

# POLITECNICO DI TORINO



Dipartimento di Meccanica

Master Degree in Mechanical Engineering

## Experimental and numerical characterization of adhesive joints with composite substrates

Relatore:

Prof. Luca Goglio

Correlatore:

Ing. Raffaele Ciardiello

Studente:

Alessandro Benelli

Anno Accademico 2020/2021



# Contents

<b>List of Figures</b>	<b>6</b>
<b>List of Tables</b>	<b>11</b>
<b>1 Introduction</b>	<b>14</b>
<b>2 Adhesive</b>	<b>16</b>
2.1 Adhesive Joint . . . . .	16
2.1.1 Adhesion . . . . .	17
2.1.2 Joint design . . . . .	18
2.2 Stresses on adhesive joints . . . . .	20
2.2.1 Adhesive joint failure . . . . .	22
2.3 Adhesive classification . . . . .	23
2.3.1 Polymer base . . . . .	24
2.3.2 Methods of reactions . . . . .	25
2.3.3 Type of applications . . . . .	26
2.4 Adhesive joint test . . . . .	27
2.4.1 Single Lap joint test . . . . .	27
2.4.2 TAST test . . . . .	27

---

2.4.3	Peel test . . . . .	28
2.4.4	ARCAN test . . . . .	28
2.5	Wetting . . . . .	30
2.5.1	Techniques to improve bonding . . . . .	31
2.6	Description of the used adhesives . . . . .	32
2.6.1	BETAFORCE 2850L . . . . .	32
2.6.2	Epoxy adhesive . . . . .	32
<b>3</b>	<b>Composite Material</b>	<b>34</b>
3.1	Introduction to composite material . . . . .	35
3.1.1	Unidirectional composites . . . . .	36
3.1.2	Load transfer matrix-fiber . . . . .	38
3.1.3	Properties of a single lamina . . . . .	39
3.1.4	Stresses and strain in casual direction . . . . .	40
3.1.5	Classical lamination theory for laminates . . . . .	41
3.2	Pre-preg composite . . . . .	44
3.3	Out-of-Autoclave Pre-preg . . . . .	44
3.3.1	Layer's properties . . . . .	44
3.3.2	Resin properties . . . . .	45
3.3.3	Fiber properties . . . . .	46
3.3.4	Common possible defects . . . . .	47
<b>4</b>	<b>Experimental part</b>	<b>48</b>
4.1	Prepregs material . . . . .	48

---

4.2	Mould design . . . . .	49
4.3	U-shape substrate production . . . . .	50
4.3.1	Mould preparation . . . . .	50
4.3.2	Pre-preg preparation . . . . .	50
4.3.3	Lamination of prepreg . . . . .	51
4.3.4	Vacuum bagging . . . . .	52
4.3.5	Curing process . . . . .	55
4.3.6	Demould the finished part . . . . .	57
4.3.7	Controlling and finishing the demoulded part . . . . .	58
4.4	Double U-shaped specimen production . . . . .	58
4.4.1	Substrates preparation . . . . .	59
4.4.2	Bonding procedure . . . . .	60
4.5	Arcan test . . . . .	61
4.5.1	Pure shear loading condition . . . . .	62
4.5.2	Pure tensile loading condition . . . . .	64
4.5.3	Mixed loading condition . . . . .	67
4.5.4	Final comparison . . . . .	71
<b>5</b>	<b>Numerical Theory</b>	<b>76</b>
5.1	The finite element method . . . . .	76
5.2	1-D problem . . . . .	76
5.2.1	1D finite element discretization . . . . .	79
5.2.2	Dynamic problem - Time integration . . . . .	82
5.3	Non -linear finite element analysis . . . . .	83

---

5.3.1	Types of non linear behaviour . . . . .	84
5.4	Summary: Step-by-step FEM . . . . .	85
<b>6</b>	<b>Numerical Simulation</b>	<b>87</b>
6.1	Set Up . . . . .	87
6.1.1	Geometry . . . . .	87
6.1.2	Material model . . . . .	90
6.1.3	Boundary Conditions . . . . .	94
6.1.4	Contact . . . . .	97
6.1.5	Output set up . . . . .	99
6.2	Results . . . . .	100
<b>7</b>	<b>Conclusion</b>	<b>104</b>
<b>8</b>	<b>Bibliography</b>	<b>106</b>

# List of Figures

2.1	Adhesive joint structure . . . . .	17
2.2	Simple heading joint . . . . .	19
2.3	Scarf joint . . . . .	19
2.4	Single-lap joint . . . . .	19
2.5	Chamfered single-lap joint . . . . .	19
2.6	Single-lap joint with offset . . . . .	20
2.7	Single-strapped joint . . . . .	20
2.8	Double-strapped joint . . . . .	20
2.9	Tensile Stress [13] . . . . .	21
2.10	Shear Stress [13] . . . . .	21
2.11	Compression Stress [13] . . . . .	22
2.12	Cleavage Stress [13] . . . . .	22
2.13	Peel Stress [13] . . . . .	22
2.14	Failure Modes [14] . . . . .	23
2.15	Stress-Strain behaviour of different polymers [10] . . . . .	24
2.16	Peel tests [7] . . . . .	29
2.17	Arcan type device [3] . . . . .	30

---

2.18	Wetting [16] . . . . .	30
3.1	Weight comparison of side panels: using skin-stringer or sandwich structures would reduce the total weight by 24% or 13% respect the aluminium based structures.[19] . . . . .	34
3.2	Typical composite materials [19] . . . . .	35
3.3	Infinitesimal fiber scheme . . . . .	39
3.4	Coordnate systems: T,L orthotropic axis; X,Y arbitrary axis[19] . . . . .	41
3.5	Plate cross section before and after the deformation [19] . . . . .	42
3.6	Layup scheme of a laminate inside the vacuum bag ready to be cured [22] . . . . .	45
3.7	Change in properties of the epoxy resin during a typical cure cycle [23] . . . . .	46
3.8	Possible defects in the proximity of a corner[22] . . . . .	47
4.1	Sheets of Prepregs XC110 Twill Prepreg Carbon fiber . . . . .	48
4.2	Drawing of Arcan specimen used in the past . . . . .	49
4.3	Drawing of the mould for the substrate production . . . . .	49
4.4	Application of the release agent . . . . .	51
4.5	Bridging defect . . . . .	52
4.6	Usage of dibbers . . . . .	52
4.7	Second layer lamination . . . . .	53
4.8	Cutting excess material . . . . .	53
4.9	Peel ply adjusting . . . . .	54
4.10	Breather adjusting . . . . .	54
4.11	Single - double bag comparison . . . . .	55
4.12	Part ready to be cured . . . . .	56

---

4.13	Curing cycle of XC110 Twill Prepreg Carbon fiber . . . . .	56
4.14	Demoulding process . . . . .	57
4.15	Cutting process . . . . .	58
4.16	Drilling process and final substrate . . . . .	59
4.17	Measuring sequences to delimit the bonding zone with the transparent tape . . . . .	60
4.18	Shims placed on the top surfaces of half of the substrates that will be bonded with the polyurethane adhesive . . . . .	60
4.19	Tested configurations with Arcan fixture . . . . .	62
4.20	Polyurethane pure shear loading test with 1 mm and 2 mm substrates	63
4.21	Cohesive failure surfaces for pure shear test of polyurethane adhesive joint for both 1mm(left) and 2mm(right) thick substrates . . . . .	64
4.22	Epoxy pure shear loading test with 1 mm and 2 mm substrates . . .	65
4.23	Cohesive failure surfaces for pure shear test of epoxy adhesive joint for both 1mm(left) and 2mm(right) thick substrates . . . . .	65
4.24	Polyurethane pure tensile loading test with 1 mm and 2 mm substrates	66
4.25	Cohesive failure surfaces for pure tensile test of polyurethane adhesive joint for both 1mm(left) and 2mm(right) thick substrates . . . . .	66
4.26	Epoxy pure tensile loading test with 1 mm and 2 mm substrates . . .	67
4.27	Cohesive failure surfaces for pure tensile test of epoxy adhesive joint for both 1mm(left) and 2mm(right) thick substrates . . . . .	68
4.28	Polyurethane mixed loading condition tests with 1 mm and 2 mm substrates . . . . .	68
4.29	Cohesive failure surfaces for mixed loading conditions tests of polyurethane adhesive joint for both 1mm(left) and 2mm(right) thick substrates . .	69
4.30	Epoxy 45° loading condition test with 1 mm and 2 mm substrates . .	70

---

4.31	Cohesive failure surfaces for mixed loading condition test of epoxy adhesive joint for both 1mm(left) and 2mm(right) thick substrates . . .	71
4.32	Load and Stiffness variation in the polyurethane adhesive joint . . . . .	71
4.33	Load and Stiffness variation in the polyurethane adhesive joint . . . . .	73
4.34	Stiffness at 80% of the max load and displacement at the peak of the load variation in the polyurethane adhesive joint . . . . .	73
4.35	Change in the behaviour of the adhesive joint with epoxy changing the loading angle. . . . .	74
4.36	Load and Stiffness variation in the epoxy adhesive joint . . . . .	74
4.37	Stiffness at 80% of the max load and displacement at the peak of the load variation in the epoxy adhesive joint . . . . .	75
5.1	Elastic string problem scheme . . . . .	77
5.2	Linear finite elements [26] . . . . .	81
6.1	Lines for the surface creation . . . . .	88
6.2	Surface drawn in Rhinoceros . . . . .	88
6.3	Automesh function: In the left side there is the implementation of the auto-mesh function and the re-meshing process of the vertical surfaces, while in the right side of the figure there is the meshed substrate . . . . .	89
6.4	Box solid geometric property . . . . .	90
6.5	Complete geometry model . . . . .	90
6.6	Material model 54-55 used for each the substrates . . . . .	91
6.7	Bi-linear traction separation law for MAT_138 . . . . .	93
6.8	Set of nodes to be properly constrained . . . . .	94
6.9	BOUNDARY_SPC constraints cards . . . . .	95

---

6.10	Boundary_Prescribed_Motion card . . . . .	96
6.11	Velocity imposed by the traction machine versus time . . . . .	96
6.12	Offset distance between shells of different thickness in the epoxy case simulation . . . . .	98
6.13	Contact keyword . . . . .	99
6.14	Cross sections . . . . .	100
6.15	Comparison between real and numerical curve in the pure shear con- ditions . . . . .	102
6.16	Comparison between real and numerical curve in the pure shear con- ditions . . . . .	103

# List of Tables

2.1	Betaforce 2850L . . . . .	33
2.2	BETAMATE 1640 . . . . .	33
3.1	Properties of the mostly used fibers [19] . . . . .	36
4.1	Curing cycle of XC110 Twill Prepreg Carbon fiber . . . . .	57
4.2	Experimental parameters for polyurethane adhesive joint with carbon fiber substrates . . . . .	72
4.3	Standard deviations of the experimental parameters for polyurethane adhesive joint with carbon fiber substrates . . . . .	72
4.4	Experimental parameters for epoxy adhesive joint with 1mm thick carbon fiber substrates . . . . .	74
4.5	Experimental parameters for epoxy adhesive joint with 2mm thick carbon fiber substrates . . . . .	74
6.1	Offset distance between shells of different thickness in the epoxy case simulation . . . . .	98

# Abstract

The use of adhesives in the last decade has grown substantially in various industrial fields, particularly in the marine, aerospace and automotive sectors. The constant research for lightweight commonly leads the industries to choose composite materials for developing more efficient products, due to their good mechanical properties and very low weight per unit of volume. Although composite materials present many advantages, they cannot be joined with traditional techniques, such as bolted joints, which involve drilled holes that are harmful to these materials, then adhesive joints are preferred. The adoption of adhesive joints leads also to a more uniform stress condition along the joint, moreover can prevent the corrosion of substrates with their sealant properties.

In this thesis work, an experimental and numerical investigation on adhesive joint subjected to different loading conditions has been carried out. The aim of the thesis is to analyze the behavior of two different adhesives, used in the automotive industries, by means of U-shaped specimens made of carbon fibers. The adhesives are tested through the Arcan test, equipment widely used for testing welded joints, that allows testing the adhesive at different loading conditions. The test leads to the characterization of the adhesive joints under different loading angles, which in particular are  $0^\circ$  (pure shear loading condition),  $45^\circ$  (combined shear-tensile loading condition) and  $90^\circ$  (pure tensile loading condition). This is very important in the automotive industry since the adhesive joints are mainly designed to support shear loads while in real working cases, such as impacts, they can be subjected to combined loads. The tests aim to find the mechanical behavior of the adhesive joints in relation to the loading angles. Two adhesives are used to bond two sets of substrates (2 layers and 4 layers) with different thicknesses to show the correlation between the adhesive behavior and the stiffness of the substrates. The adhesives are a 2-component polyurethane adhesive which is characterized by a ductile behavior and a 1-component epoxy that presents a stiffer behavior compared to the polyurethane. In the first part of the activity, the substrates were prepared in the lab by using prepreg

---

made of carbon fiber layers cured in the oven under vacuum. In the second part of the thesis adhesive joints were prepared and tested. Finally, a Finite Element Model was developed to study the mechanical properties of the joints. The numerical simulation has been carried out using the software LS-Dyna and was validated through iterative procedures comparing the numerical results with the experimental ones to obtain important information such as peel and shear stress in the inner section of the adhesive joints. The aim of the thesis is to assess whether and how the adhesive type and the stiffness of the substrates can influence the mechanical properties of the adhesive joints and define a failure envelope in a stress space based on the tested mixed-stress conditions.

# 1. Introduction

The history of adhesives is strictly related to the history of humankind. Unlike other species that use instinct to accomplish a task, human beings observe and adopt the techniques of many species, always trying to improve the outcome. In ancient times human beings observed the interesting phenomenon of sticky substances. In the beginning, our ancestors used mud, clay, snow or other natural materials to keep wind or even rain out of their dens, similar material are used today to perform similar functions in the modern buildings (*sealants*). The first rudimentary *composite* was composed by straws or other vegetable materials used to reinforce mud or clay. Soon, to enhance the joining process of materials, observing human discovered sticky materials. In particular they noticed that hot sources change the state of some materials, causing them to soften and became sticky, then hardened again exploiting the cool of the night. This was the first approach to the wide world of *adhesive* technology. [1]

Modern adhesive and sealant industry has its history strictly correlated to the development of aerospace and automotive industries. The reason why is because, for example in the automotive industry, there is a constant research for lighter vehicles, able to reduce fuel consumption and fuel emissions, due to the restriction imposed by the EU in terms of CO<sub>2</sub> emissions. [2]. This goal is achievable by using lighter materials, such as composite materials or light metal alloys. In order to not lose the mechanical properties of this light structures, it is important to guarantee a more uniform distribution of stress and not modify the material properties during the joining process. Adhesive joining techniques do not affect the structure of the substrate to join unlike traditional techniques such as bolted joints, that can introduce cracks in the structures. Moreover the use of adhesive instead of traditional techniques can prevent or reduce corrosion phenomena.[3]

In the last years the joining of composite materials with adhesives is an increasingly attractive topic for companies in the automotive field, due to the introduction in the market of electric cars. In order to increase as much as possible the range of

of an electric car, the wiser choice is to reduce as much as possible the weight of the entire structure, as for the reduction of fuel emissions. By using advanced materials, such as carbon fiber reinforced polymer (CFRP), along with adhesives that do not change the property of the composite, is possible to drastically increase the range of a car without losing performance. [4][5]. Moreover the main path toward lightweight vehicle design is the possibility to assemble hybrid structures, that would be difficult and sometimes impossible to do with traditional joining techniques.

The adhesive bonding joining technique can be easily adopted both for metal and composite structures, but the prediction of the behaviour of those bonded joints is still not easy to understand and compute. Using the Arcan fixture technology is possible to define the behaviour of the adhesive joints in different loading conditions. Using this fixture is possible to test each joint under pure tensile load, pure shear and even in a combined shear and tensile load condition. [6]

In this thesis work two different adhesives have been tested. The first adhesive is a polyurethane, which is ductile and guarantees a big elongation before the complete rupture. Instead the second one is a structural epoxy adhesive, very stiff with high load carrying capacity. The aim is to analyze and understand a possible correlation between the response of the adhesive joint to different kind of load and the thickness of the substrates. For what it concerns the substrate, they have been manufactured from prepreg sheets of carbon fiber inside the DIMEAS laboratories at the Politecnico di Torino. Two different thicknesses will be analyzed and studied, 1mm and 2mm.

Nowadays is very important to have a numerical model that is able to simulate the reality, so as last step in this work, a FEM model, with the software LS-Dyna, is roughly created. The simulation results are discussed and compared to the real one in the last chapter.

## 2. Adhesive

Adhesive have been used for thousand of years, but until 100 years ago, the vast majority was from natural products such as bones, skins, fish, milk and plants. Nowadays instead, adhesives based on synthetic polymers have been introduced. The formation of a bonded joint can be described in two different stages: [7]

- the adhesive in the solid state must be spread easily on the surface and wet properly the substrates to be bonded;
- the liquid adhesive must harden in order to be able to support the loads during is serving life;

Naturally is necessary to understand the capacity of the joints to support the load under various factors such as the environment that the joint will be subjected to. Adhesives are divided in two big categories: the ones that historically were cured on heating are called "Thermosetting" the others are called "Thermoplastic". However, many thermoset adhesive cure at room temperature so the real distinction between the two type is that the first ones do not soften on eating after curing, because the polymer chains are chemically cross linked, instead the second ones soften on heating. Is very easy to understand that in general thermoset adhesive have better thermal, fluid, and environmental resistance than the thermoplastic, however the first ones are not easily removable or recyclable.

### 2.1 Adhesive Joint

The use of adhesive has progressively increased over the years and is continuously growing in many industrial areas such as automotive, marine and aerospace industries. The main reasons which let this type of joining technique to be used so widely are: [8] [9] [10]

- lighter assemblies with respect to welded or bolted joints;
- relatively uniform distribution of the stresses;
- possibility to attach together very different materials;
- can prevent or reduce corrosion between dissimilar materials
- the micro structure of the substrates is not affected in any way, so we do not weaken the structure.

It is possible to analyse the structure of adhesive joint [Fig.2.1] which consists of two substrates surfaces with the adhesive material filled the gap between them. The two substrates can be made of the same material or different, it can be a metallic one or a ceramic so is very important to chose wisely the best adhesive for the application. Once bonding is completed the substrates are called adherends. Finally it is possible to define also 2 "Boundary Layers" in which the adhesive properties have been changed by impurities and product of reactions at the substrate surfaces.[11]

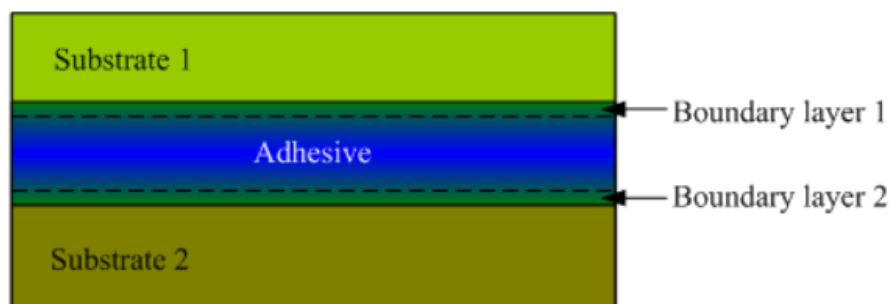


**Figure 2.1:** Adhesive joint structure

### 2.1.1 Adhesion

The principle behind an adhesive bonding is a phenomenon called "Adhesion", which is very complex. As a matter of fact, one of the main difficulties in the study of adhesion mechanisms lies in the fact that the subject is at the boundary of several scientific fields such as: macro-molecular science, physical chemistry of surfaces, material science, mechanics and micro-mechanics of fracture. Consequently, the study of this phenomena could be done by different type of approaches, sometimes contradictory, depending very much on one's field of expertise. The most common approaches are:[1]

- Mechanical interlocking: the major factor to establish adhesive strength is to interlock the adhesive into the cavities, pores and asperities of the solid surface. Indeed, in order to establish a strong adhesion is necessary to increase the roughness of the surfaces so that the penetration of the adhesive is possible.
- Electronic theory: the resultant electrostatic forces can play a major role in the total adhesive force due to the possible formation of a double electrical layer at the interface induced by an electron transfer mechanism between the substrate and the adhesive, having different electronic band structures that can equalize the Fermi levels.<sup>1</sup>
- Theory of boundary layers and inter-phases: the cohesive strength of a weak boundary layer can always be considered as the main factor in the determining the level of adhesion, even when the failure appears to be inter facial.
- Adsorption theory: this is probably the most widely used approach, it consist in believing that the adhesive will adhere to the substrate because of inter-atomic and inter-molecular forces (Van del Walls forces) established at the interface, provided that an intimate contact is achieved.
- Diffusion theory: the adhesion strength of polymers to themselves (autohesion) or to each other is due to mutual diffusion (inter-diffusion) of macro-molecules across the interface, thus creating an inter-phase.
- Chemical bonding theory: the chemical bonds formed across the adhesive-substrate interface are considered as the main forces that participate the the total level of adhesion between both material, instead physical interactions, such as Van der Walls, are called secondary force interactions.

Actually each of these theories is valid to some extent, depending on the nature of the solid in contact and the conditions of formation of the bonded system. Therefore it is not possible to state which is the best because their respective importance depends largely on the system chosen.

### 2.1.2 Joint design

The geometric features of a joint, and especially the type of the joint, have a strong effect on the producibility of a structure in adhesive bonding operations. Further-

---

<sup>1</sup>The Fermi level of a solid-state body is the thermodynamic work required to add one electron to the body. It is a thermodynamic quantity.

more each type of joint has its own characteristic. Are now listed the most used ones: [12]

- Simple heading joint [Fig.2.2]: is the easiest to make, however cohesive peel strength of cured adhesive is very limited.
- Scarf joint [Fig.2.3]: higher strength than the simple heading joint but requires the additional operation of chamfering and is not really easy to make. Is a good choice for thick substrates.

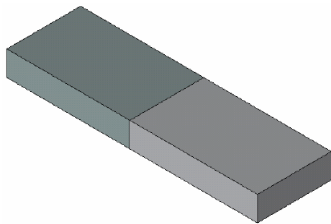


**Figure 2.2:** Simple heading joint

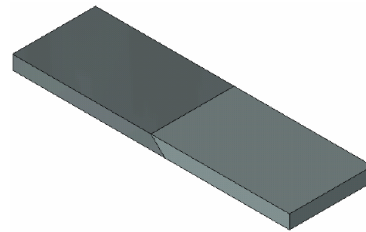


**Figure 2.3:** Scarf joint

- Single-lap joint [Fig.2.4]: is the most frequently used but the eccentricity of load causes deterioration of the strength properties. Commonly used for thin sections.
- Chamfered single-lap joint [Fig.2.5]: it guarantees an higher strength than the single-lap due to a lower concentration of stresses at the ends of the overlap. It requires troublesome chamfering of edges.

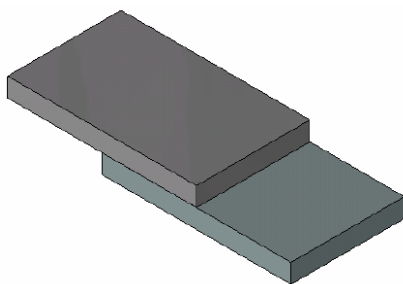


**Figure 2.4:** Single-lap joint

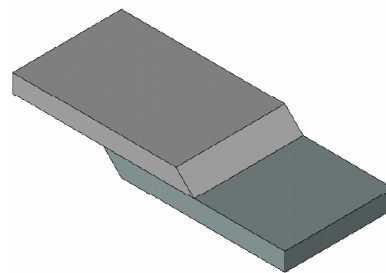


**Figure 2.5:** Chamfered single-lap joint

- Single-lap joint with offset [Fig.2.6]: is very easy to make and moreover eliminates eccentricity of loads, but requires the additional operation of bending the overlap section.

- Single-strap joint [Fig.2.7]: is easy to make but requires the application of a strap. It is used if a smooth surface is needed.

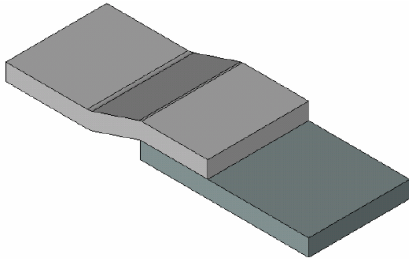


**Figure 2.6:** Single-lap joint with offset

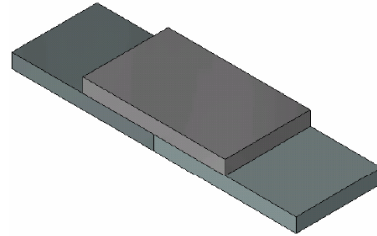


**Figure 2.7:** Single-strap joint

- Double-strap joint [Fig.2.8]: is more difficult to make than a single-strap joint, increases the weight of the structure and the fabrication of one additional strap, but eliminates the eccentricity of loads and has good strength characteristics.

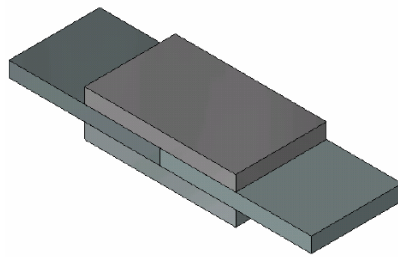


**Figure 2.8:** Double-strap joint

## 2.2 Stresses on adhesive joints

Regardless of the joint type used, it's important to understand the different stresses that are applied onto a bonded assembly. Adhesive and tapes perform at their best when the stress is two-dimensional to the adhesive, so that the load is distributed all over the entire area of the bonding surface. Adhesive and tapes perform at their worst when the stress is one-dimensional to the adhesive, concentrating a load onto the leading edge of a bond line[13]:

- Tensile Stress [Fig.2.9]: is pull exerted equally over the entire joint. Pull direction is straight, in plane and away from the adhesive bond. The load is distributed across the entire area of the bond line.

- Shear Stress [Fig.2.10]: is pull directed across the adhesive, forcing the substrate to slide over one another. As the previous case, the force is in-plane, and the force is distributed across the entire area of the bond line.

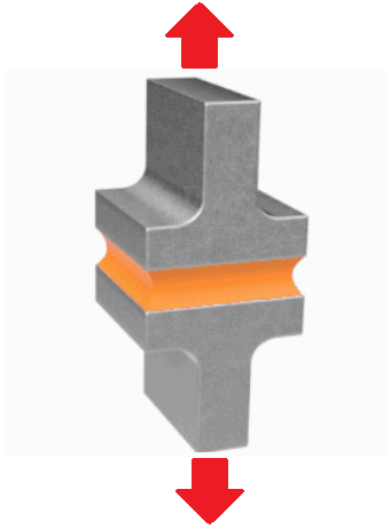


**Figure 2.9:** Tensile Stress [13]

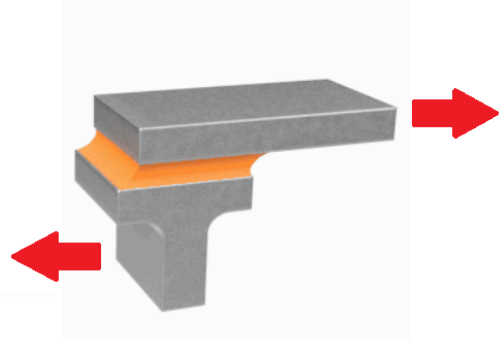


**Figure 2.10:** Shear Stress [13]

- Compression Stress [Fig.2.11]: like tension, is a force applied to a bond that is in-plane and straight. Unlike tension, the force is being applied toward the adhesive. Force is distributed across the entire area of the bond line.
- Cleavage Stress [Fig.2.12]: is pull concentrated at one edge of the joint, exerting a prying force on the bond. While one end of the adhesive is experiencing concentrated stress on the leading edge, the other is theoretically under zero stress. This type of stress occurs with two rigid substrates.
- Peel Stress [Fig.2.13]: as the previous case, peel is a pull that is also concentrated at one edge of the joint. Though one of the substrate is flexible, resulting in even more concentration at the leading edge than with a cleavage joint.



**Figure 2.11:** Compression Stress [13]

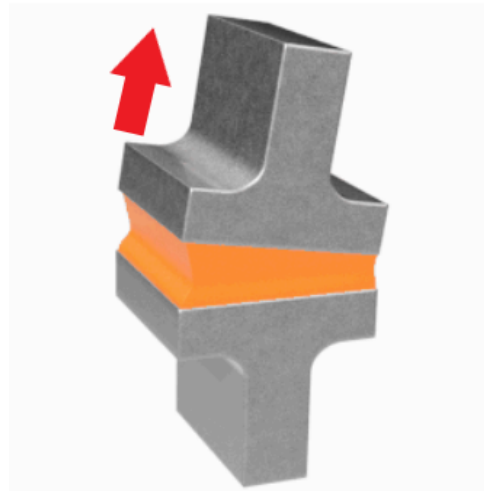


**Figure 2.12:** Cleavage Stress [13]



**Figure 2.13:** Peel Stress [13]

### 2.2.1 Adhesive joint failure

In order to classify the rupture modes of adhesive joints it is possible to follow the guidelines of the ASTM D5573. The main rupture modes suggested by the standard is shown in Fig. 2.14. The factors which determine the failure mode of a specimen is the difference between the cohesive and adhesive resistances and the resistance of the substrates. The failure will first occur in the least resistance spot. The failure of the substrate, in turn, can occur in two ways: stock-break or fiber-tear. The typical type of rupture are:[14]

- Adhesive failure [Fig. 2.14a]: inter-facial failure between the adherend and

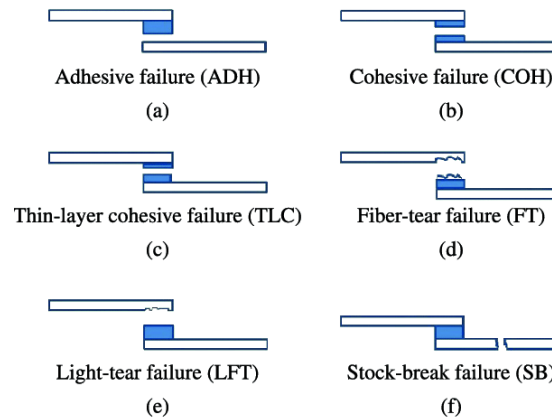


**Figure 2.14:** Failure Modes [14]

the adhesive. It might be caused by to an error during the preparation of the joint or to a comp ability problem between the adhesive and the substrate's material or also to an higher cohesive resistance than the adhesive one.

- Cohesive failure [Fig. 2.14b]: this is the mode of failure desirable at the end of a test because it means that the adhesion was stable during the whole time. A layer of adhesive remains attached to the substrates.
- Thin-layer cohesive failure [Fig. 2.14c]: similar to the previous mode but in this case the adhesive left in the two substrates is not equivalent.
- Fiber-tear failure [Fig. 2.14d]: it could happen only in a composite material. The failure does not happen in the adhesive, how it should be, but in the composite material's fibers. This might be caused by an adhesive resistance higher than the adherend's fibers.
- Light-fiber-tear failure [Fig. 2.14e]: as in the previous mode the failure occurs in the material's fibers, however in this case the failure is closer to the interface between the adherend and the adhesive.
- Stock-break failure [Fig. 2.14f]: As in the last two cases the failure is in the fiber but away from the overlap between the adherend and the adhesive.

## 2.3 Adhesive classification

There are a lot of possible way to classify the adhesives, but the most used are:

1. Polymer base (i.e. natural or synthetic)
2. Methods of reactions
3. Type of functions

### 2.3.1 Polymer base

In order to be able to describe polymers and their composites which are used in the production of adhesives, a general classification of engineering polymers need to be considered first. The nature of a polymer defined as a plastic, an elastomer (rubber), or a fiber depends on the strength of its inter-molecular bonds and molecular structure. At temperature above  $T_g$ <sup>2</sup> elastomers are typically non crystalline polymers with very weak inter-molecular forces. Polymers with moderate inter-molecular forces are classified as plastics, instead polymers with strong hydrogen bonds and especially those with high crystallinity can be made into strong fibers Fig.2.15.[10]

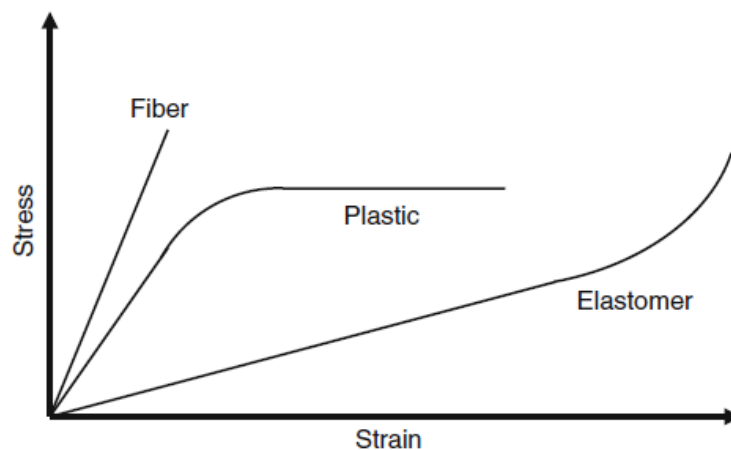


Figure 2.15: Stress-Strain behaviour of different polymers [10]

#### Thermoplastics

This adhesives are formed by polymers that can change their structure from liquid to solid just by subtracting heat. They present a linear or laminated structure, indeed they have a lower mechanical and thermal resistance than the Thermosetting one.[10]

---

<sup>2</sup>The glass-transition temperature  $T_g$  of a material characterizes the range of temperatures over which this glass transition occurs. It is always lower than the melting temperature,  $T_m$ , of the crystalline state of the material, if one exists.

### Thermosets

Thermosetting adhesives are typically available in liquid, paste, and solid forms. As discussed by Lin and Pearce ([15]) these polymers consist of three-dimensional cross-linked networks of infinite or immeasurably high weight molecules, indeed are stronger than the previous ones. They are commonly used for structural application with also high temperature involved.[10]

### Natural

This type of adhesive are obtained from natural resources, such as, starch, protein or animal glues. They have low mechanical resistance but high temperature resistance. resistance.[10]

### Elastomers (rubbers)

This one are made from natural or synthetic resin, their typical ability is to undergo very large elongation and are characterized by a significant amount of resilience<sup>3</sup>. [10]

## 2.3.2 Methods of reactions

Except for pressure-sensitive adhesive, which undergo no phase change for application, adhesive are typically applied as low-viscosity liquids to wet properly the adherend surfaces and to flow into their crevices and asperities. Liquid form of adhesive is typically obtained by three methods:[10]

1. heating the solid adhesive to the point of a facile flow
2. dispersing/dissolving the adhesive material in a solvent
3. starting with the adhesive material in liquid monomer form which is subsequently polymerized. These liquid forms are subsequently solidified by:
  - cooling

---

<sup>3</sup>Resilience is represented by the area under the elastic portion of the stress-strain curve, and therefore, refers to a material's ability to undergo elastic deformations.

- solvent evaporation
- chemical reaction

Therefore, adhesive can be classified based on the method of "activation" as follow:

- Solvent-activated: These types of adhesives become tacky when wetted with an organic solvent. The presence of an organic solvent, however, may present fire and health hazards.
- Water-activated: These types of adhesives are generally based on polyvinyl alcohol, starch or protein glues.
- Hot melts: These adhesives are generally thermoplastic 100% nonvolatile materials heated up to the melting point in order to be applied to the substrates . With these types of materials, the adhesive bond is primarily mechanical, as achieved after solidification.
- Reactive-adhesives: These adhesive polymerize either at low and high temperatures, Moreover, they guarantee an high adhesion force in time, even in severe environmental conditions.

### 2.3.3 Type of applications

The last classification is based on the function of the adhesive:

- Structural adhesive: refer to a relatively strong adhesives that are normally used well below their glass transition temperature ( $T_g$ ). Common examples of structural adhesives include epoxies, cyanoacrylates, and certain urethane and acrylic adhesives. Such adhesives can carry significant stresses, and lend themselves to structural applications.[16]
- Non-structural adhesive: refer to adhesive primarily used for applications of facades, or better for aesthetic purpose. [16]
- Semi-structural adhesive: equal to the previous one but the failure would be less critical. [16]

## 2.4 Adhesive joint test

There are many test methods as well as many configurations for the determination of failure strength data.

### 2.4.1 Single Lap joint test

The most common configurations in order to evaluate the mechanical properties of bonded joints is 'Single Lap Joint' [Fig.2.4]. The SLJ configuration is very common because is generally used in many practical applications and moreover because are rather simple to manufacture and pretty cheap. However using this kind of configuration it is possible to encounter some issues like the control of the adhesive's thickness or the right alignment of the specimen. Moreover this type of joint is prepared by clamping the two substrates together with clamps and keep this configuration until the curing process is over, so some problems may be encountered:[7]

- Guaranteeing the initial alignment of the substrates is not trivial, some reference blocks could be used being very careful to not bonding these blocks to the specimen.
- When the alignment is obtained, it is not easy to keep it during all the curing process, especially when the specimen has to be cured inside an oven.
- Control the thickness of the adhesive is almost impossible, unless by using son kind of filler beds.
- The number of specimen that can be prepared is quite limited due to the fact that this kind of joint is very time consuming.

### 2.4.2 TAST test

From the previous section it was easy to understand that the conventional single lap shear joint puts the adhesive in a complicated state of stress, therefore is not suitable for the determination of the true adhesive properties. The thick adherend shear test (TAST) indeed is one of the most used types of failure strength test because it is easy to make and test the specimens. The concept behind this test is the fact that when using stiff and thick metallic adherends, the adhesive is in a state of uniform

shear over almost the whole overlap section and the peel stress is reduced as much as possible. Two different forms of the test are used:

1. Developed by Krieger in the United States (ASTM D3983)
2. Developed by Althof and Neumann in Europe (ISO 11003-2)

The two tests mainly differ only on the size of the specimens, the Althof specimen is half the size of the Krieger's.[7]

### 2.4.3 Peel test

Since many years, peel tests have been used to compare the relative strength of different adhesives, different surface preparation techniques and so on. However the most interesting way to exploit this kind of test is to determine the adhesive toughness by suitable data treatment. One of the strengths of this type of test is the fact that it is possible to test the specimen under a combination of mode I<sup>4</sup> and mode II<sup>5</sup> by varying the peel angle, that is the angle with which the force is applied. There are different peel test methods:

- Fixed Arm [Fig.2.16a]
- T-peel [Fig.2.16b]
- Floating roller [Fig.2.16c]
- Climbing drum [Fig.2.16d]

which are all very similar, they differ just in the way that the load is applied to the specimen.[7]

### 2.4.4 ARCAN test

In order to optimize adhesive bonded assemblies, the development of reliable tools is necessary. A large database of experimental data are needed to develop a good

---

<sup>4</sup>Is the loading conditions that occurs more often and produces the most damage. It is also called 'Opening Mode' and consist in a Tensile stress normal to the plane of the crack.[17]

<sup>5</sup>Is the second most studied case and is also called 'Sliding Mode'.It consists in a shear stress acting parallel to the plane of the crack.[17]

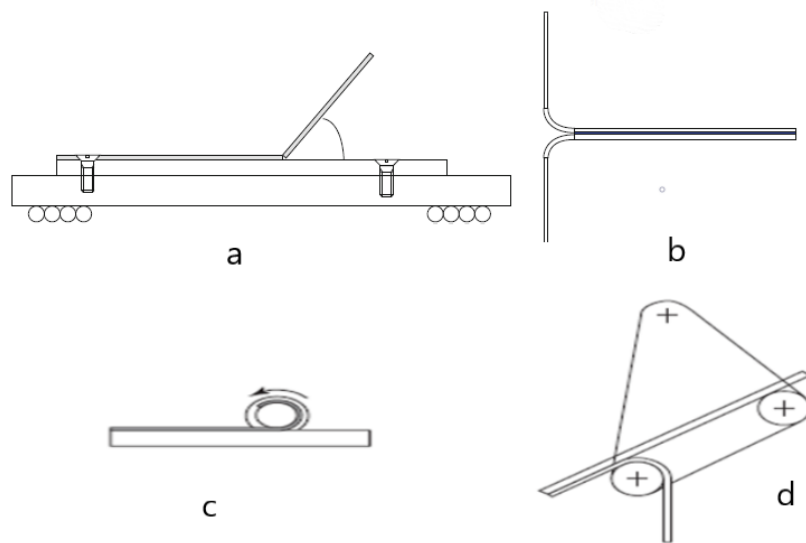


**Figure 2.16:** Peel tests [7]

numerical model that works best. Those experimental data have to be obtained in a simple way, for example using a tensile testing machine. The Arcan-type device allows the same bonded specimen to be loaded under mixed loading condition as well as pure tensile and pure shear conditions. This kind of test, in other words, is the one that let understand the behaviour of the material under different loading conditions, using just a tensile testing machine, and the big amount of data that generates can be used to develop a very good numerical model.[7]

### Arcan-type Device

The Arcan-type device consists on two half-moon shaped parts made of highly rigid steel. If the specimens used in the test are the double-U shaped (also called KS2 specimen), those two plates are equipped by two sets of drilled holes:

- The external holes are intended to fix the Arcan fixture to the tensile testing machine
- The internal holes are needed in order to clamp the specimen to the fixture.

Is easy to understand from Fig.[2.17] that by changing the fixing holes between the plates and the tensile testing machine, the loading angle varies, therefore it is possible to load the specimens with any combination of mode I and mode II as requested.

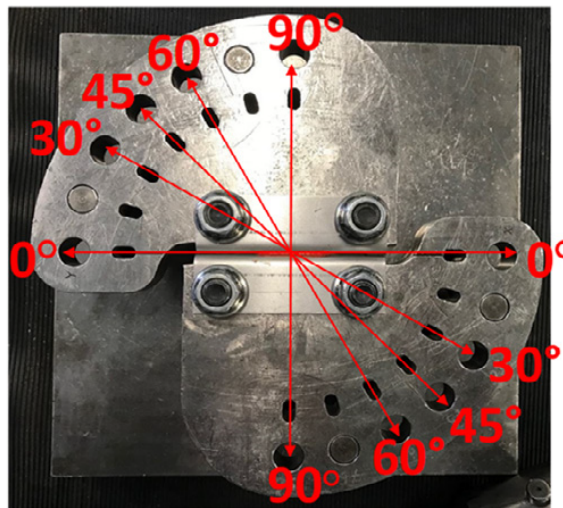


Figure 2.17: Arcan type device [3]

## 2.5 Wetting

Wetting is the ability of liquids to form interfaces with solid surfaces. To determine the degree of wetting, the contact angle ( $\alpha$ ) that is formed between the liquid and the solid surface is measured. The smaller the contact angle and the smaller the surface tension, the greater the degree of wetting.[16] The wetting ability depends

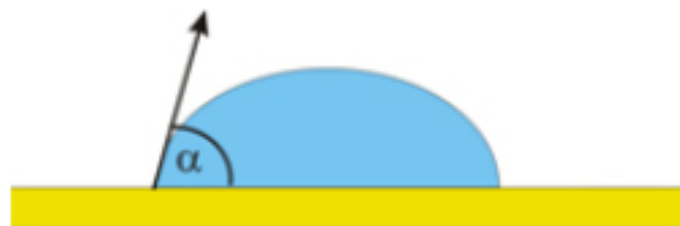


Figure 2.18: Wetting [16]

mostly on rheological properties:

- Viscosity: is responsible for the forces that affect the mobility of the fluid, in other words the fluid resistance to flow. High viscosity is advantageous in order for example to avoid too much running of the adhesive out of the edges of the bonded joints. Depending on the method of application different values of viscosity are needed, for example in the spraying technique very low viscosity are requested.

- Thixotropy: is the property of a fluid to temporarily change the state of the fluid to a lower viscosity as a result of the action of mechanical forces, such as stirring, shaking or kneading.

However the wetting ability of the substrates is a necessary condition but is not sufficient so that the adhesion take place, moreover a good wetting property does not guarantee a great strong bonding conditions.

### 2.5.1 Techniques to improve bonding

In order for strong and lasting adhesion to be achieved, the substrate structure must meet certain requirements, namely:[18]

- Elimination of 'weak boundary layers' at the surface such as contaminants, oxidized layers
- Improve wetting of the substrates
- Induce chemical modifications, such as the introduction of polar chemical groups or coupling agents onto the surface which are available for bonding
- Increase the surface roughness in order to improve the mechanical interlocking or to increase the bondable surface area

To meet the requirements just listed it is possible to do a surface treatment. The effectiveness of any surface treatment depends on the type of substrate and the extent of the treatment. For instance using some solvent cleaning will remove surface contaminants in some substrates but in other ones may interact with the surface, causing morphological changes. Surface treatments can also exploit acid or laser techniques, also called etching treatments, because they may cause chemical modifications at low level but may also introduce large texture changes at high treatment levels. Moreover electrical discharge treatment may cause a temperature rise on a surface and therefore it is possible to have surface texture changes due to localized melting.

## 2.6 Description of the used adhesives

The adhesives that have been tested are a 2-component polyurethane adhesive which is characterized by a ductile behavior and a 2-component methacrylate that presents a fragile behavior compare to the polyurethane.

### 2.6.1 BETAFORCE 2850L

The first tested adhesive is BETAFORCE 2850L which is a 2-component polyurethan adhesive with very long open time <sup>6</sup> and used especially for structural bonding. The properties listed in its technical data sheet are:

- Good adhesion to plastics, composite and painted surfaces
- Good adhesion to coated metal surfaces
- Accelerated adhesion at elevated temperature
- High mechanical strength and elongation at break
- Low temperature dependency of the modulus
- Glass transition temperature outside the application range

In addition from the data sheet it is possible to extrapolate the most important technical data [Tab:2.1]: The substrate must be cleaned, in particular the surfaces must be free of dust, oil and grease. The composite substrates should be cleaned with 'BETACLEAN 3350' as recommended by the producers. The adhesive is particularly resistant to aqueous chemicals, petrol and alcohol.

### 2.6.2 Epoxy adhesive

The second adhesive that have been tested is BETAMATE 1640 a one component epoxy supplied by Dow Automotive. This adhesive is a structural one with the following properties, listed in its datasheet:

---

<sup>6</sup>The open time is the time which the adhesive need to bond, is affected by the environmental conditions.

<b>MECHANICAL PROPERTIES OF THE TWO COMPONENTS</b>		
<b>Component</b>	<b>A</b>	<b>B</b>
Basis	Isocyanate (hardener)	Polyol (resin)
Colour	Black	White
Density [g/cm <sup>3</sup> ]	1.17	1.43
<b>ADHESIVE</b>		
Processing temperature [°C]	18-28	
Open Time [min]	35-50	
Tensile strength [MPa]	10	
Elongation at break [%]	150	
E-modulus [MPa]	21	
Glass transition temperature [°C]	-45	

**Table 2.1:** Betaforce 2850L

- Excellent process and storage stability
- High durability of the adhesive and the adhesive bond
- Stiffness and crash stability increase of the entire car body
- Up to eight weeks open time in the uncured bond
- Precurable

For what it concerns the application of it, it is suggested to heat up the adhesive to decrease its viscosity, also the substrates should be at 15°C or higher. In addition from the data sheet it is possible to extrapolate the most important technical data [Tab:2.2]: The adhesive contains small glass spheres of 0,2mm diameter.

<b>ADHESIVE</b>	
Processing temperature [°C]	35-65
Density [g/ml]	1.22
Tensile strength [MPa]	9-13
Elongation at break [%]	7
E-modulus [MPa]	2270

**Table 2.2:** BETAMATE 1640

### 3. Composite Material

The constant need to increase performance has led, for some years now, the research to look for solutions in order to reduce the overall weight of a structure as much as possible, while maintaining the same mechanical characteristics. The first industry to have a lot of interest in the loss of weight of the structure was the aircraft industry, indeed reducing the aircraft weight could be the answer to improved aircraft efficiency and performance. One important example of weight reduction is in the realization of a fuselage panel, which was originally manufactured from aluminum and then using laminated graphite epoxy stringers or laminated graphite epoxy sandwich. The weight comparison between the three structures is represented in Fig.3.1. [19]

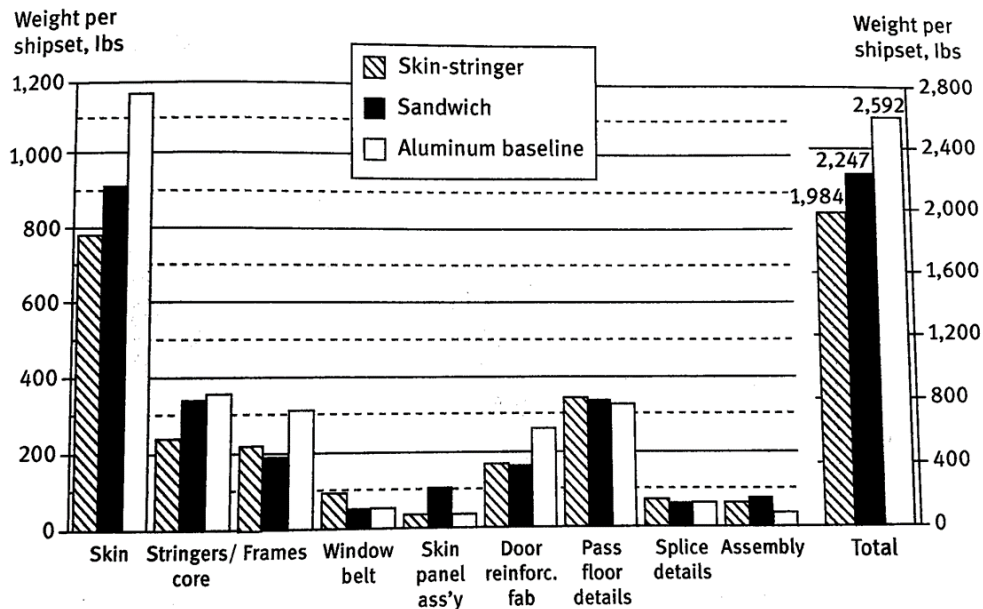


**Figure 3.1:** Weight comparison of side panels: using skin-stringer or sandwich structures would reduce the total weight by 24% or 13% respect the aluminium based structures.[19]

## 3.1 Introduction to composite material

The common definition of a composite material is that is made of two constituents:

1. fiber, also called the reinforcement, which gives to the material the strength and they are meant to support the external loads;
2. glue, normally called matrix, which has the following two main functions, to protect the fibers from abrasion or environmental agents and also to maintain the reinforcements in the correct orientation.

The matrix is a polymer, indeed is characterized by low strength and stiffness however is very important that is able to transmit the outside load to the fibers, which are characterized by high strength and stiffness. The composites can be of various types and in the literature are usually cataloged in a block diagram as in the Fig.3.2.

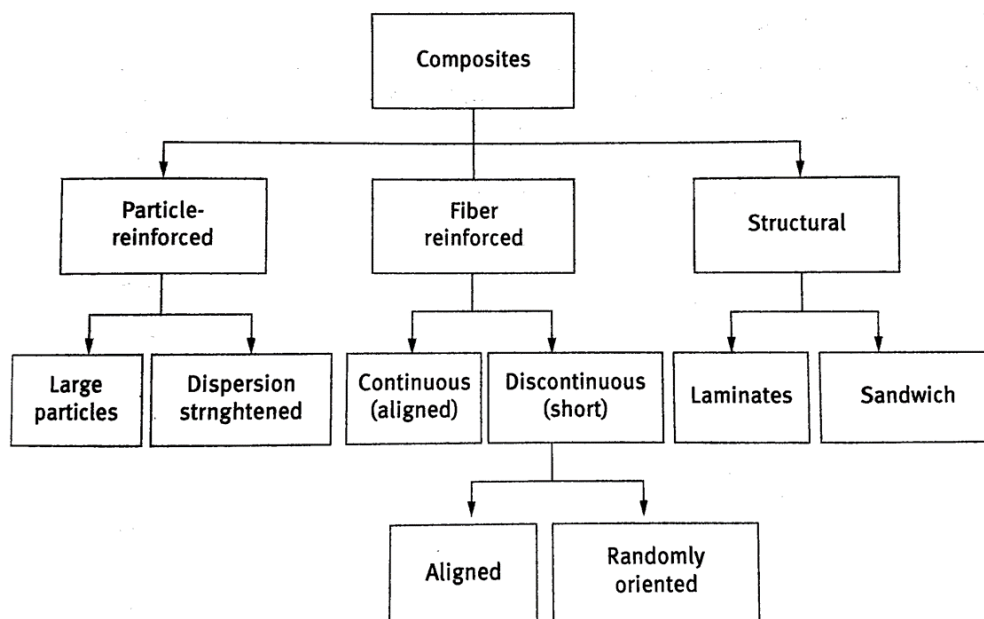


Figure 3.2: Typical composite materials [19]

Two different types of polymer based matrices are available:

1. Thermosets: contain polymers that during the curing process form an irreversible chemical bond. Thermosets are ideal for high temperature applications. The cross linking process that happens during the curing stage means

that the material with a thermoset polymer base cannot be recycled and even reshaped or remolded;

2. Thermoplastics: contain polymers soften when heated, this means that the curing process is completely reversible and no chemical bonding takes place. The previous characteristic allows thermoplastics to be remolded or recycled but usually are more expensive than thermosets. They can melt if heated, this means that they are not ideal for high temperature applications.

Matrix and fiber have very different properties but the combination of them result in a high strength and stiffness with low density material which is the main advantages of composite materials over the existing materials, like metals or plastics. [19] The typical properties of the more commonly used fibers reinforcement are reported in the Tab.3.1.

Material	Density $\rho[kg/m^2]$	Fiber diameter $[\mu m]$	Young's Modulus $E[GPa]$	Tensile strength [GPa] $[GPa]$
Boron	2600	140	410	4.0
Carbon	1800	5.5-7	230-295	3.5-5.6
E-Glass	2500	10	70	1.5-2.0

**Table 3.1:** Properties of the mostly used fibers [19]

### 3.1.1 Unidirectional composites

Unidirectional composites are composed by a glue (matrix), which holds together the fibers that are placed all in the same direction. Each material can be assumed to have three different principal directions, the main one also called longitudinal (where in this case the fibers are aligned) and two secondary ones also known as transverse directions. Differently from an isotropic material (such as metallic materials), a composite material needs more elastic constants to be completely defined:

- Young's modulus in the longitudinal direction
- Young's modulus in the transversal direction
- shear modulus in the lamina plane
- Poisson's coefficient in the lamina plane
- Poisson's coefficient in the transverse plane

which means that also the strength of a composite lamina is characterised by five different values:

- tensile strength in the longitudinal direction
- compressive strength in the longitudinal direction
- tensile strength in the transverse direction
- compressive strength in the transverse direction
- shear strength in the lamina plane

In order to calculate all the properties of the unidirectional layer it is possible to exploit the 'Rule of Mixture' [Eq.3.2], which is a very easy law based on the properties of the two constituents of the layer (matrix and fibers) and their volume proportions. It is important to underline that using this particular law, it is assumed that the constituents are bonded together well and they behave as a single component which can be expressed physically by means of a simple strain compatibility rule [Eq.3.1], which says that the strain of the fiber  $[\varepsilon_f]$  is equal to the one of the matrix  $[\varepsilon_m]$  and so we can define a total strain of the composite component.

$$\varepsilon_c = \varepsilon_f = \varepsilon_m = \varepsilon \quad (3.1)$$

$$\begin{cases} E_L = E_1 = E_f V_f + E_m V_m \\ \nu_{12} = \nu_f V_f + \nu_m V_m \end{cases} \quad (3.2)$$

In the expressions [Eq.3.2] the members are:

- $E_{11}$  is the longitudinal, or major, modulus;
- $E_f E_m$  are the respective longitudinal moduli of the fibers and the matrix;
- $\nu_{12}$  is the major Poisson's coefficient of the composite material;
- $\nu_f \nu_m$  are the respective longitudinal Poisson's coefficients of the fibers and the matrix;
- $V_f V_m$  are the volume proportions of the matrix and fibers respect to the entire component, note that  $V_m + V_f = 1$

The Poisson's ratio ( $\nu_{12}$ ) is obtained starting from its own definition  $\nu_{12} = -\frac{\epsilon_2}{\epsilon_1}$ . The expression of the second constant of the material, the transverse modulus can be obtained by considering the transverse deformability of the composite layer as a summation of the deformabilities of the three parts that together are forming a single layer (matrix-fiber-matrix). Skipping all the mathematical passages it is possible to state the equation of the transverse modulus [Eq.3.3].[20]

$$\frac{1}{E_{22}} = \frac{V_f}{E_f} + \frac{V_m}{E_m} \Rightarrow E_{22} = E_T = \frac{E_f}{V_f + \left(\frac{E_f}{E_m}\right)V_m} \quad (3.3)$$

Considering the longitudinal strains in a lamina submitted to transverse stress it is possible to derive the expression of the Poisson's coefficient in the transverse direction:

$$\frac{\nu_{12}}{E_L} = \frac{\nu_{21}}{E_T} \Rightarrow \nu_{21} = \nu_{12} \frac{E_T}{E_L} \quad (3.4)$$

The last material constant to be define is the shear modulus of the composite, which is the shear modulus of the lamina. It is known that by definition  $\gamma = \frac{\tau}{G}$  and doing some mathematical passages it is possible to obtain [19]:

$$G_{12} = \frac{G_m}{V_f \frac{G_m}{G_f} + V_m} \quad (3.5)$$

### 3.1.2 Load transfer matrix-fiber

Talking about composite material is necessary to understand well one of the most important concept, the transfer of the load between the matrix and the fiber. Firstly is important that fiber and matrix are well bonded to have the correct stress transfer when the composite material is subjected to various loading conditions. If an external traction stress is applied to the material, the load is transferred to the fiber by means of a shear stress across the interface. The fiber is subjected to a tensile stress which increases from zero, at the interface, to a maximum value equal to the breaking stress of the fiber. As the strain increases due to the external load, the fibers break as soon as the ultimate stress of the fibers is reached, in its weakest point. The fiber continue to break anytime the stress is equal to the fiber ultimate stress, when the ultimate stress is reached exactly in the middle of the fiber means that the "critical length" is reached. Following the analysis of Kelly and Tyson is possible to relate this critical length to the shear stress at the interface fiber-matrix. Considering an infinitesimal part of the fiber [Fig.3.3] and analysing its equilibrium is possible to obtain the Eq.3.6.

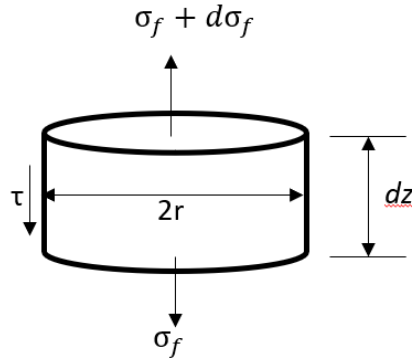


**Figure 3.3:** Infinitesimal fiber scheme

$$\begin{aligned} \pi r^2 \sigma_f + 2\pi r \tau \frac{dz}{r} &= \pi r^2 (\sigma_f + d\sigma_f) \\ \tau_y &= \frac{\sigma_f d}{2L_c} \end{aligned} \quad (3.6)$$

In Eq.3.6  $\tau_y$  is the shear strength at the interface or in other words is the maximum shears stress for that particular critical length  $L_c$ , which is equal to the yield stress and it is assumed to be constant along the interface. [21]

### 3.1.3 Properties of a single lamina

A lamina, also know as ply or layer, has two major dimensions and a third one that is very small compared with the previous two. Therefore the 3D representation can be simplified to a 2D plane stress condition [Eq.3.7].

$$\begin{cases} \sigma_{33} = 0 \\ \tau_{13} = 0 \\ \tau_{23} = 0 \end{cases} \quad (3.7)$$

Therefore the stiffness matrix [Eq.3.8] and the compliance matrix [3.9] for the a single lamina assume the reduced form:

$$[\sigma] = [E] \{\varepsilon\} \quad (3.8)$$

$$\begin{Bmatrix} \sigma_1 \\ \sigma_2 \\ \tau_{12} \end{Bmatrix} = \begin{bmatrix} E_{11} & E_{12} & 0 \\ E_{12} & E_{22} & 0 \\ 0 & 0 & E_{33} \end{bmatrix} \begin{Bmatrix} \varepsilon_1 \\ \varepsilon_2 \\ \gamma_{12} \end{Bmatrix}$$

$$\begin{aligned} \{\varepsilon\} &= [S] \{\sigma\} \\ \begin{pmatrix} \varepsilon_1 \\ \varepsilon_2 \\ \gamma_{12} \end{pmatrix} &= \begin{bmatrix} S_{11} & S_{12} & 0 \\ S_{12} & S_{22} & 0 \\ 0 & 0 & S_{33} \end{bmatrix} \begin{pmatrix} \sigma_1 \\ \sigma_2 \\ \tau_{12} \end{pmatrix} \end{aligned} \quad (3.9)$$

Rarely in literature it is possible to find a third equation for the deformation of the thickness together with the above mentioned ones [Eq.3.10], leaving then the assumption made in Eq.3.7.

$$\varepsilon_{33} = -\frac{\gamma_{13}}{E_1}\sigma_{11} - \frac{\gamma_{23}}{E_2}\sigma_{22} \quad (3.10)$$

Therefore is necessary to define the shear strain as in Eq.3.11.

$$\begin{pmatrix} \gamma_{23} \\ \gamma_{13} \end{pmatrix} = \begin{bmatrix} \frac{1}{G_{23}} & 0 \\ 0 & \frac{1}{G_{13}} \end{bmatrix} \begin{pmatrix} \tau_{23} \\ \tau_{13} \end{pmatrix} \quad (3.11)$$

Finally is possible to express the stresses as function of strains [Eq.3.12]. [19]

$$\begin{pmatrix} \sigma_{11} \\ \sigma_{22} \\ \tau_{12} \end{pmatrix} = \begin{bmatrix} Q_{11} & Q_{12} & Q_{13} \\ Q_{21} & Q_{22} & Q_{23} \\ Q_{31} & Q_{32} & Q_{33} \end{bmatrix} \begin{pmatrix} \varepsilon_{11} \\ \varepsilon_{22} \\ \gamma_{12} \end{pmatrix} = \begin{bmatrix} \frac{E_L}{1-\nu_{LT}\nu_{TL}} & \frac{\nu_{LT}E_T}{1-\nu_{LT}\nu_{TL}} & 0 \\ \frac{\nu_{LT}E_T}{1-\nu_{LT}\nu_{TL}} & \frac{E_T}{1-\nu_{LT}\nu_{TL}} & 0 \\ 0 & 0 & G_{LT} \end{bmatrix} \begin{pmatrix} \varepsilon_{11} \\ \varepsilon_{22} \\ \gamma_{12} \end{pmatrix} \quad (3.12)$$

### 3.1.4 Stresses and strain in casual direction

In a real case usually the load is not oriented along the two the principal directions of the lamina, such as longitudinal and transverse, Which means that in order to analyze a casual stress and strain condition it is necessary to consider a rotated coordinate system. In Fig. 3.4 is possible to see the two coordinate systems and the angle  $\theta$  which relates them through the rotation matrix 3.13.

$$[T] = \begin{bmatrix} \cos^2\theta & \sin^2\theta & 2\cos\theta\sin\theta \\ \sin^2\theta & \cos^2\theta & -2\cos\theta\sin\theta \\ -\cos\theta\sin\theta & \cos\theta\sin\theta & \cos^2\theta - \sin^2\theta \end{bmatrix} \quad (3.13)$$

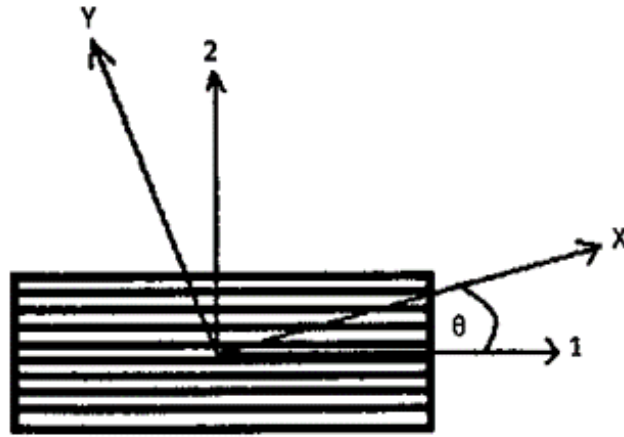


Figure 3.4: Coordinate systems: T,L orthotropic axis; X,Y arbitrary axis[19]

Knowing the rotation matrix is possible to transform the stresses and strains from the arbitrary directions to the orthotropic coordinate system:

$$\begin{aligned} \begin{Bmatrix} \sigma_T \\ \sigma_L \\ \tau_{TL} \end{Bmatrix} &= [T] \begin{Bmatrix} \sigma_x \\ \sigma_y \\ \tau_{xy} \end{Bmatrix} \\ \begin{Bmatrix} \varepsilon_T \\ \varepsilon_L \\ \frac{\gamma_{TL}}{2} \end{Bmatrix} &= [T] \begin{Bmatrix} \varepsilon_x \\ \varepsilon_y \\ \frac{\gamma_{xy}}{2} \end{Bmatrix} \end{aligned} \quad (3.14)$$

Is possible now to derive the expression of the transformation of the stresses and strain from the lamina axis to the laminate axis [Eq.3.15]:

$$\begin{Bmatrix} \sigma_T \\ \sigma_L \\ \tau_{TL} \end{Bmatrix}^k = [T]^{-1} [Q]^k [T] \begin{Bmatrix} \varepsilon_x \\ \varepsilon_y \\ \gamma_{xy} \end{Bmatrix}^k = \begin{bmatrix} \overline{Q}_{11} & \overline{Q}_{12} & \overline{Q}_{16} \\ \overline{Q}_{12} & \overline{Q}_{22} & \overline{Q}_{26} \\ \overline{Q}_{16} & \overline{Q}_{26} & \overline{Q}_{66} \end{bmatrix}^k \begin{Bmatrix} \varepsilon_x \\ \varepsilon_y \\ \gamma_{xy} \end{Bmatrix}^k = [\overline{Q}]^k \begin{Bmatrix} \varepsilon_x \\ \varepsilon_y \\ \gamma_{xy} \end{Bmatrix}^k \quad (3.15)$$

The "k" exponent indicates the number of the ply which is considered.

### 3.1.5 Classical lamination theory for laminates

When a structure have to be studied, is necessary to investigate the laminate behaviour and not the single layer response. Using the 'Classical Lamination Theory', which is based on Kirchhoff-Love plate theory, is possible to analyse the mechanical behaviour of a laminate. Being this theory based of Kirchhoff-Love plate theory the

assumptions of the latter have to be considered:

- Thickness of the plate does not change during the deformation
- The cross section of a laminate is planar before deformation and remains planar after it

Looking at the Fig.3.5 and considering  $w$  as the displacement in the  $z$ -direction, is possible to express the following relations [Eq.3.16]:

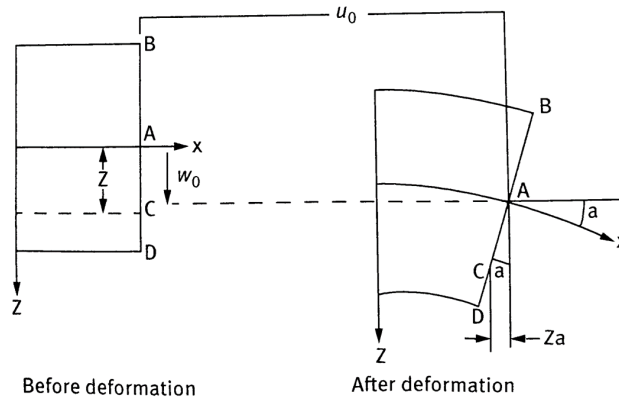


**Figure 3.5:** Plate cross section before and after the deformation [19]

$$\begin{cases} u = u_0 - z \frac{\partial w}{\partial x} \\ v = v_0 - z \frac{\partial w}{\partial y} \end{cases} \quad (3.16)$$

Is possible to define also the strains ( $\varepsilon_x \varepsilon_y \gamma_{xy}$ ) and the curvatures ( $k_x k_y k_{xy}$ ):

$$\begin{Bmatrix} \varepsilon_x \\ \varepsilon_y \\ \gamma_{xy} \end{Bmatrix} \equiv \begin{Bmatrix} \frac{\partial u}{\partial x} \\ \frac{\partial v}{\partial y} \\ \frac{\partial u}{\partial y} + \frac{\partial v}{\partial x} \end{Bmatrix} = \begin{Bmatrix} \frac{\partial u_0}{\partial x} \\ \frac{\partial v_0}{\partial y} \\ \frac{\partial u_0}{\partial y} + \frac{\partial v_0}{\partial x} \end{Bmatrix} - z \begin{Bmatrix} \frac{\partial^2 w_0}{\partial x^2} \\ \frac{\partial^2 w_0}{\partial y^2} \\ \frac{2\partial^2 w_0}{\partial x \partial y} \end{Bmatrix} = \begin{Bmatrix} \varepsilon_x^0 \\ \varepsilon_y^0 \\ \gamma_{xy}^0 \end{Bmatrix} + z \begin{Bmatrix} k_x \\ k_y \\ k_{xy} \end{Bmatrix} \quad (3.17)$$

Recalling Eq.3.15 the stresses at the lamina level will be:

$$\{\sigma\}^k = [Q]^k \{\varepsilon^0\} + z[\bar{Q}]^k \{k\} \quad (3.18)$$

Now is possible to pass from stresses to the resultants of force ( $N_x N_y N_{xy}$ ) and moment ( $M_x M_y M_{xy}$ ) considering  $h$  as the thickness of the laminate:

$$\begin{aligned} N_x &\equiv \int_{-h/2}^{h/2} \sigma_x dz & N_y &\equiv \int_{-h/2}^{h/2} \sigma_y dz & N_{xy} &\equiv \int_{-h/2}^{h/2} \tau_{xy} dz \\ M_x &\equiv \int_{-h/2}^{h/2} \sigma_x z dz & M_y &\equiv \int_{-h/2}^{h/2} \sigma_y z dz & M_{xy} &\equiv \int_{-h/2}^{h/2} \tau_{xy} z dz \end{aligned} \quad (3.19)$$

Substituting the stresses exploiting Eq.3.18 is possible to obtain the following relations, which relate the resultants of force and moment to the strain in the mid-plane ( $\{\varepsilon^0\}$ ) and the curvature ( $k$ ) [Eq.3.20]:

$$\begin{aligned} \begin{Bmatrix} \{N\} \\ \{M\} \end{Bmatrix} &= \begin{bmatrix} [A] & [B] \\ [B] & [D] \end{bmatrix} \begin{Bmatrix} \{\varepsilon^0\} \\ \{k\} \end{Bmatrix} \\ \begin{Bmatrix} \begin{Bmatrix} N_x \\ N_y \\ N_{xy} \end{Bmatrix} \\ \begin{Bmatrix} M_x \\ M_y \\ M_{xy} \end{Bmatrix} \end{Bmatrix} &= \begin{bmatrix} \begin{bmatrix} A_{11} & A_{12} & A_{16} \\ A_{12} & A_{22} & A_{26} \\ A_{16} & A_{26} & A_{66} \end{bmatrix} & \begin{bmatrix} B_{11} & B_{12} & B_{16} \\ B_{12} & B_{22} & B_{26} \\ B_{16} & B_{26} & B_{66} \end{bmatrix} \\ \begin{bmatrix} B_{11} & B_{12} & B_{16} \\ B_{12} & B_{22} & B_{26} \\ B_{16} & B_{26} & B_{66} \end{bmatrix} & \begin{bmatrix} D_{11} & D_{12} & D_{16} \\ D_{12} & D_{22} & D_{26} \\ D_{16} & D_{26} & D_{66} \end{bmatrix} \end{bmatrix} \begin{Bmatrix} \begin{Bmatrix} \varepsilon_x^0 \\ \varepsilon_y^0 \\ \gamma_{xy}^0 \end{Bmatrix} \\ \begin{Bmatrix} k_x \\ k_y \\ k_{xy} \end{Bmatrix} \end{Bmatrix} \end{aligned} \quad (3.20)$$

where all the constants inside the matrix A B and D are:

$$\begin{aligned} A_{ij} &\equiv \int_{-h/2}^{h/2} \bar{Q}_{ij}^k dz = \sum_{k=1}^n \bar{Q}_{ij}^k (h_k - h_{k-1}) \\ B_{ij} &\equiv \int_{-h/2}^{h/2} \bar{Q}_{ij}^k z dz = \frac{1}{2} \sum_{k=1}^n \bar{Q}_{ij}^k (h_k^2 - h_{k-1}^2) \\ D_{ij} &\equiv \int_{-h/2}^{h/2} \bar{Q}_{ij}^k z^2 dz = \frac{1}{3} \sum_{k=1}^n \bar{Q}_{ij}^k (h_k^3 - h_{k-1}^3) \end{aligned} \quad (3.21)$$

where the couples ( $i,j$ ) are (1,1) (1,2) (2,2) (1,6) (2,6) (6,6).[19]

In conclusion is possible to obtain, with some passages, the expression of elongations and curvatures, that are reported in [Eq.3.22] and is possible to notice how the elongations and curvatures both depend either on forces and moments.

$$\begin{aligned} \begin{Bmatrix} k_x \\ k_y \\ k_{xy} \end{Bmatrix} &= [F] \begin{Bmatrix} N_x \\ N_y \\ T_{xy} \end{Bmatrix} + [G] \begin{Bmatrix} M_x \\ M_y \\ M_{xy} \end{Bmatrix} \\ \begin{Bmatrix} \varepsilon_x^0 \\ \varepsilon_y^0 \\ \gamma_{xy}^0 \end{Bmatrix} &= [H] \begin{Bmatrix} N_x \\ N_y \\ T_{xy} \end{Bmatrix} + [L] \begin{Bmatrix} M_x \\ M_y \\ M_{xy} \end{Bmatrix} \end{aligned} \quad (3.22)$$

Where the matrix in Eq.3.22 are defined:

$$\begin{cases} [F] = \{[I] - [D]^{-1}[B][A]^{-1}[B]\}^{-1}\{-[D]^{-1}[B][A]^{-1}\} \\ [G] = \{[I] - [D]^{-1}[B][A]^{-1}[B]\}^{-1}[D]^{-1} \\ [H] = [A]^{-1}[I] + [B][F] \\ [L] = -[A]^{-1}[B][G] \end{cases} \quad (3.23)$$

## 3.2 Pre-preg composite

Most of the high performance structures begin their life as a layers of Pre-Preg, which are carbon fiber beds pre-impregnated with a catalyzed but uncured resin. Commonly layers are stacked into a mold to form a laminate (lamination process), enclosed in a vacuum bag and placed inside an autoclave, which is a pressurized oven. Pressure and temperature mixed together cure the laminate. The applied pressure help to decrease as much as possible the defect of porosity, which is a big issue for composite parts made from Pre-preg layers. Autoclave processing is a very well working process but has big drawbacks, such as big costs and the inflexibility of the manufacturing process. [22]

## 3.3 Out-of-Autoclave Pre-preg

As the demand for composite material parts grows the need for cheaper and faster manufacturing process comes into conflict with the very expensive autoclave manufacturing process. A new generation of pre-preg (VBO Pre-preg<sup>7</sup>) layers has been studied and introduced. 'VBO' pre-pregs are able to cure and generate very good quality final parts without using the autoclave but using just a vacuum bag and an oven. [22]

### 3.3.1 Layer's properties

Early generation 'VBO' were deigned to cure at low temperature ( $\simeq 60^{\circ}\text{C}$ ) and then a high temperature post cure process was performed, this lead to advantages in terms of costs but three big drawbacks were presented:

1. High porosity in the final part due to the low pressure applied during the curing process;
2. Very short storage time at room temperature;
3. Low mechanical performance, in particular low toughness.

---

<sup>7</sup>VBO stands for vacuum bag only pre-preg material

The first and the last point are strictly correlated and the key to obtain a low porosity VBO-parts is to remove all the trapped air during lay-up. To solve this problem the VBO layers are 'breathable', made of partially impregnated micro structures composed by both dry and resin rich areas. Dry areas are intended to be 'engineered vacuum channels' which allow the migration of air towards the boundaries. Once the air is out of the layer must be sucked outside of the vacuum bag system, and this is made possible by the use of a breather film which makes the air flow continuous towards the sucking point of the vacuum pump. A scheme of the set-up for the laminate to be cured is presented in Fig.3.6. A very important parameter during

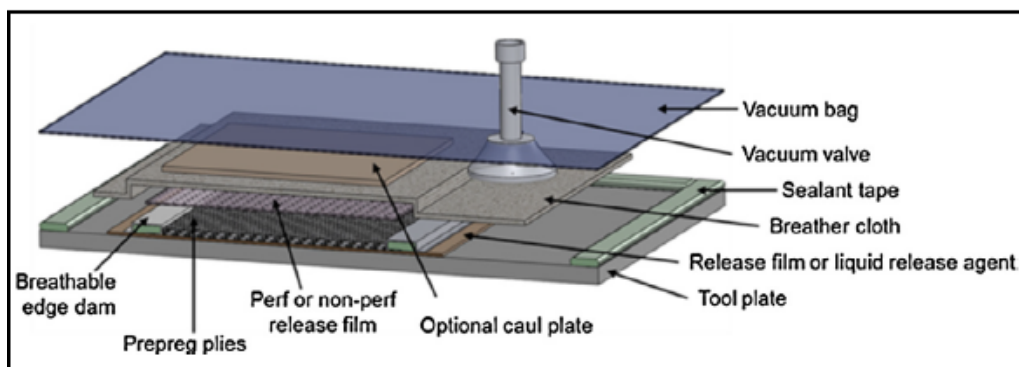


**Figure 3.6:** Layup scheme of a laminate inside the vacuum bag ready to be cured [22]

the design process of a layer of Prepreg is the 'degree of impregnation' (DI), in fact it is reported in [22] that a fully impregnated prepreg layer led to a laminate void content exceeding the 5%, instead in the partially impregnated layer of prepreg the final laminate result in a nearly void-free component. The last concept can be explained by the fact that a completely wet layer does not allow the correct escape of the air while, designing dry channels, the air is able to escape from the laminate much more easily. [22]

### 3.3.2 Resin properties

The resin that wets the pre-preg layers has to be viscous enough to let the air escape from the material during the lamination process while, during the curing process must possess a low viscosity so that all the fibers can be wetted. The resin must have a precise kinetics behaviour, such as [Fig.3.7]:

- the resin at room temperature needs high viscosity in order to maintain the air flow channels for the air to get out from the laminate

- during the first step of the curing process the temperature increase causes the viscosity of the resin to decrease initially, so that it can wet all the fibers of the laminate
- when the temperature gets to medium-high temperature of curing (from 90°C to 130°C), the resin start the polymerization until achieving the vitrification in the post curing process at high temperature ( $\simeq 170^\circ\text{C}$ )

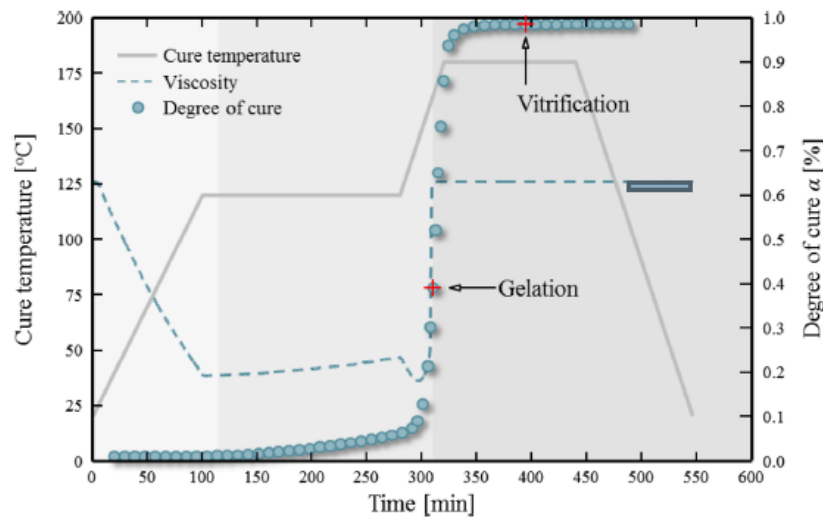


**Figure 3.7:** Change in properties of the epoxy resin during a typical cure cycle [23]

Can be also seen from Fig.3.7 that in order to achieve a complete degree of cure a post curing process at high temperature is necessary.

### 3.3.3 Fiber properties

Selection of the right fibers is a very important to obtain a final component able to carry out what is designed for. It is important to underline that the fiber volume fraction ratio that is reachable using an out of autoclave prepreg is not comparable to the one achievable with the use of autoclave during the curing process. There is no surprise that two identical material, which are cured differently, the first in the autoclave and the second without using it, the first one will result in a thinner component due to the pressure which helps a lot reducing the thickness of the final part. However, using a 'VBO' prepreg a fiber volume fraction of 60% is reachable without any problem. [22]

### 3.3.4 Common possible defects

This kind of technology could be used also to manufacture big and complex geometries but being very careful to not generate any kind of big defects. Laminating big objects full of difficult curvatures is a huge challenge respect to the lamination of flat laminate and this could lead to different defects that cannot occur in a flat laminate [Fig.3.8]:[22]

- Delamination between two layers
- Macro voids probably induced by not a sufficient vacuum pressure, and also trapped air between the layers
- Corner thickening in particular the external layers do not follow well the mould and there is not a proper continuous curvature in the final part
- Corner thinning occurs when the layers in the internal curvature have a more sharp edge respect to what they should have

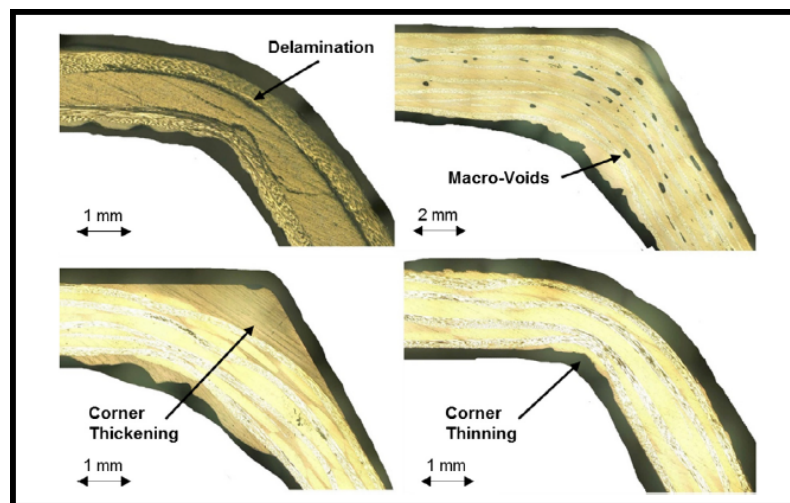


**Figure 3.8:** Possible defects in the proximity of a corner[22]

## 4. Experimental part

In this chapter will be treated the experimental part, in other words the preparation of the specimens from the design of the mold until the application of the adhesive to create the bonded joint. In the end of the chapter the experimental arcan test will be explained and the obtained results shown.

### 4.1 Prepregs material

"Prepregs" are sheets of composite material such as carbon fibers or glass fibers which had already the activated resin matrix impregnated into the reinforcement [Fig.4.1]. During all the process the resin is theoretically curing from the point of manufacture. Fortunately, the reactivity is very very low which means that it cures incredibly slowly at ambient temperature. Knowing that is easy to understand that the sheets of prepreg can be easily stored and handled for a certain amount of time, which is known with the name of prepreg's outlife. By storing the pre-impregnated material in a freezer at a very low temperature, the life of the uncured prepreg will extend to many months or even years, this period of time is defined as prepreg's freezer life.[24].



**Figure 4.1:** Sheets of Prepregs XC110 Twill Prepreg Carbon fiber

## 4.2 Mould design

In order to create a proper mold for the creation of the substrates, the design started from the technical drawing of a previous arcan specimen, already used in the past, which was made by steel [Fig.4.2]. The best configuration, in order to create void

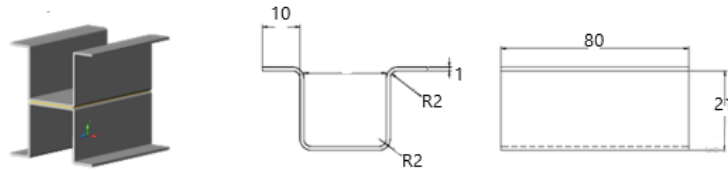


**Figure 4.2:** Drawing of Arcan specimen used in the past

during the curing process, was studied and the mould's shape was decided. As it possible to notice the mould was designed to create 10 substrate per time [Fig.4.3]. Moreover another important design parameter was necessary to take into account,

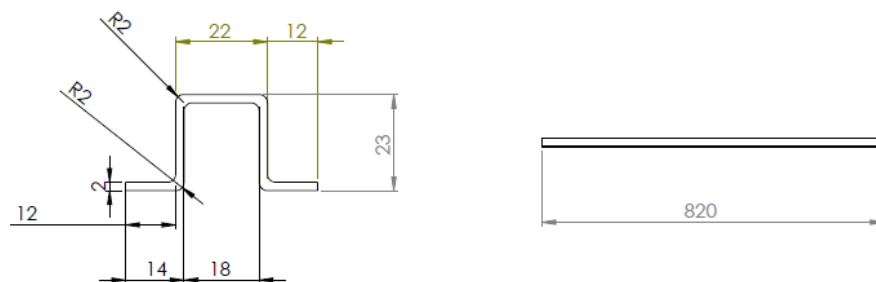


**Figure 4.3:** Drawing of the mould for the substrate production

the mould material. It is important to underline that not all materials are suitable for this purpose indeed there is a list of compatibility of some possible mould materials with the prepreg carbon fiber material:[24]

- Prepreg carbon fiber - Fully compatible
- High temperature epoxy - Fully compatible
- Toughened glass - Fully compatible (for flat sheets/panels)
- Aluminum - Fully compatible
- Stainless steel - Fully compatible

- Vinylester - Semi-compatible, can affect surface finish and need to take into account the maximum cure temperature of the prepreg
- Polyurethane tooling board - Not compatible because at elevated temperature this material inhibits the cure of epoxies.

Aluminum was chosen and as manufacturing process the folding procedure was adopted because it is a lot cheaper than cutting process, where so much material would be discarded and wasted.

## 4.3 U-shape substrate production

It is important to underline that in order to create a suitable specimen which can undergo the Arcan test it is necessary to join together two different substrates, in this section will be analyzed the production of the single substrate.

### 4.3.1 Mould preparation

For necessity and also for convenience, the mold has been cut in half, in fact the glass plate where the aluminum mold will be placed is not big enough moreover smaller prepreg sheets will be used making the manufacturing process easier. It is very important to clean properly the glass so that any dust or other particulates do not interfere with the correct production of the substrate. The last two useful steps before starting the lamination of the carbon fiber sheets are fixing the two moulds in the glass plate with sealant tape, and also waxing them. Before starting to place the pre-preg into the mould is recommended to first apply a release agent in accordance with its instructions. In this case TR-104 HIGH TEMP RELEASE MOLD was used and it was let rest for at least 10 minutes [Fig.4.4].

### 4.3.2 Pre-preg preparation

When the easy release wax is dry it is convenient to start preparing the material needed for the lamination, in particular it is necessary to cut the sheets of prepreg into smaller pieces. In the uncured state those sheets of material are very easy to cut so it is possible to do it with a simple sharp knife. In this particular case each

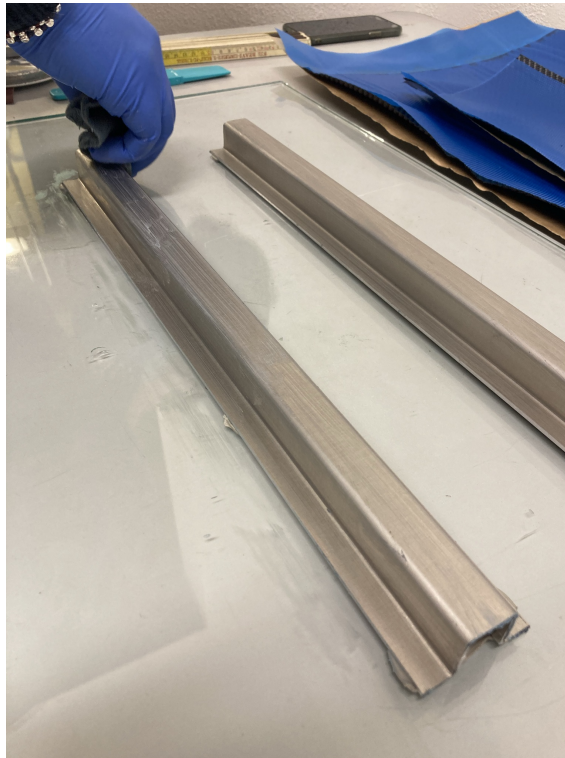


**Figure 4.4:** Application of the release agent

layer is composed of just one rectangular piece of 100 mm by 420 mm. It was not cut precisely because later during the lamination the material in excess will be cut out. [24]

### 4.3.3 Lamination of prepreg

The sheets of prepreg are very easy to handle but great care must be taken in order to ensure that the material is lay down in the mould in the proper way. Manufacturers generally suggest to lay it down from the centre lowest point and systematically continue in the other directions, in this way would be theoretically easy to avoid any type of defects, like 'bridging'[Fig.4.5] [24]. During the procedures of lamination would be useful to use some laminating tools called 'dibbers' [Fig.4.6], which can be made by hand, bought ready made or they could be edges of other tools. Again is very important in each stage of lamination to ensure there are no bridges or voids both between the mould and the first sheet of material and also between two stacked up adjacent layers. In some spot such as corners, could be very useful to make some little cut in the sheet so that following the curvature of the mould would be easier [24]. In this particular project the final substrate will be made of [Fig.4.7] 2 or 4 stacked up layers and care has been taken that the fibers of each layer were parallel

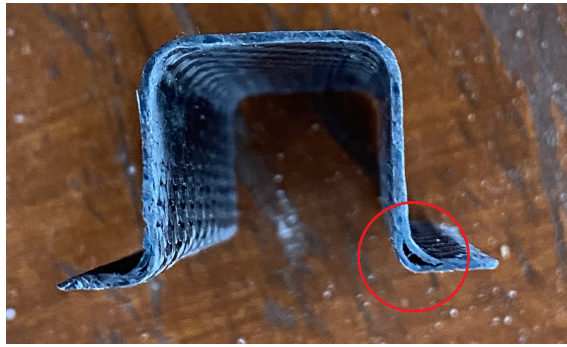


**Figure 4.5:** Bridging defect

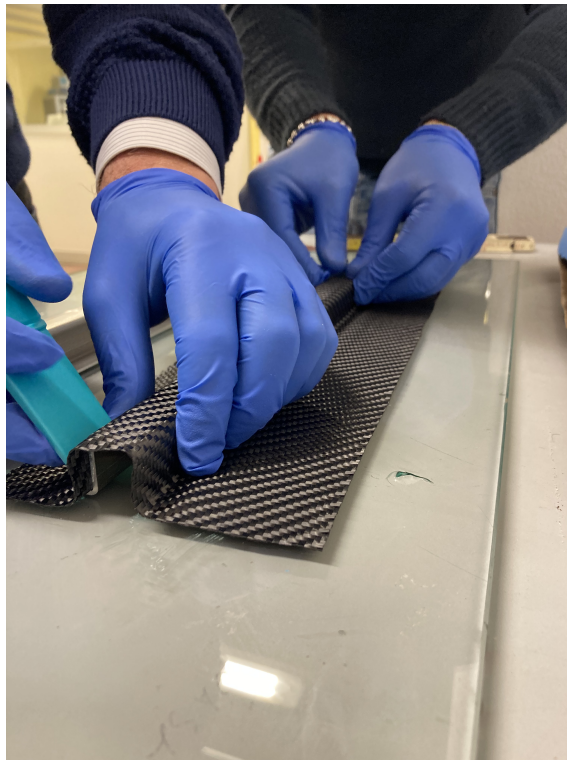


**Figure 4.6:** Usage of dibbers

to the mould long axis. Before moving on to the next step the material in excess was cut out and removed, using together a cutter and dibbers tool in order to cut the excess material while the sheets of pre-preg are force to stay in place [Fig. 4.8].

#### 4.3.4 Vacuum bagging

When the pre-preg is fully laid up, it is possible to vacuum bag the part ready for curing. Before create void is important to prepare correctly the part. The first thing to apply is a non-perforated release film [Fig.4.9], in this case a layer of peel ply was used, it is very important that also this layer is carefully pressed onto the mould

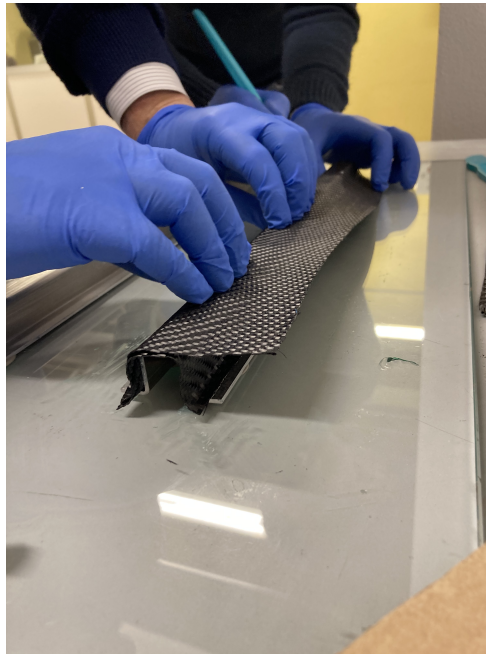


**Figure 4.7:** Second layer lamination

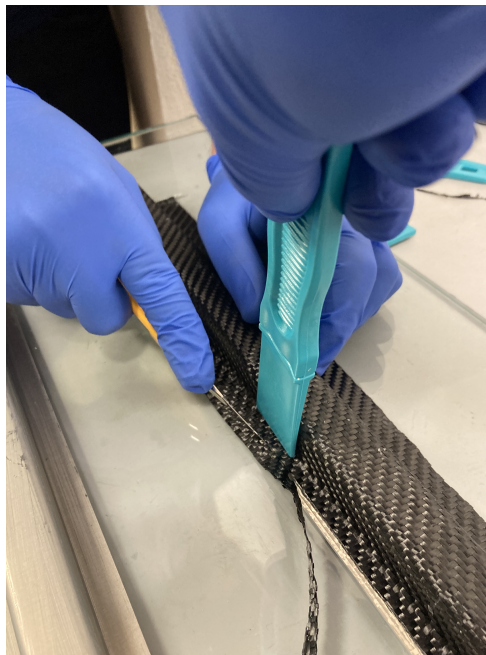


**Figure 4.8:** Cutting excess material

without creating any bridges. During this process in order to help hold the peel ply down in the mold, some flash release tape was used. Peel ply is also very useful when the composite part will be attached with some adhesive, indeed the peel ply create a rough surface which is ideal for adhesive application. As a second step is important to place a breather film [Fig.4.10] in order to ensure a continuous air path. This sheet of soft material is not always used, but in this case, since the shape of the part is not really complex, it was used all over the surface with a double layer in the spot



**Figure 4.9:** Peel ply adjusting

where the air connector is placed, in other words where the air is sucked out. At



**Figure 4.10:** Breather adjusting

the beginning it was decided to have a single big vacuum bag [Fig.4.11A] to create void simultaneously in both the two moulds but to achieve a better result it was decided to use two different bags [Fig.4.11B] and obviously the previous procedure was followed for each mould. The last step before placing the bag is lay down the

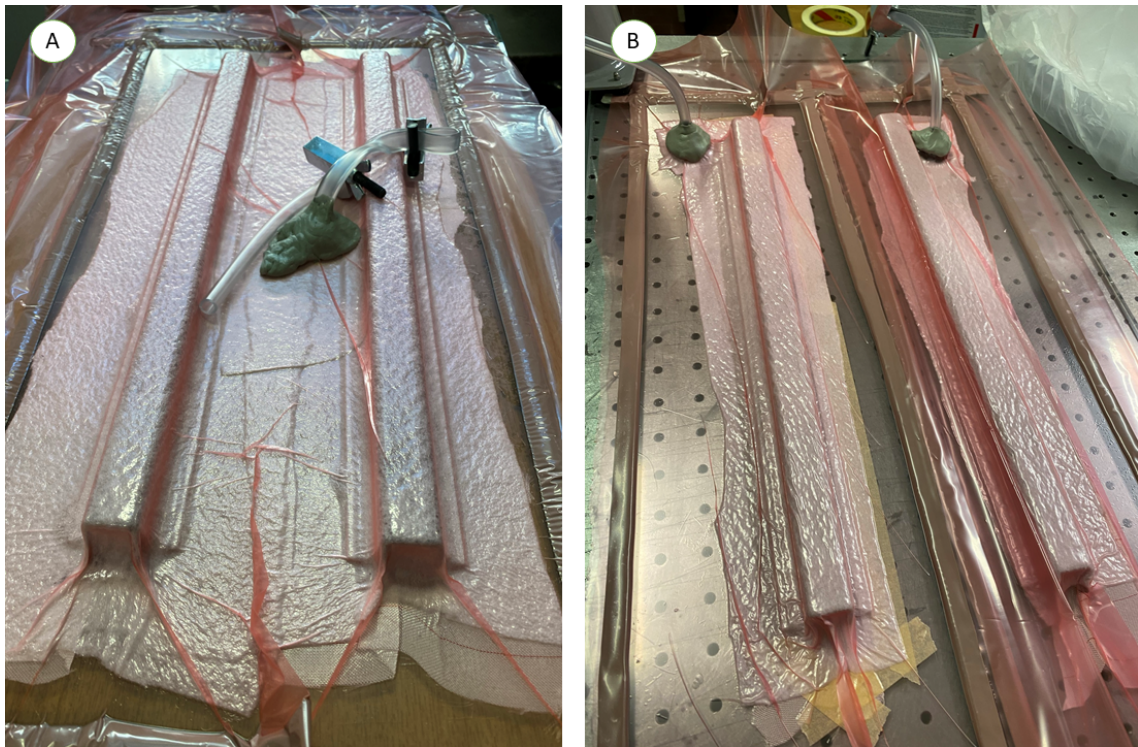


**Figure 4.11:** Single - double bag comparison

sealant tape which is necessary to let the bag seal the two parts inside moreover, it was decided to create a fold in the middle of the bag to let the manipulation of it during the void creation easier. The bag must be place carefully and without creating any fold over the sealant tape, otherwise the air could escape from it and the creation of the void would be impossible. The vacuum is created in two steps by using a vacuum pump. In the first one the void is only created partially so that the position of the bagging film is easier. This stage is helpful to get the film into all the corners and details. Once a good position of the bag is achieved it is possible to pull the full vacuum. Once the full vacuum is pulled, is good manner to carry out a leak test for at least ten minutes, in other words is important to verify that after at least ten minutes the void is unchanged and no air enters in the bag, this is easily checked by using a manometer between the bag and the vacuum pump.

#### 4.3.5 Curing process

Once the leaking test is successfully terminated it is possible to place the part under vacuum inside the oven (OV 301 curing oven was used) in order to let the resin fully cure. When everything is placed carefully inside the oven [Fig.4.12] and the door is properly shut it is possible to set the curing cycle of the prepreg material

[Fig4.13].[24]



Figure 4.12: Part ready to be cured



Figure 4.13: Curing cycle of XC110 Twill Prepreg Carbon fiber

Standard Cure Cycle					
Step	Start Temp	Ramp Rate	Duration	End Temp	Elapsed Time
1	~20°C	1°C/min	00:50	70°C	00:50
2	70°C	Soak	04:00	70°C	04:50
3	70°C	2°C/min	00:25	120°C	5:15
4	120°C	Soak	01:00	120°C	6:15
5	120°C	Natural Cool	—	~20°C	7:15

**Table 4.1:** Curing cycle of XC110 Twill Prepreg Carbon fiber

### 4.3.6 Demould the finished part

When the curing process is over it is possible to demould the finished part, after allowing the part to fully cool down to room temperature. If for some reason the part is trying to be demoulded before is cooled down it is possible that the shock temperature would cause some deformations and possible surface defects. Once the part is cool, it is possible to remove it from the oven and wrap off the bag, the breather and the peel ply [Fig.4.14]. Now is possible, using demoulding wedges or other pointed items, such as a pocket knife, to demould the finished part being careful to avoid scratching the mould, [Fig.4.14].

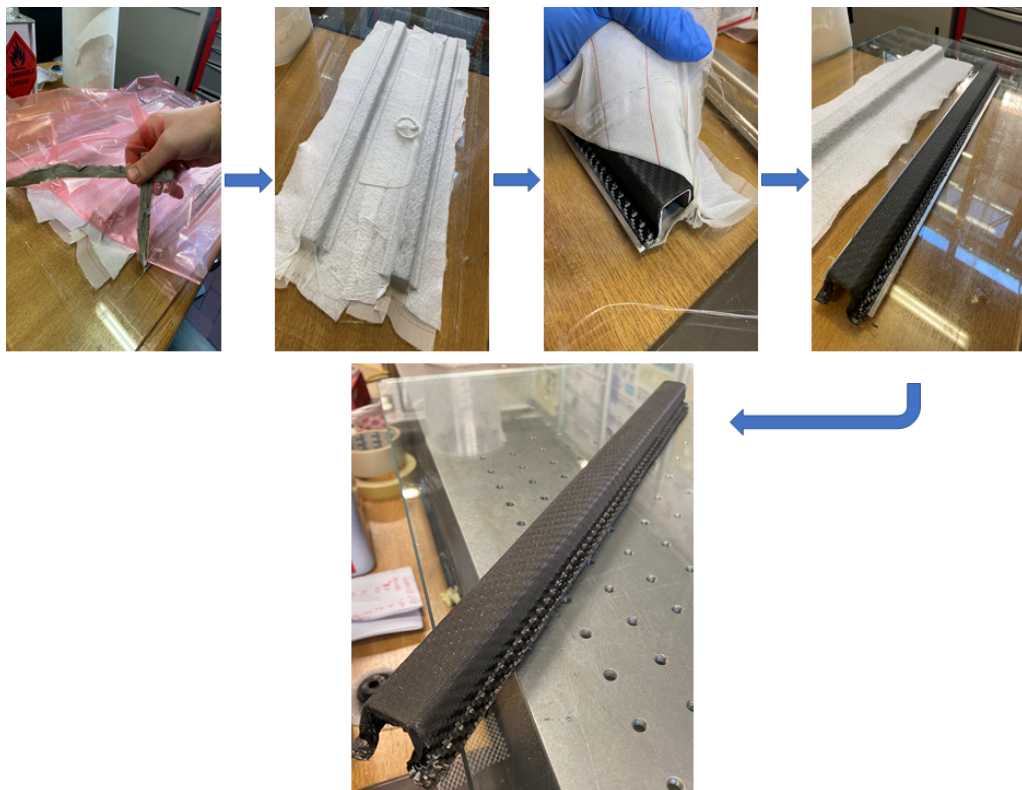


**Figure 4.14:** Demoulding process

### 4.3.7 Controlling and finishing the demoulded part

The last step in order to obtain a ready to be used carbon fiber substrate is to cut the part in 80 mm long substrates and also drill the holes that will be necessary to mount it in the traction machine to perform the arcan test. In order to cut the long part in smaller substrates a classic fine-toothed metal saw was used [Fig.4.15].

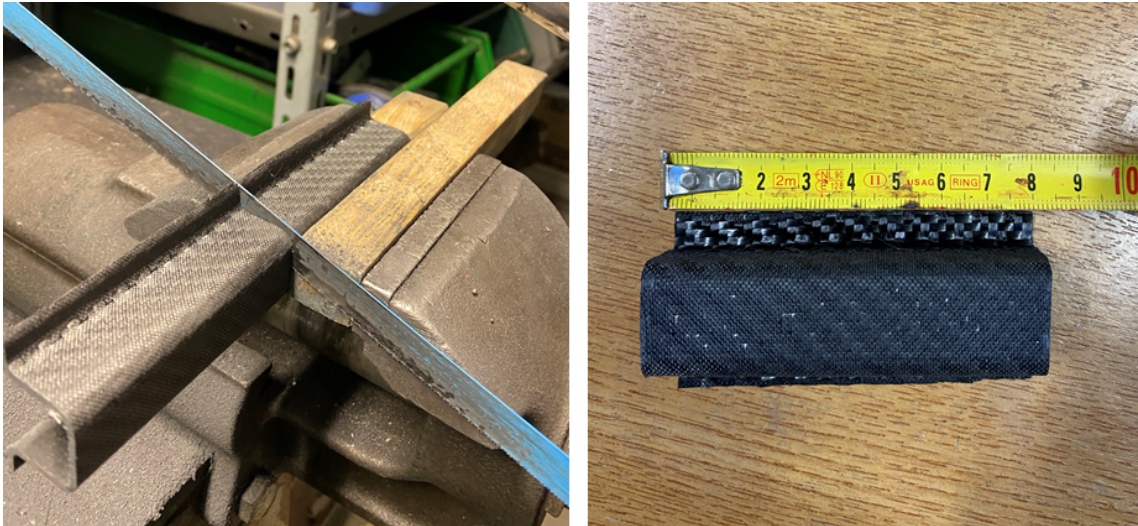


**Figure 4.15:** Cutting process

For what it concerns the holes to be drilled in the substrates, they were drilled by using a drill press with a drill of 10.2 mm. In order to stress the substrate the least possible, the latter was clamped in the clamping system of the drill by using also two blocks of wood and a block of teflon. The wood block inside the substrate has rounded edges otherwise during clamping the sharp edges tend to widen the substrate from the inside [Fig.4.16].

## 4.4 Double U-shaped specimen production

In order to perform the arcan test, two substrates must be joined together, by using the two adhesives already described in 2.6. In the following sections the preparation of the substrates and the following bonding will be described.

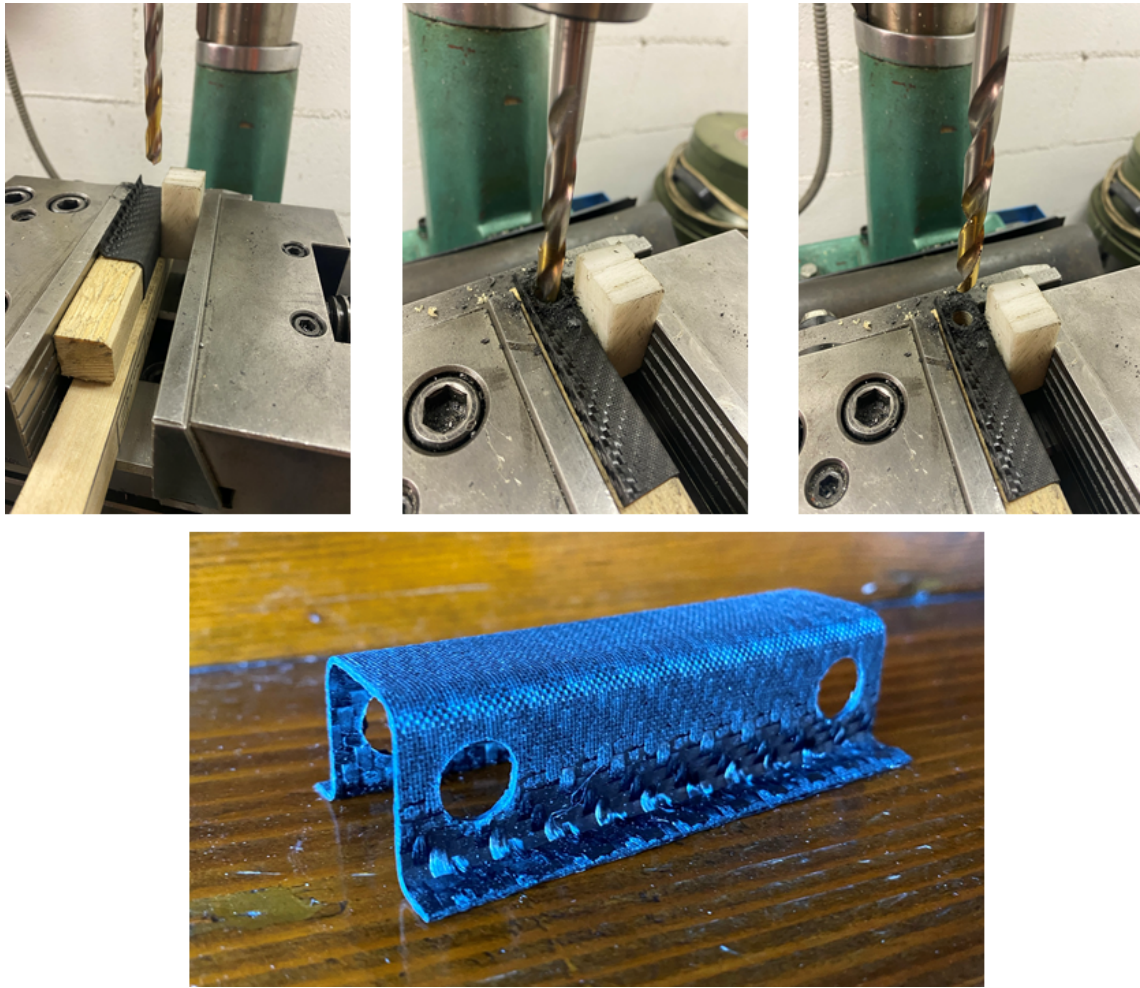
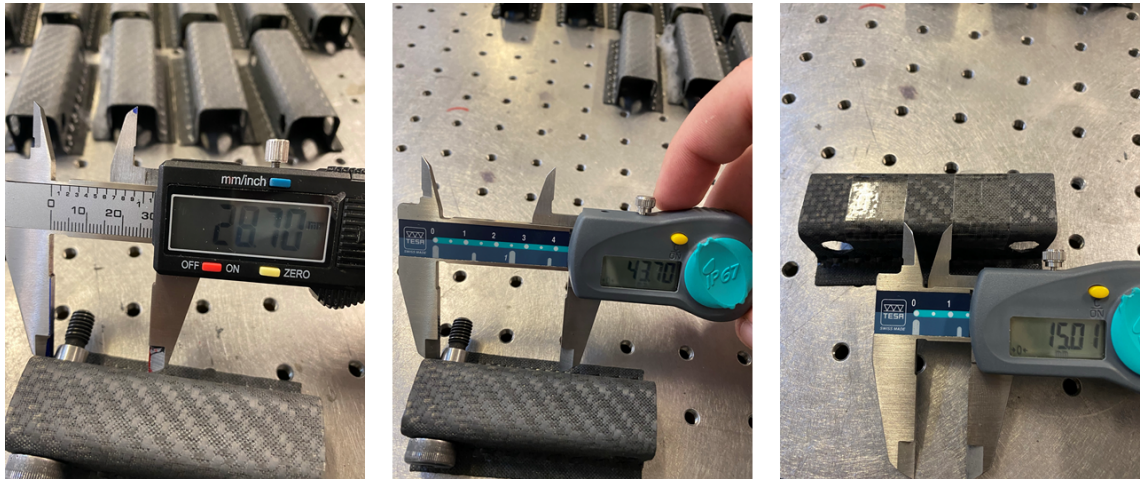


Figure 4.16: Drilling process and final substrate

#### 4.4.1 Substrates preparation

In order to have a good adhesion between the adhesive and the substrate, the latter have to be prepared. After the substrates have been cut and holes have been drilled, dust and contaminants settled on the top surfaces, jeopardizing proper adhesion. Therefore the surfaces interested in the bonding process have been treated with medium-fine sandpaper (P150) and then cleaned with pure acetone. As second step is important to delimit the bonding region, which in this case is placed in the middle and extend for 15 mm throughout the whole width of the top surface of the substrate. In order to do so transparent tape have been used. As reference the drilled hole are considered because the length of the substrates is not exactly equal for all of them, due to the manual cutting procedure adopted [Fig.4.17]. Moreover before apply the adhesives, the thickness of it have to be chosen. The thickness of the polyurethane chosen is 1.5 mm so in half of the substrates in which this adhesive will be applied shims must be placed [Fig.4.18]. Instead for what it concerns the epoxy adhesive,



**Figure 4.17:** Measuring sequences to delimit the bonding zone with the transparent tape

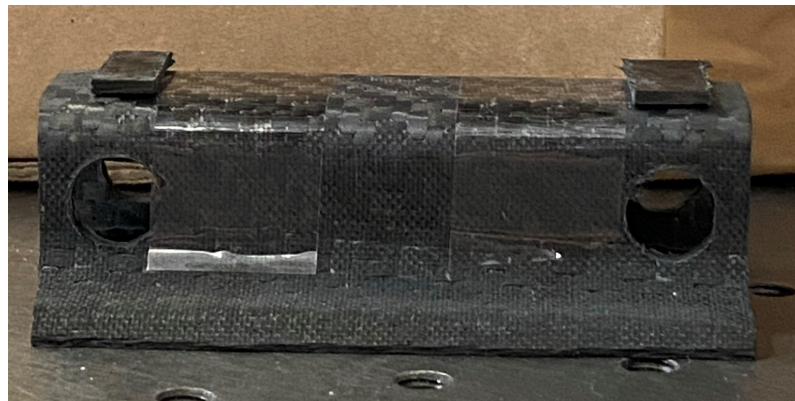


**Figure 4.18:** Shims placed on the top surfaces of half of the substrates that will be bonded with the polyurethane adhesive

shims are not necessary because the glass spheres inside the adhesive guarantee a thickness of 0.2mm.

#### 4.4.2 Bonding procedure

The bonding procedure of the two adhesives is slightly different. For what it concerns the Polyurethane adhesive, it was applied by a pneumatic double cartridge gun dispenser, with a static mixer mounted in the end, which guarantees a mixing ration of 1:1 between the component A and B. The adhesive was applied on the substrates with the shims fixed on the top, subsequently the substrate without the shims was placed on the top and pushed toward the other one causing the adhesive to spread well and let the excessive adhesive to get out of the bonding region. Once the two substrates are in the final position the adhesive in excess, which has come out from the edges, was removed by means of a cotton swab. Finally the specimens

bonded were left curing with weight on top of them to let it cure properly at room temperature for an entire night. To have strong adhesion also a post cure in the oven for 8 hours at 80°C was processed. Regarding the bonding procedure of the second adhesive, is important that before applying it, is necessary to warm the adhesive up to 60°C in order to have the correct viscosity to obtain an effective application. The adhesive was applied by means of a manual single cartridge gun dispenser. Once the adhesive is in place and the excessive adhesive cleaned out, the bonded specimens have been mounted on equipment that keeps them in the correct position during the curing process in the oven. The duration of the process depends on the value of temperature adopted, higher the temperature, lower the time, in this case a 45 minutes cure at 160°C was performed.

## 4.5 Arcan test

In this section the tests performed will be explained and the results discussed. Two different adhesives have been tested:

1. Polyurethane adhesive
2. Epoxy adhesive

Each adhesive bonds two equal carbon fiber substrates by exploiting a bonding area of 15mm by 17mm. The thickness of the two adhesive is not equal but for the first one (polyurethane), as already said, a thickness of 1.5 mm by using shims is imposed, instead for the epoxy the thickness of 0.2mm is guaranteed due to the glass spheres of that diameter present inside the adhesive. The second adhesive have been tested in 3 different configurations instead for the high repeatability of data of the test regarding the polyurethane, 5 configurations have been tested. Each configuration is characterized by a different loading angle ( $\alpha$ ), which is the inclination between the center of symmetry of the specimen, where the fracture is expected, and the direction of the applied load. The load conditions chosen are the following: 4.19

- Pure shear,  $\alpha = 0^\circ$
- Combination of loads,  $\alpha = 30^\circ$   $\alpha = 45^\circ$   $\alpha = 60^\circ$  (30° and 60° just for the polyurethane)
- Pure tensile,  $\alpha = 90^\circ$

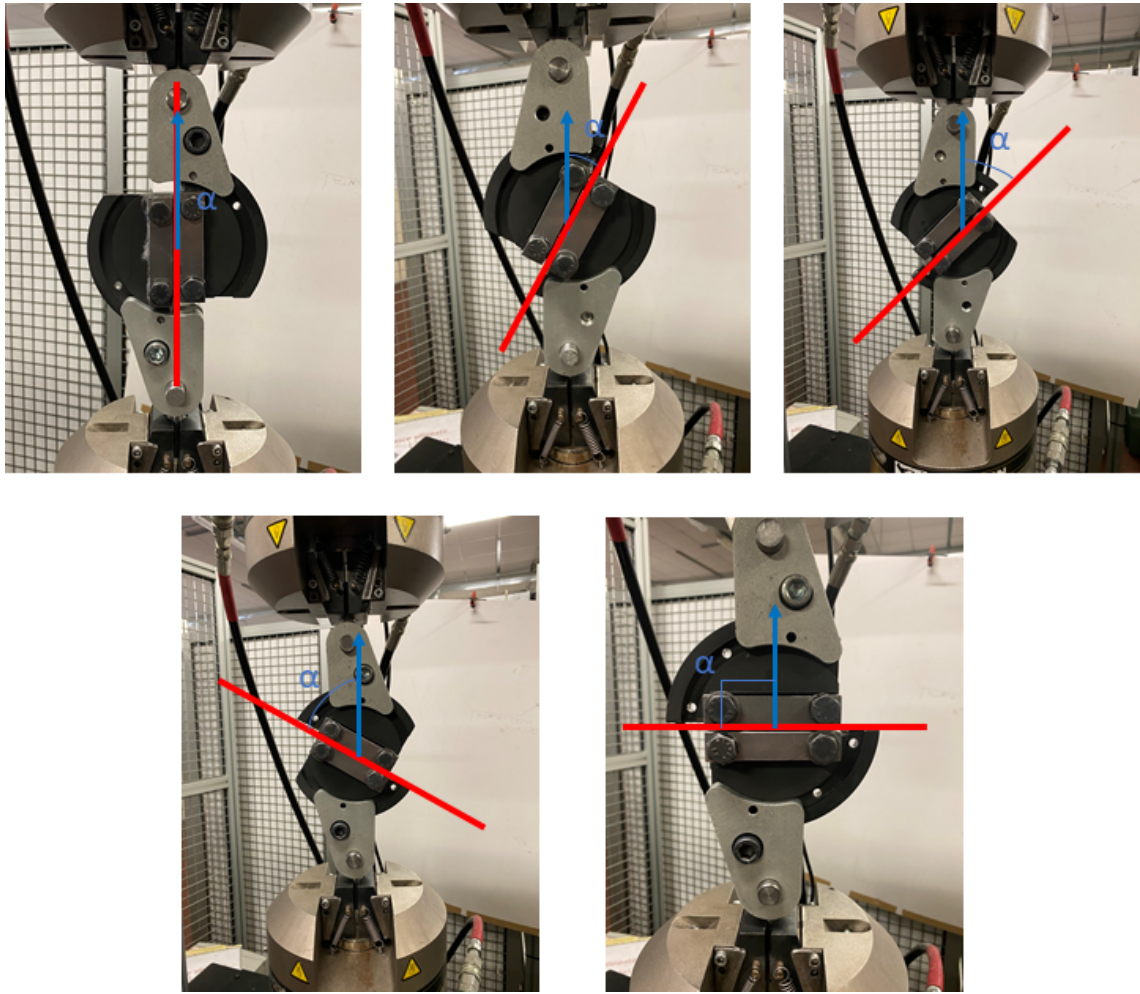


**Figure 4.19:** Tested configurations with Arcan fixture

In the following sections the tests will be presented so that a comparison between the loading curve will be possible. Firstly the behaviour of the bonded joint, with different thickness of substrates, but in the same loading conditions will be compared. Afterwards the change in the response of the joint changing the angle of the applied load for the specimens made with the same substrates will be analyzed. It is important to underline that the failure mode for all the specimens tested, except for one case that will be discussed later, is the cohesive one, which is what is necessary in order to properly obtain the adhesive properties. In the following sections just the representative curves of each case will be shown, because the curves obtained from the tests were very repeatable.

#### 4.5.1 Pure shear loading condition

The loading conditions is the first one represented in the fig.4.19.

## Polyurethane

The obtained experimental results are shown in fig.4.20 and it is possible to notice that the two curves are really similar but in the case of the 2 mm substrates the failure takes place before than with the 1 mm substrates, this is probably due to the more stiffness that characterize the thicker specimen. Is possible to have a look

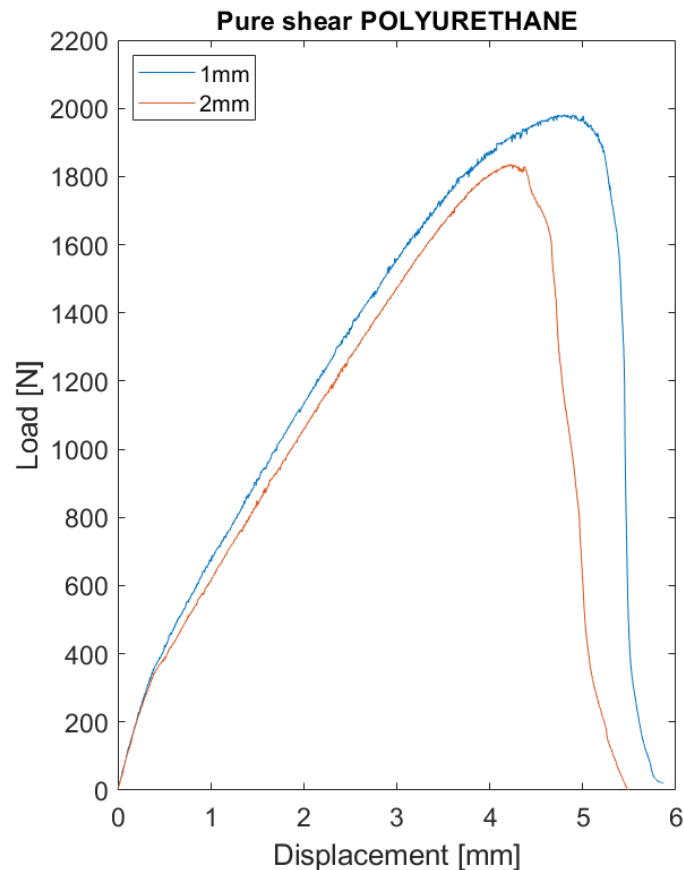


**Figure 4.20:** Polyurethane pure shear loading test with 1 mm and 2 mm substrates

at the surfaces of failure of the adhesive joints [Fig.4.21], and it is clear that the bonding areas were well limited with the transparent tape, and the failure mode in each of the tested configurations is the cohesive one.

## Epoxy

The results obtained are shown in fig.4.22. From those curves is possible to immediately notice an high difference in terms of load peak. In the joint with thinner substrates, is possible to see a failure in the substrates, close to the holes where the specimen is attached to the fixture. Which means that for this particular test a

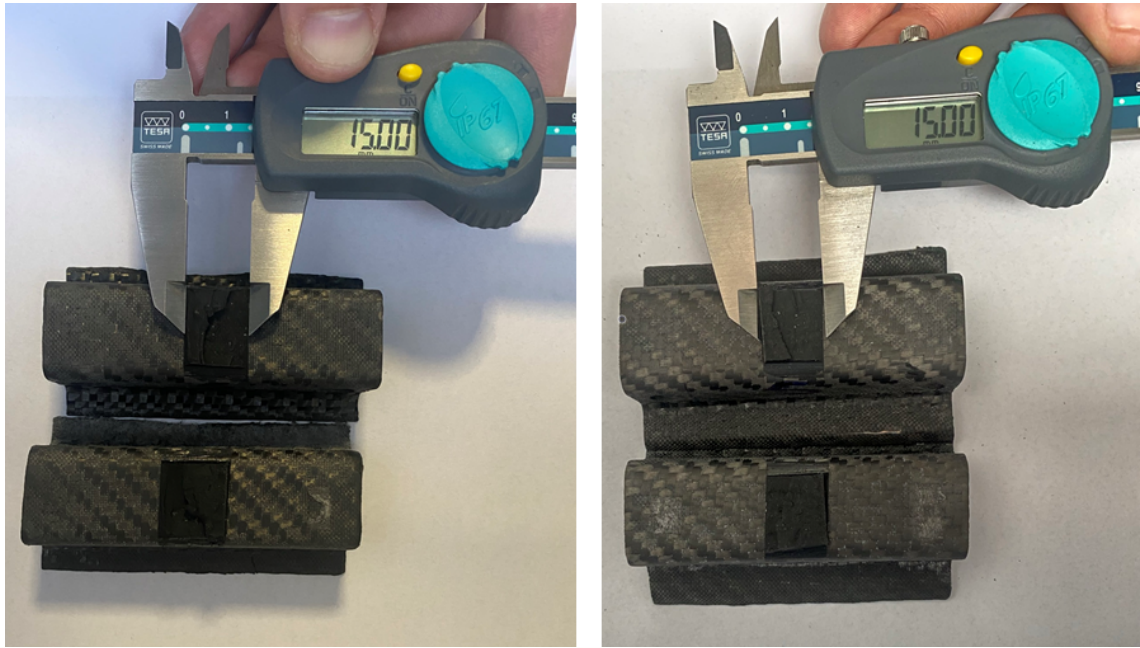


**Figure 4.21:** Cohesive failure surfaces for pure shear test of polyurethane adhesive joint for both 1mm(left) and 2mm(right) thick substrates

proper comparison between the two different curves is not realistic. As done previously is possible to check the surfaces of failure of the adhesive joints [Fig.4.23], and it is clear that, as before, the bonding areas were well limited with the transparent tape. In this case the failure mode is cohesive for the thicker specimen while for the thinner specimen is possible to notice a consistent delamination in the carbon fiber substrate, as highlighted in the figure by the red arrows.

## 4.5.2 Pure tensile loading condition

The loading conditions is the last one represented in the fig.4.19.

### Polyurethane

As in the pure shear case, for the polyurethane, the peak of the load is very similar in both cases but this time is even more clear that the 2 mm substrates gives to the adhesive joint more stiffness. The greater stiffness of the red curve is noticeable through the different slopes of the two curves and moreover the failure, in the stiffer joint, takes place before than in the other case. The failure surfaces, as shown in fig.4.25, represent a cohesive failure in both cases.

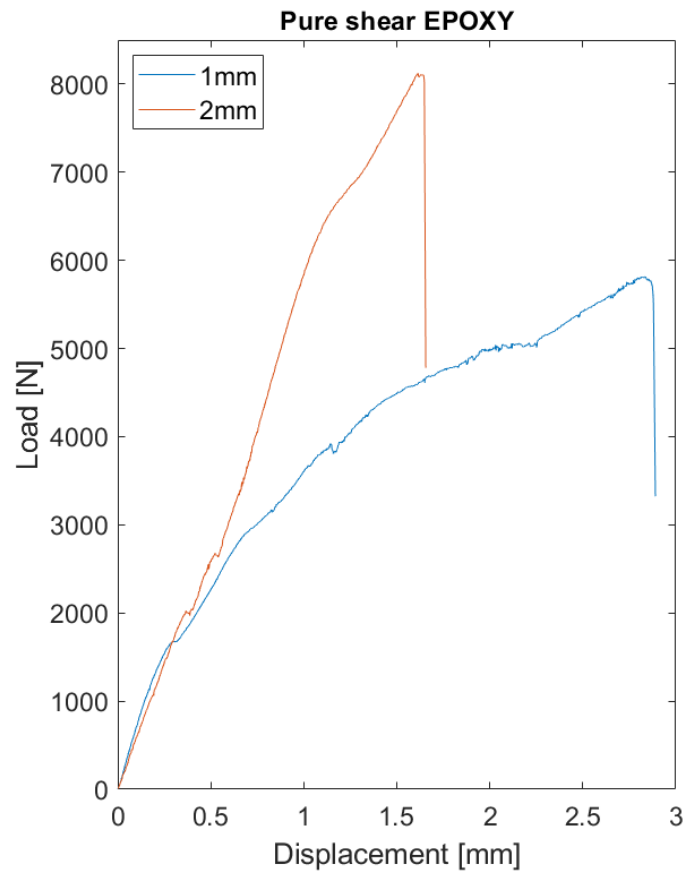


Figure 4.22: Epoxy pure shear loading test with 1 mm and 2 mm substrates

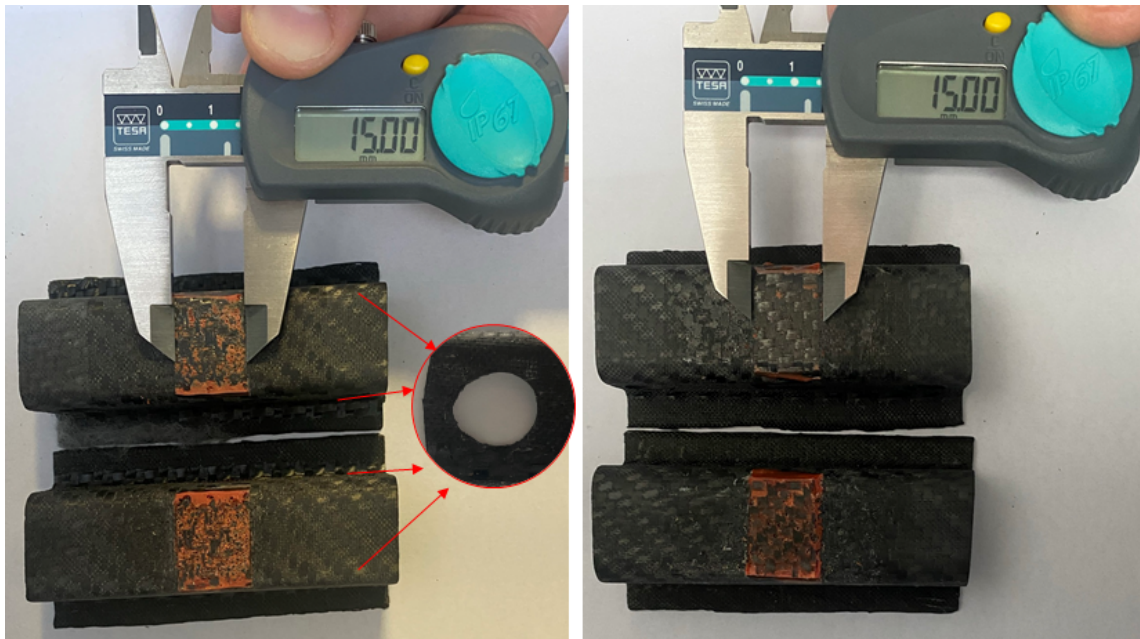


Figure 4.23: Cohesive failure surfaces for pure shear test of epoxy adhesive joint for both 1mm(left) and 2mm(right) thick substrates

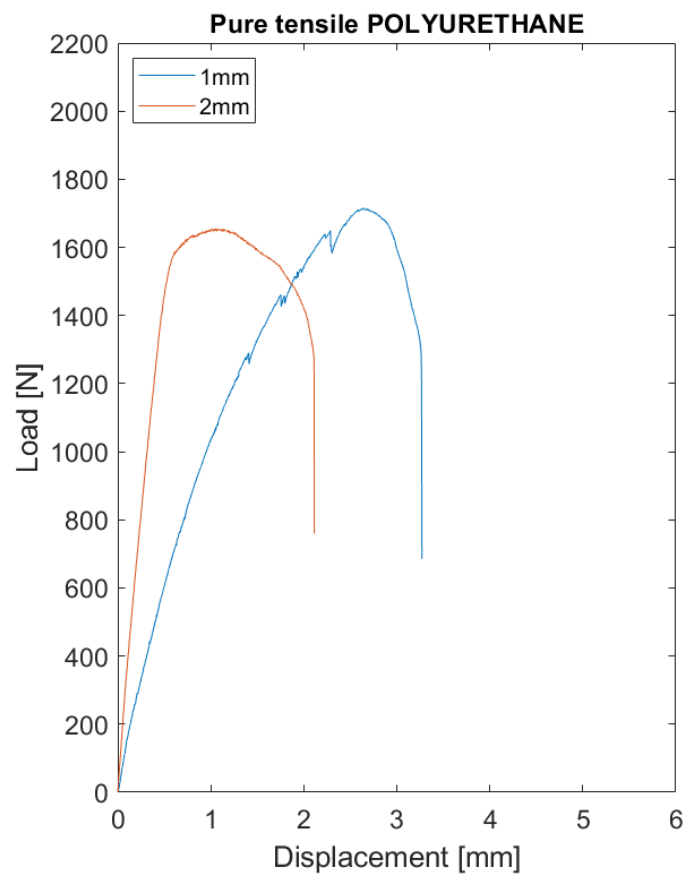


Figure 4.24: Polyurethane pure tensile loading test with 1 mm and 2 mm substrates

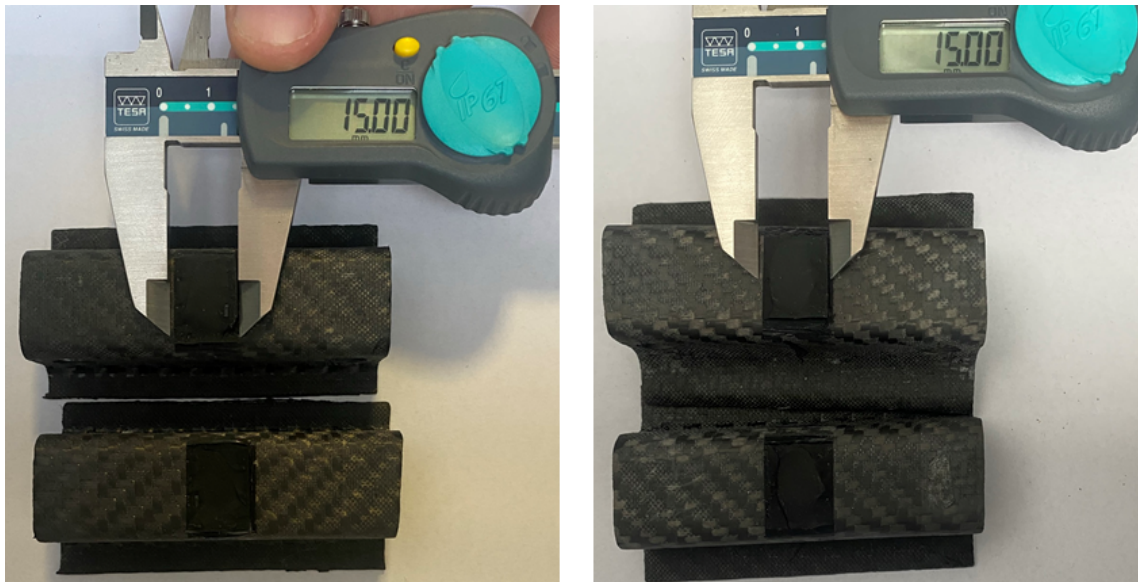
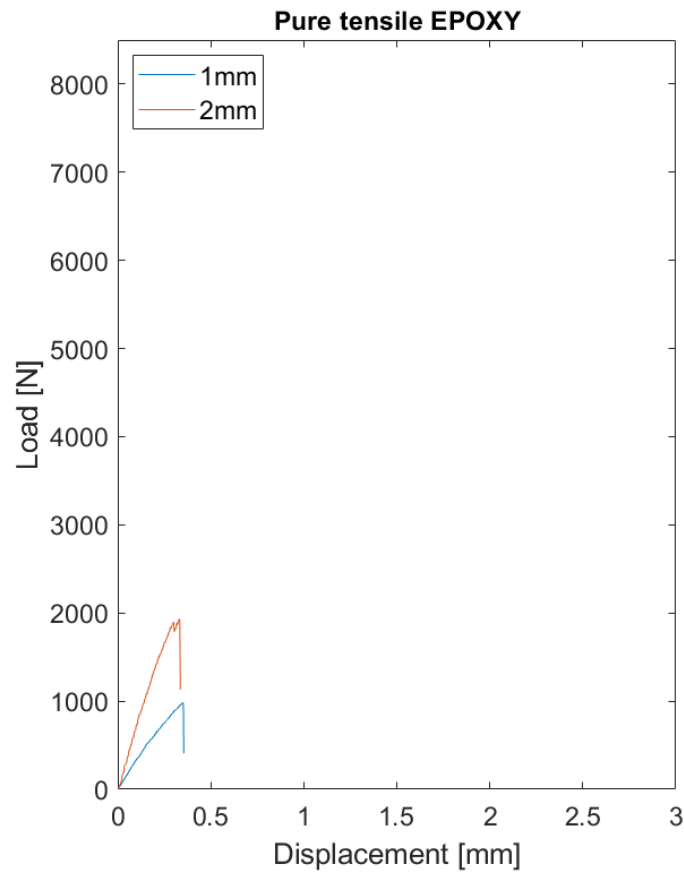


Figure 4.25: Cohesive failure surfaces for pure tensile test of polyurethane adhesive joint for both 1mm(left) and 2mm(right) thick substrates

## Epoxy

Consistently with the pure shear case the epoxy adhesive has a similar change in behaviour changing the thickness of the substrates, the joint is stiffer and can carry a bigger load increasing the substrate's thickness indeed. For what it concerns



**Figure 4.26:** Epoxy pure tensile loading test with 1 mm and 2 mm substrates

the surfaces of failure for this configuration, they are shown in fig.4.27. For this configuration the substrates do not have any kind of delamination in their structure.

### 4.5.3 Mixed loading condition

For what it concerns the mixed loading conditions the configuration that have been tested are the three remaining in the fig. 4.19.

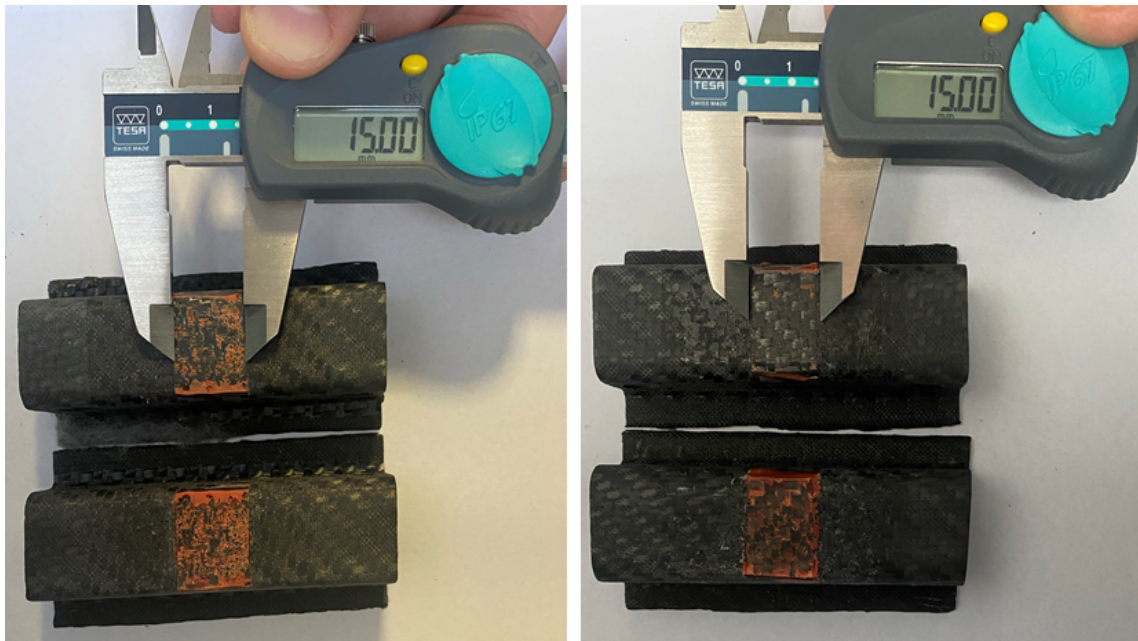


**Figure 4.27:** Cohesive failure surfaces for pure tensile test of epoxy adhesive joint for both 1mm(left) and 2mm(right) thick substrates

### Polyurethane 30° 45° 60°

In the mixed loading conditions, as for the previous 2 cases, the peak of the load for each configuration, is similar in both cases, but differently that previously the adhesive joints with thicker substrates can carry slightly more load than the thinner configurations. Moreover the stiffness of the joint, accordingly with the two pure loading cases, is greater in those with the thicker substrates. The failure surfaces

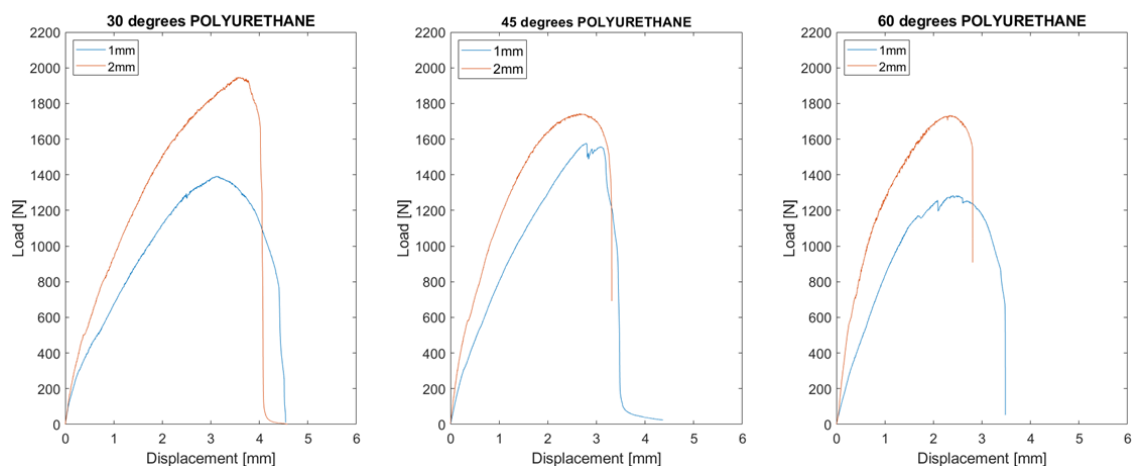
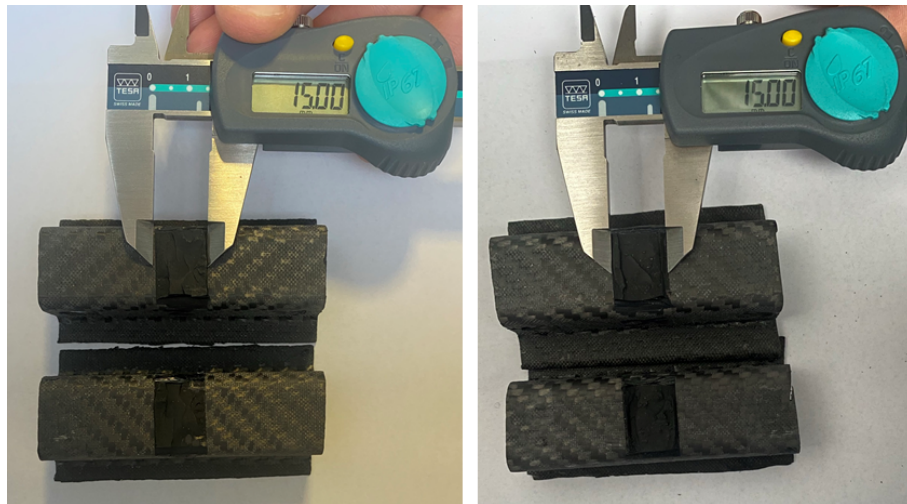
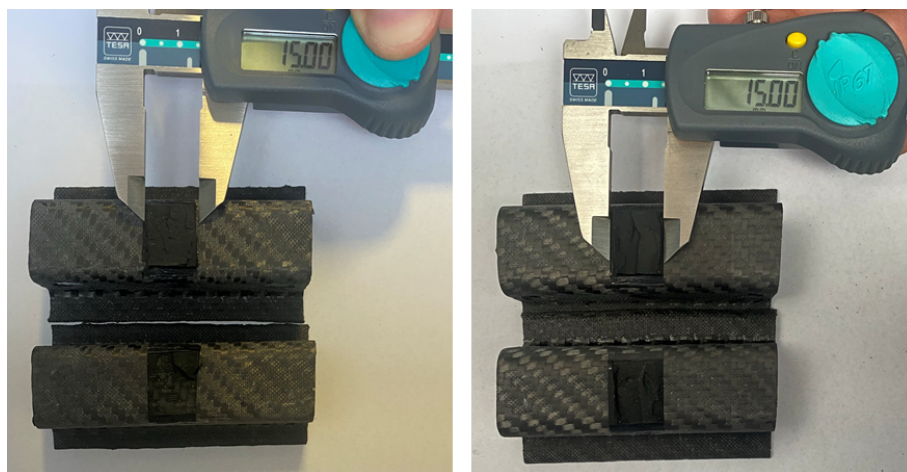


**Figure 4.28:** Polyurethane mixed loading condition tests with 1 mm and 2 mm substrates

can be observed and checked in Fig.4.29 and a cohesive failure mode is confirmed also in this case.



(a) 30 degrees loading angle



(b) 45 degrees loading angle



(c) 60 degrees loading angle

**Figure 4.29:** Cohesive failure surfaces for mixed loading conditions tests of polyurethane adhesive joint for both 1mm(left) and 2mm(right) thick substrates

## Epoxy 45°

The behaviour of the adhesive joint with the epoxy adhesive is consistent in each test that have been done, in fact also in this configuration, increasing the thickness of the two substrates the joint can carry bigger loads and the stiffness of the joint is greater [Fig.4.30].

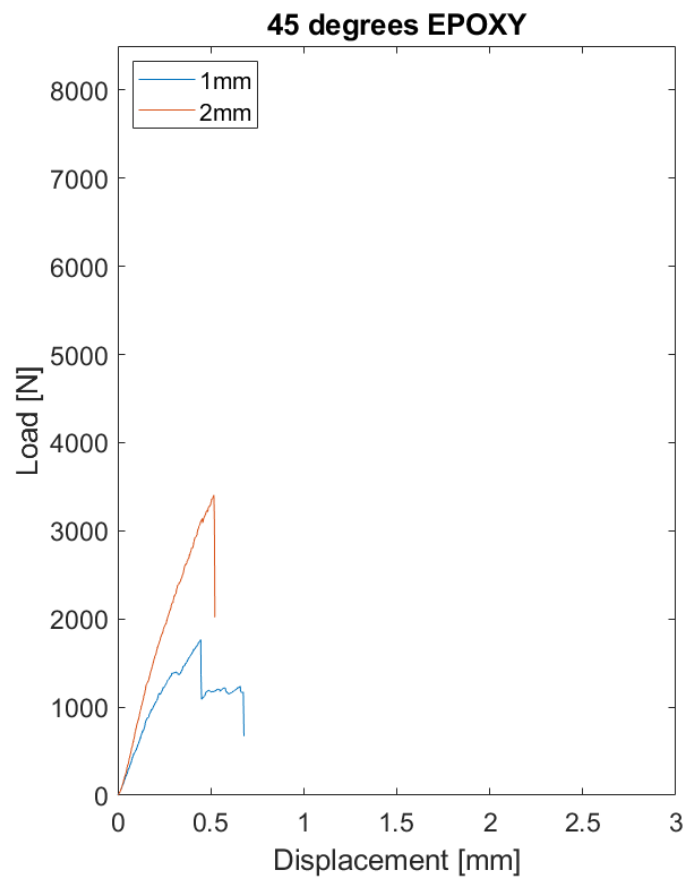


**Figure 4.30:** Epoxy 45° loading condition test with 1 mm and 2 mm substrates

Also in this case the surfaces of failure are of the cohesive type and are reported in fig.4.31.

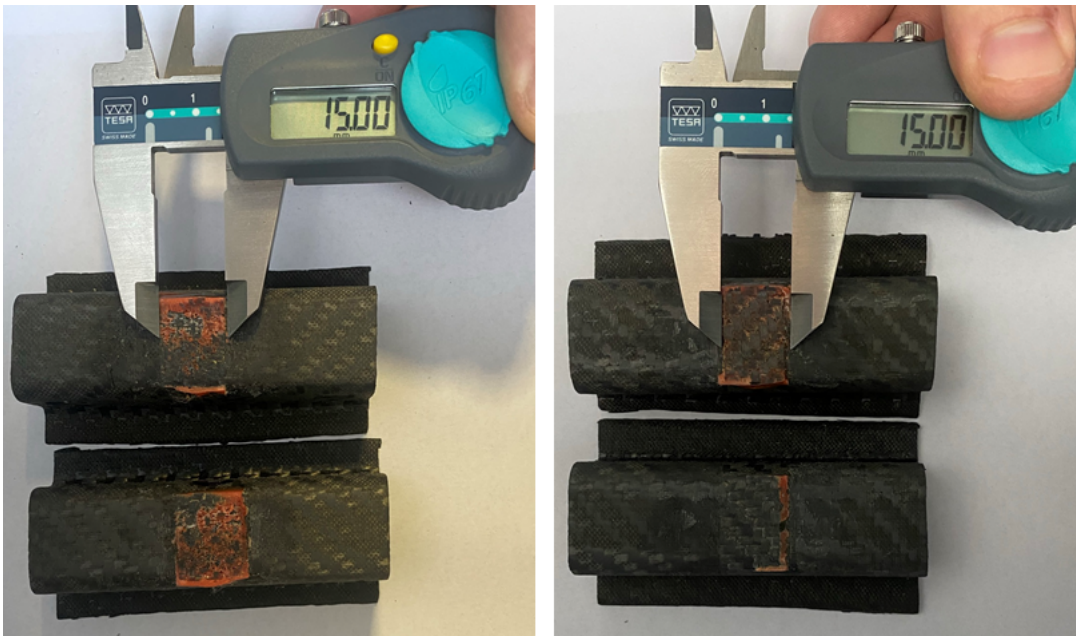


**Figure 4.31:** Cohesive failure surfaces for mixed loading condition test of epoxy adhesive joint for both 1mm(left) and 2mm(right) thick substrates

#### 4.5.4 Final comparison

The two adhesives have completely different behaviour, the polyurethane is ductile and can be defined as a semi-structural adhesive, instead the epoxy adhesive is a structural adhesive and is more stiff than the first one. It is possible to see the change in behaviour of the adhesive joint with the polyurethane adhesive, changing the loading angle [Fig.4.32]. In the figure is possible to notice that it seems

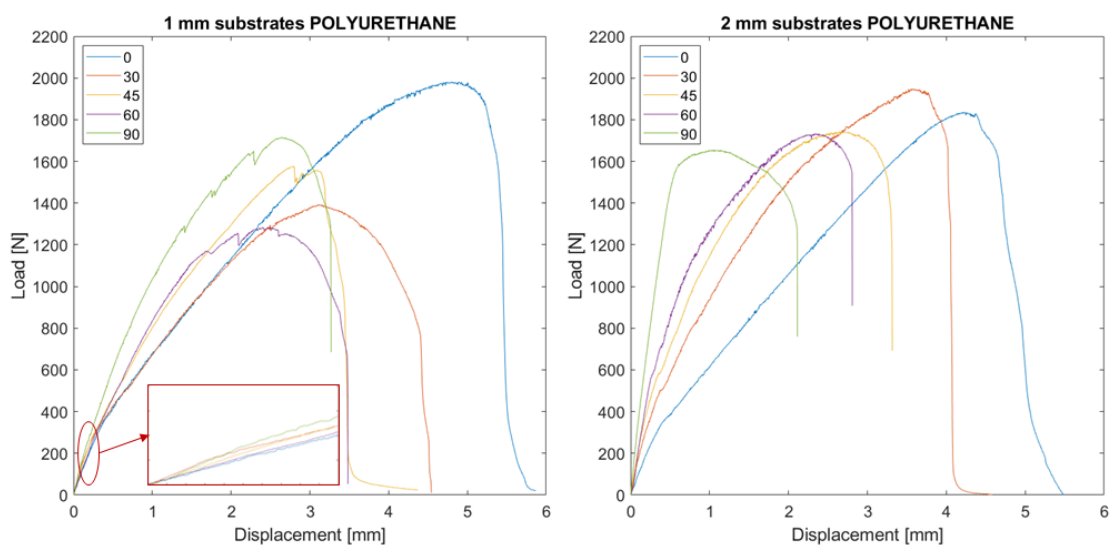


**Figure 4.32:** Load and Stiffness variation in the polyurethane adhesive joint

that increasing the loading angle the peak of the load slightly changes, but for this

particular ductile adhesive the change is not really evident. Moreover with the loading angle also increases the stiffness of the adhesive joint, which is well visible in the 2mm substrates joint. Instead in the 1mm substrates case an enlargement is needed, where is possible to see that the less stiff configuration is the one in pure shear ( $0^\circ$ ), and the stiffer is the pure tensile configuration ( $90^\circ$ ). All the configuration have been tested at least 3 times so all the reference value are listed in Tab.4.2 with their standard deviations in Tab.4.3. The tables can be resumed by a double y-axis

<b>1 mm polyurethane joint</b>					
<b>Configuration</b>	0	30	45	60	90
<b>Max Load [N]</b>	1965	1401	1598	1269	1675
<b>Stiffness [N/mm]</b>	917	872	1332	1075	1460
<b>Stiffness (@ 0.8Load) [N/mm]</b>	503	546	657	732	815
<b>Displacement @peak [mm]</b>	4.57	3.12	3.03	2.36	2.74
<b>2 mm polyurethane joint</b>					
<b>Max Load [N]</b>	1746	1966	1743	1759	1611
<b>Stiffness [N/mm]</b>	907	1315	1769	2417	3665
<b>Stiffness (@ 0.8Load) [N/mm]</b>	484.37	669.52	894.62	1108.12	2957.82
<b>Displacement @peak [mm]</b>	4.2	3.44	2.68	2.31	1.14

**Table 4.2:** Experimental parameters for polyurethane adhesive joint with carbon fiber substrates

<b>Standard deviations of Tab.4.2 [1 mm polyurethane joint]</b>					
<b>Configuration</b>	0	30	45	60	90
<b>Max Load [N]</b>	75.40	5.22	14.30	10.55	40.87
<b>Stiffness [N/mm]</b>	31.77	6.23	114.81	20.05	103.50
<b>Stiffness (@ 0.8Load) [N/mm]</b>	16.38	9.84	20.36	49.69	38.68
<b>Displacement @peak [mm]</b>	0.213	0.04	0.17	0.02	0.08
<b>Standard deviations of Tab.4.2 [2 mm polyurethane joint]</b>					
<b>Max Load [N]</b>	59.62	13.47	9.24	18.35	23.41
<b>Stiffness [N/mm]</b>	40.60	26.81	53.41	61.84	70.11
<b>Stiffness (@ 0.8Load) [N/mm]</b>	6.75	0.77	45.59	24.79	224.30
<b>Displacement @peak [mm]</b>	0.25	0.05	0.08	0.05	0.07

**Table 4.3:** Standard deviations of the experimental parameters for polyurethane adhesive joint with carbon fiber substrates

bar graph [Fig.4.33] and [Fig.4.34].

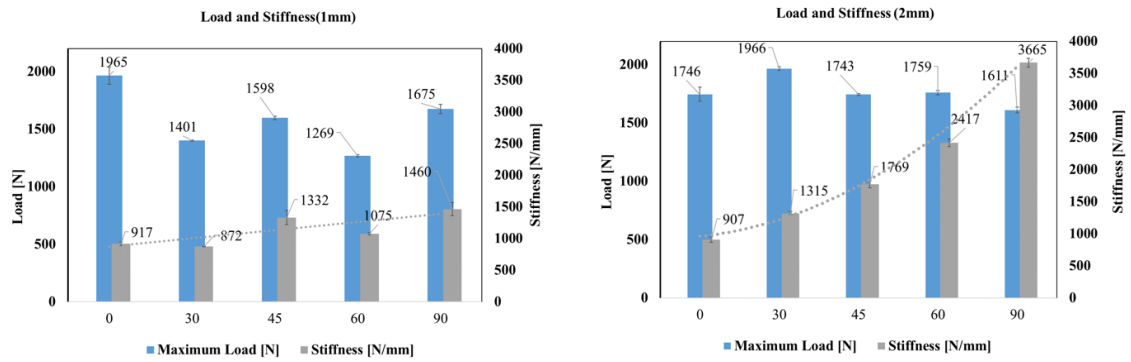


Figure 4.33: Load and Stiffness variation in the polyurethane adhesive joint

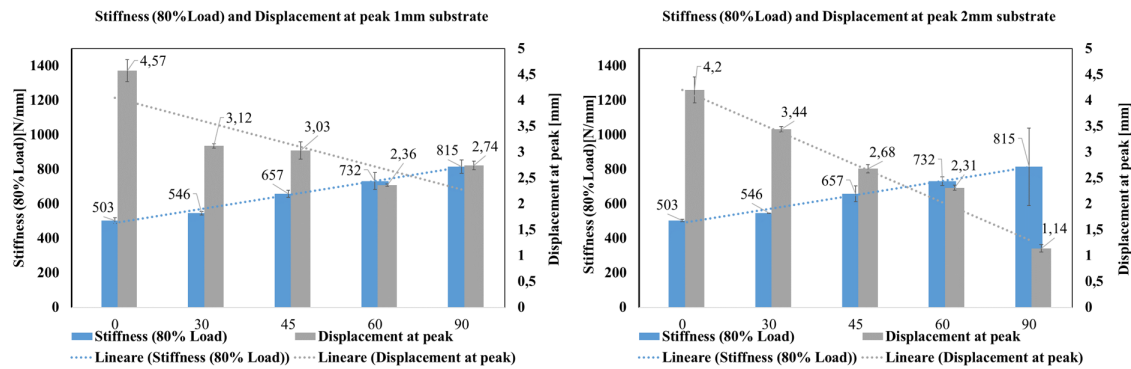


Figure 4.34: Stiffness at 80% of the max load and displacement at the peak of the load variation in the polyurethane adhesive joint

For what it concerns the epoxy joints, it is possible to compare the curves that characterize the joint with the same substrates, in each configuration [Fig.4.35]. Increasing the loading angle, in this adhesive, is very straightforward that the peak of the carried load is decreasing a lot passing from a pure shear loading condition (0°) to a pure tensile case (90°), both in the 1mm substrates joint and in the 2mm one. Regarding the slope of the curves, for this adhesive the behaviour for the joints with 1mm thick substrates and for the 2 mm one is not consistent with the first adhesive. Looks like that for both types of substrates the adhesive joints is becoming stiffer in the 45° configuration followed by the pure tensile case, but the difference is minimal.

Due to the fact that the same configuration has been repeated at least 4 times for this adhesive, also the standard deviations of the most important result have been computed. All the technical data are grouped in the following graphs [Fig.4.36][Fig.4.37] and table [Tab.4.4] for the 1mm substrates joints, instead for the thicker substrates joints in the table [Tab.4.5].

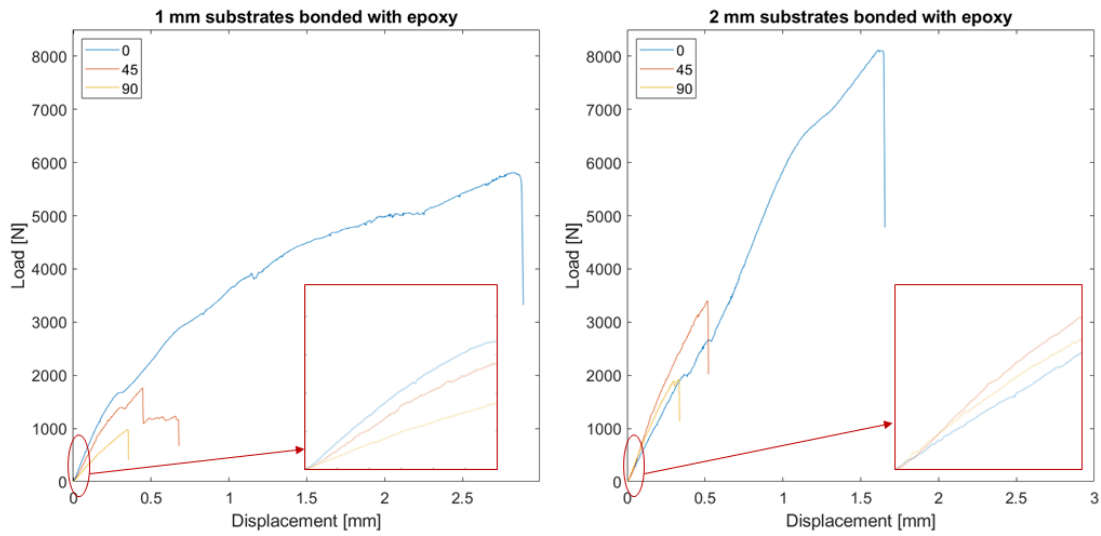


Figure 4.35: Change in the behaviour of the adhesive joint with epoxy changing the loading angle.

1 mm Epoxy joint				Standard Deviations		
Configuration	0	45	90	0	45	90
Max Load [N]	6045	1600	964	290.63	115.63	12.64
Stiffness [N/mm]	2950	4579	3075	709.83	554.94	204.32
Stress [MPa]	23.71	6.27	3.78	1.14	0.91	0.05
Max Displacement [mm]	4.59	0.53	0.36	0.94	0.11	0.01

Table 4.4: Experimental parameters for epoxy adhesive joint with 1mm thick carbon fiber substrates

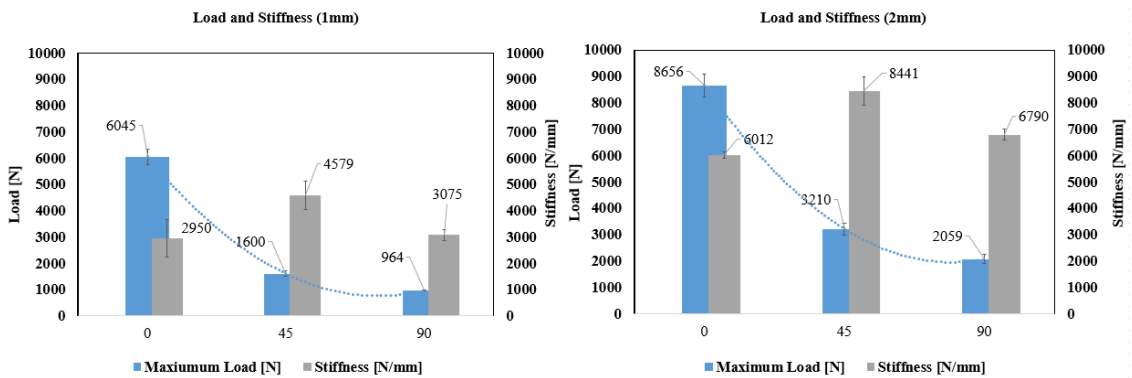
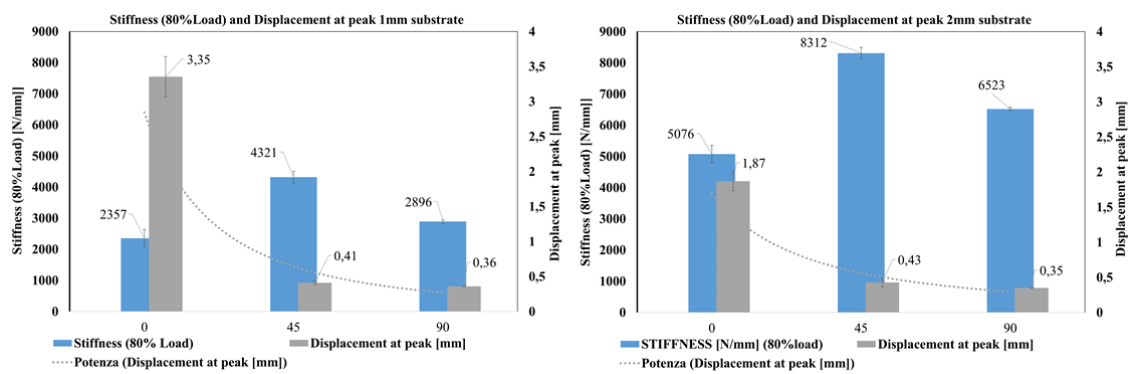


Figure 4.36: Load and Stiffness variation in the epoxy adhesive joint

2 mm Epoxy joint				Standard Deviations		
Configuration	0	45	90	0	45	90
Max Load [N]	8656	3210	2059	425.77	224.35	175.60
Stiffness [N/mm]	6012	8441	6790	119.04	525.13	205.73
Stress [MPa]	33.95	12.59	8.07	1.67	1.76	0.69
Max Displacement [mm]	1.90	0.82	0.37	0.14	0.27	0.02

Table 4.5: Experimental parameters for epoxy adhesive joint with 2mm thick carbon fiber substrates



**Figure 4.37:** Stiffness at 80% of the max load and displacement at the peak of the load variation in the epoxy adhesive joint

## 5. Numerical Theory

In this chapter a brief review of the most relevant theory that the numerical simulations are based on will be presented.

### 5.1 The finite element method

The finite element method (FEM) was firstly introduced and developed in the aerospace industry but then transformed into an analysis tool for a quite broad field of continuum mechanics. The FEM could be described as a numerical technique used to find approximate solutions to a partial differential equations. In a continuum problem each variable, such as displacement, stress and temperature, has an infinite number of values in the chosen region due to them being a function of each and every point in the solution region. An infinite number of values leads to an infinite number of unknowns, the goal of the finite element method is to reduce the problem into one with a finite number of unknowns. This reduction of solution points is done dividing the solution region into elements in which each unknown variable is expressed by interpolation functions.[25]

### 5.2 1-D problem

In order to apply the finite element method to a real case it is necessary to understand it in the easiest case, which exploit the model of a thin elastic string which can be seen as a boundary value problem [Fig.5.1]. An elastic string with constant round cross section and a small density force per unite of volume lying on the mid plane of the string and orthogonal to the axis of the latter and the two extreme fixed will be studied. The small force will induce a small displacement of the string which varies along the axis of it. It is possible to state that the displacement will

be co-planar with the force and moreover one component will be negligible respect to the other one [Eq.5.1]. In the figure 5.1 is possible to notice:

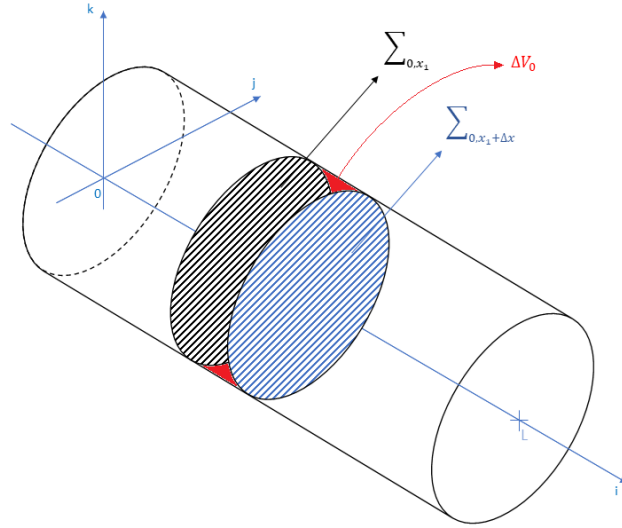


**Figure 5.1:** Elastic string problem scheme

- $L$  is the total length of the string
- The two cross sections  $\Sigma_{0,x_1}$  and  $\Sigma_{0,x_1+\Delta x}$
- $\Delta V_0$  which is the control volume before any load is applied to the string

$$\begin{cases} f = 0 \vec{i} + 0 \vec{j} + f_3 \vec{k} \\ u = u_1 \vec{i} + u_2 \vec{j} + u_3 \vec{k} \simeq u_3 \vec{k} = u(x) \end{cases} \quad (5.1)$$

When the force is applied the small volume element  $\Delta V_0$  transforms into  $\Delta V$  consequently also the cross sections become  $\Sigma_{x_1}$  and  $\Sigma_{x_1+\Delta x}$ , so it is possible to write the equilibrium equation:

$$\int_{\Delta V} f dV + \int_{\Sigma_{x_1+\Delta x}} \bar{\sigma} n d\Sigma - \int_{\Sigma_{x_1}} \bar{\sigma} n d\Sigma = 0 \quad (5.2)$$

where:

- $\Delta V$  is the transformed element

- $\sum_{x_1}$  and  $\sum_{x_1+\Delta x}$  are the transformed cross sections
- $\bar{\sigma}$  is the stress tensor of the string

$$\bar{\sigma} = \begin{pmatrix} \sigma_1 \tau_{12} \tau_{13} \\ \tau_{21} \sigma_2 \tau_{23} \\ \tau_{31} \tau_{32} \sigma_3 \end{pmatrix} \quad (5.3)$$

- $\mathbf{n}$  is the normal to the transformed section oriented in the  $\vec{i}$  direction.

Assuming small displacement it is possible to switch to a one-dimensional problem because as first approximation it is possible to consider:

- the transformed element ( $\Delta V$ ) equal to the original one ( $\Delta V_0$ )
- the transformed cross sections ( $\sum_{x_1}$  and  $\sum_{x_1+\Delta x}$ ) equal to the original ones ( $\sum_{0,x_1}$  and  $\sum_{0,x_1+\Delta x}$ )

Considering the assumptions above it is possible to work out the expression of the mean force over the section of the string along the interval  $[0,L]$ :

$$\int_{\Delta V} f dV \simeq \int_{\Delta V_0} f dV = \int_{x_1}^{x_1+\Delta x} \left( \int_S f(x, x_2, x_3) dx_2 dx_3 \right) dx |S| = \int_{x_1}^{x_1+\Delta x} \tilde{f}(x) dx \quad (5.4)$$

Stating that  $|S|$  is the area of the section the mean value of the force over the section the interval is:

$$\tilde{f}(x_1) = \frac{1}{|S|} \int_S f(x_1, x_2, x_3) dx_2 dx_3 \quad (5.5)$$

The surface integral can be treated similarly so the final string's equilibrium state is:

$$|S| \int_{x_1}^{x_1+\Delta x} \tilde{f}(x) dx + |S| \bar{\sigma} \tilde{\mathbf{n}}|_{x_1+\Delta x} - |S| \bar{\sigma} \tilde{\mathbf{n}}|_{x_1} = 0 \quad (5.6)$$

$$\int_{x_1}^{x_1+\Delta x} \tilde{f}(x) dx + \bar{\sigma} e_{1|x_1+\Delta x} - \bar{\sigma} e_{1|x_1} = 0 \quad (5.7)$$

$$\int_{x_1}^{x_1+\Delta x} f_3(x) dx + \tau_{31|x_1+\Delta x} - \tau_{31|x_1} = 0 \quad (5.8)$$

$$f_3(x_1) + \frac{d\tau_{31}}{dx}(x_1) = 0, \quad x_1 \in (0, L) \quad (5.9)$$

In order to obtain the final expression which express the string's equilibrium state, the equation 5.6 is divided by  $|S|$  and  $\tilde{\mathbf{n}}$  is assumed to be  $\simeq e_1$ , instead for what

it concern the next equation just the component along  $\vec{k}$  is considered. The last equation can be obtained dividing by  $\Delta x$  and taking the limit so that  $\Delta x$  goes to 0, and the differential equation number 5.9 is obtained. Considering now the Hooke's law <sup>8</sup> and developing some simple steps and simplifications, such as  $u_1$  negligible with respect to  $u_3$  is possible to obtain the approximate constitutive equation:

$$\tau_{31} = \mu \frac{\partial u_3}{\partial x_1} \quad (5.10)$$

The coefficient  $\mu$  is called shear modulus and is related to the Young's modulus  $E$  and the Poisson coefficient  $\nu$ <sup>9</sup>. Substituting the constitutive equation in the string equilibrium the following system of equation can be expressed:

$$\begin{cases} -\frac{d}{dx} \left( \mu \frac{du}{dx} \right) + f = 0 & \text{in}(0, L) \\ u(0) = u(L) = 0 \end{cases} \quad (5.11)$$

If  $f$  and  $\mu$  are continuous functions the boundary value problem can be solved and admits one and one only solution. However the procedure to find the analytical solution may be very complex and long due to the presence of integrals, moreover this procedure cannot be generalised to the bi-dimensional problem. This is the reason why it is important to discretize the problem and reduce the system to a linear algebraic system.

### 5.2.1 1D finite element discretization

Finite element method are based on the variational formulation of the boundary value problem to be approximated. Is necessary to recall the variational formulation of the previous elastic string problem [Eq.5.11], introduce a generic function  $v$  and then integrate [Eq.5.12]. The  $v$  function is an 'admissible displacement' physically talking instead a 'shape function' from the mathematical point of view, but is easy to understand that this function must be continuous (the elastic string shouldn't break) and is null at the endpoints where the string is fixed.

$$-\int_0^L \frac{d}{dx} \left( \mu \frac{du}{dx} \right) v dx = \int_0^L f v dx \quad (5.12)$$

<sup>8</sup>This law relates the stress tensor  $\bar{\sigma}$  to the strain tensor  $\bar{\epsilon}$   $\bar{\sigma} = 2\mu\bar{\epsilon} + \lambda tr(\epsilon)\bar{I}$

<sup>9</sup> $\mu = \frac{E}{2(1+\nu)}$

Integrating by part the left hand side of the Eq.5.12 and denoting a set of the all admissible displacements ( $V$ ), which also contains the solution of our problem  $u$  it is possible to formulate the variational formulation of the elastic string problem [Eq.5.13].

$$\begin{cases} u \in V \\ \int_0^L \mu \frac{du}{dx} \frac{dv}{dx} dx = \int_0^L f v dx \end{cases} \quad v \in V \quad (5.13)$$

Eq.5.13 describes mathematically what in mechanics is called as 'Principle of Virtual Work'. It is possible now to define a discretization method starting from Eq.5.13 and considering just a finite number of independent admissible displacements, which can be called discrete displacements  $V_h$ , defining the 'discrete variational formulation'[Eq.5.14]:

$$\begin{cases} u_h \in V_h \\ \int_0^L \mu \frac{du_h}{dx} \frac{dv_h}{dx} dx = \int_0^L f v_h dx \end{cases} \quad v_h \in V_h \quad (5.14)$$

Using the finite element method is possible to define, in an effective way, the discrete displacements to be used in the discrete variational formulation Eq.5.14. The first step is to divide the domain of the problem  $[0,L]$  in  $N+2$  nodes, which do not have to be necessarily equidistant. This nodes let the domain to be splitted up in  $N+1$  intervals of length  $h$ . Now is important to decide which degree of interpolation is necessary between two admissible displacement values, the easiest choice are polynomials of degree one, this particular selection generates the so called 'Linear finite elements'[Fig.5.2].

$$\begin{cases} 0 = x_0 < x_1 < \dots < x_{j-1} < x_j < x_{j+1} < \dots < x_N < x_{N+1} = L \\ I_j = [x_{j-1}, x_j] \quad j = 1, \dots, N+1 \\ h_j = x_j - x_{j-1} \\ V_h = v_h \in V | v_h|_{I_j} \in P_1 \quad j = 1, \dots, N+1 \end{cases} \quad (5.15)$$

Looking at Fig.5.2 is possible to write the discrete displacement as in Eq.5.16.

$$v_h(x) = v_{j-1} \frac{x_j - x}{h_j} + v_j \frac{x - x_{j-1}}{h_j} \quad (5.16)$$

The discrete displacement can be written as a liner combination of basis functions. Defining the vector  $e_j = \delta_{jk}$ , where  $\delta_{jk}$  is the Dirac's delta, which all the components are zero except for the  $j$ -th, which is equal to one, is possible to define the discrete displacement as a function of the Hat function  $\varphi$  also called Lagrange basis in  $V_h$

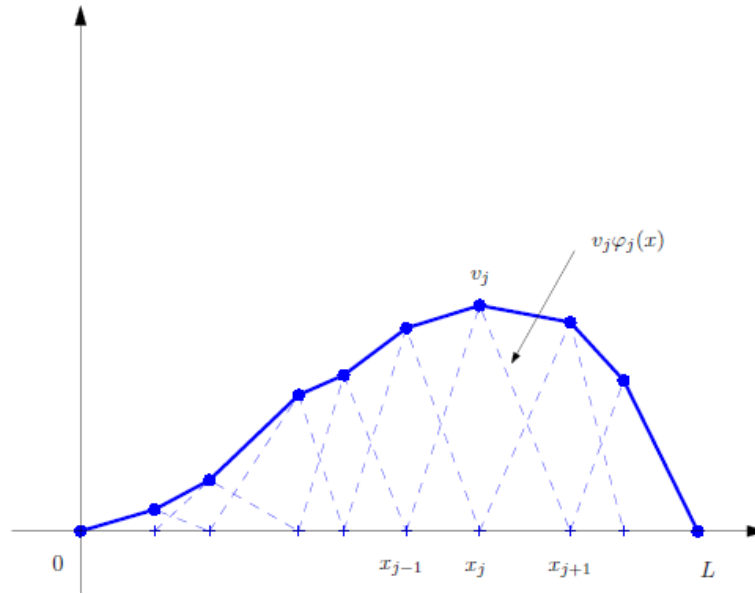


Figure 5.2: Linear finite elements [26]

[Eq.5.17].

$$v_h(x) = v_1\varphi_1(x) + v_2\varphi_2(x) + \cdots + v_{N-1}\varphi_{N-1}(x) + v_N\varphi_N(x) = \sum_{j=1}^N v_j\varphi_j(x)$$

$$\text{where } \varphi_j(x) = \begin{cases} \frac{x-x_{j-1}}{h_j} & x \in I_j \\ \frac{x_{j+1}-x}{h_{j+1}} & x \in I_{j+1} \\ 0 & \text{otherwise} \end{cases} \quad (5.17)$$

Is now possible to pass from the system [Eq.5.14] to a system of  $N$  equations [Eq.5.18].

$$\int_0^L \mu \frac{du_h}{dx} \frac{d\varphi_j}{dx} dx = \int_0^L f \varphi_j dx; \quad j = 1, \dots, N \quad (5.18)$$

By defining  $u_h = \sum_{k=1}^N u_k \varphi_k$ ,  $\int_0^L \mu \frac{d\varphi_k}{dx} \frac{d\varphi_j}{dx} dx = a_{jk}$  and  $\sum_{k=1}^N a_{jk} u_k = f_j$  is possible to reduce the equations to the matrix form [eq.5.19].

$$Au = f \quad (5.19)$$

Where A is the 'Stiffness matrix', u is the displacement vector and f is the load vector or force term. When the three term are constructed and defined is possible to solve the problem numerically exploiting the Eq.5.19.[26] This is a short presentation of the mathematical reasoning behind the FEM method which permits to pass from an analytical exact solution to a numerical approximation. In the chapter is not presented the computation of each single term of the Eq.5.19 just because is purely mathematical and not very important for the goal of the thesis, anyway the result are reported in the system [5.20] but is important to underline that this procedure

can be extended to the 2-D and then 3-D case, and that is what each simulation software based of finite element method pretty much does to solve a static problem.

$$\begin{aligned} A &= \mu \text{ tridiag}[-1 \quad 2 \quad -1] \\ f_j &= f(x_j) \frac{h_j + h_{j+1}}{2} \end{aligned} \quad (5.20)$$

### 5.2.2 Dynamic problem - Time integration

In the reality the majority of the case studies involves a structure which is subjected to a load that is time dependent. It is useful to recall the equilibrium equations of a linear dynamic system [Eq.5.21].

$$M\ddot{U} + C\dot{U} + KU = R \quad (5.21)$$

The latter equation is derived by static considerations at a certain time  $t$ , indeed a dynamic problem could be seen as a resolution of a static problem at different instant of time, spaced apart of a  $\Delta T$  interval. For sure the solution in the previous interval will be the initial conditions of the next 'static' problem. [27]

#### Central Difference scheme

LS-dyna uses the explicit difference scheme to integrate the equations of motion.[28] The scheme is based on one assumption for which the acceleration must have the following form [Eq.5.22]

$$\ddot{U} - t = \frac{1}{\Delta t^2}(U_{t-\Delta t} - 2U_t + U_{t+\Delta t}) \quad (5.22)$$

The error in Eq.5.22 is of order  $\Delta t^2$ , and to have the same order of error in the velocity expression, the latter will be of this type [Eq.5.23].

$$\dot{U}_t = \frac{1}{2\Delta t}(-U_{t-\Delta t} + U_{t+\Delta t}) \quad (5.23)$$

The displacement solution at time  $t + \Delta t$  can be computed by using the previous computation at time  $t$ , by substituting Eq.5.22 and Eq.5.23 in Eq.5.21:

$$\left(\frac{1}{\Delta t^2}M + \frac{1}{2\Delta t}C\right)U_{t+\Delta t} = R_t - \left(K - \frac{2}{\Delta t^2}M\right)U_t - \left(\frac{1}{\Delta t^2}M - \frac{1}{2\Delta t}C\right)U_{t-\Delta t} \quad (5.24)$$

From which it is possible to compute  $U_{t+\Delta t}$ , by using only the values of the previous instant of time  $t$ , this integration procedure is called Explicit integration method. It is very well known that a small time step size is needed for good simulation's results but is important, to have a stable scheme, that the time step is smaller than the critical time step which is characteristic of the mass and stiffness properties of the structure [Eq.5.25][27].

$$\Delta t \leq \Delta t_{cr} = \frac{2}{\omega_{max}} \quad (5.25)$$

### 5.3 Non-linear finite element analysis

So far everything stated is under three main assumptions:

- Displacement are infinitesimally small
- Material is linearly elastic
- The boundary conditions remains unchanged during the application of the loads

If one of the previous assumptions cannot be satisfied a non linear analysis is necessary. [27] The main difference between a linear analysis and a non linear one can be represented by the "Stiffness" of the problem. The stiffness is the ability of a part to respond to an applied load, and this behaviour is highly affected by:

- Shape: the stiffness of a structure is directly dependent from the shape, a H-beam has different stiffness from a rectangular beam
- Material: the stiffness of a structure is directly dependent from the material, an iron beam has different stiffness than a steel beam with the same shape and size
- Part Support: a beam which is clamped in one side is less stiff than a double supported beam in both sides

During the simulation the part can undergo deformations, which change the 'Stiffness' of the problem, if the change is small enough a linear study is acceptable, otherwise if the change in 'Stiffness' are not negligible a long and more complex non-linear analysis is requested.[29]

### 5.3.1 Types of non linear behaviour

As said before the origin of a non linear study is based on a not negligible change in stiffness, but the reasons why this happens could be of different types: [29]

- Non linear geometry: as already previously discussed, non linear analysis is requested in case of the part which undergoes the analysis changes its own stiffness. If changes in stiffness comes only from the changes in shape, nonlinear behaviour is also known as geometric non-linearity. This kind of non linearity happens always when the problems contains large deformations, but is possible to have to deal with non linearity also with small deformations that cause not neglecting changes in stiffness
- Non linear material: If the change of the stiffness is caused only by its material properties under the operating conditions, is necessary to deal with non linearities due to the material. A linear material model has the assumes the stress to be proportional to the strain, moreover assumes that no permanent deformations will result once the load is removed. Although this is a possible case study, sometimes the loads are high enough to cause some permanent deformations, or if the strains are very high, then a non-linear model have to be used. In particular is the material is strained beyond its yield limit a non linear material model is required.
- Loss of elastic stability (Buckling): from mechanics is well known that an applied load can modify the stiffness of a part, for example a tension load can increase the stiffness of a part instead a compressive load will decrease it. Buckling is the phenomena which occurs when a compressive load changes the structure's stiffness until reaching a zero value, in this case the structure will undergo a rapid deformation. Using a linear buckling analysis is possible to compute the 'Euler load'<sup>10</sup>, but this result is not conservative and is possible that the predicted load is much higher that the real one. Moreover, a

---

<sup>10</sup>The Euler load is the load at which a part, subjected to compressive load, will buckle

linear analysis cannot study the post-buckling behavior. In case of buckling phenomena takes place a non-linear analysis should be used.

- Contact stresses and nonlinear supports: Contact stresses are created between two contacting surfaces. The concentrated stresses in the area of contact cause a big change in the stiffness of the model, forcing the user to choose a non linear analysis. A similar situation when non linear analysis is necessary occurs when a support changes is stiffness depending on the amount of deformation that the part undergoes.
- Non linear dynamic analysis: As for static analysis in case of a dynamic study is possible to have a linear or non-linear approach. The approach to choose depends, as for static, in the change of stiffness of the problem. In case the stiffness changes just a bit, like in case of a vibrating engine which undergoes small deformations about its equilibrium point, is possible to use a linear dynamic analysis. Instead a crash simulation or an airbag explosion have to be studied with a non-linear dynamic analysis because the structure will suffer large deformation (geometric non linearity) and large strains (material non linearity).

## 5.4 Summary: Step-by-step FEM

How the finite element method works practically is described by Huebner [25]:

1. Discretization of the continuum: the region to be studied is divided into elements which may be not all equals
2. Choice of interpolation functions: to each element is assigned a finite number of nodes and the interpolation functions are used (polynomials are commonly used)
3. Establish element properties: all the properties of each element are defined
4. Assembly of element properties to get the system equations: all the element's properties are assembled, which means that the elements interconnected will have the same properties in the common boundaries.
5. State boundary conditions: known values are assigned to the boundaries before solving the system equations

6. Solving system equations: the system equations are solved depending on the type of problem, such as steady state or time dependent. In the first case linear or non linear algebraic equation are solved, in the last case linear or non linear ordinary differential equations have to be solved.
7. Make any additional computations: in this final step the already computed unknowns are exploited to calculate new dependent parameters, such as stress from displacement or the heat flux from the temperature.

## 6. Numerical Simulation

In this chapter both the numerical simulation set up and the result obtained will be discussed. For what it concerns the set up two software were used, Rhinoceros for the geometry construction and LS-Dyna for the proper simulation. The results were analyzed thanks to the software Matlab.

### 6.1 Set Up

In the following sections the numerical model implementation will be discussed step by step until the launch of the simulation, the results will be discussed at the end of the chapter.

#### 6.1.1 Geometry

In order to obtain the geometry it was necessary to create a surface of the substrate and this was done by using Rhinoceros, which is a very well known software in the Engineering and Design field indeed is one of the best software when it comes to generate, manipulate and modify surfaces. This software manages just surfaces and does not work with solids as a 3D Cad software. In this particular case the surface to create was not really difficult so by just defining the construction lines [Fig.6.1] and by using the proper Loft surface command the external surface of the substrate will be created [Fig.6.2]. Once the surface is created can be saved in STEP format, which can be easily import in the simulation pre-processor of LS-Dyna 'LS-PrePost'. As explained in the previous chapter the continuous geometry have to be discretize and this could be done by meshing it, with this operation the surfaces will be divided in a lot of small elements which are all characterize by three or four nodes, depending on the type of element chosen. The meshing procedure of the substrate, which has been repeated two times, consist of three steps:

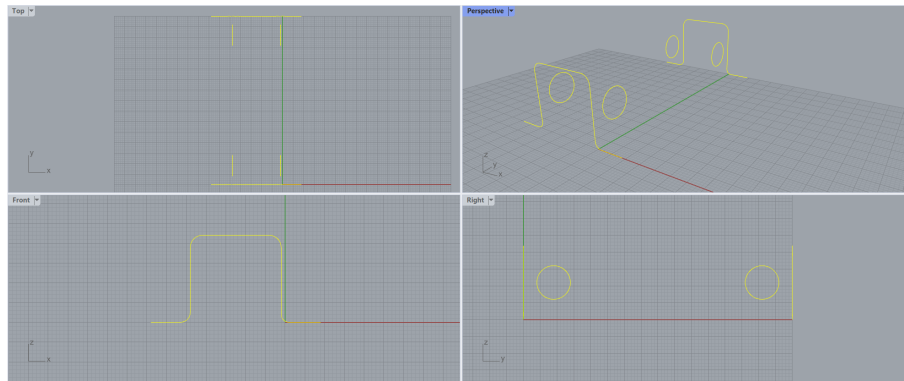


**Figure 6.1:** Lines for the surface creation

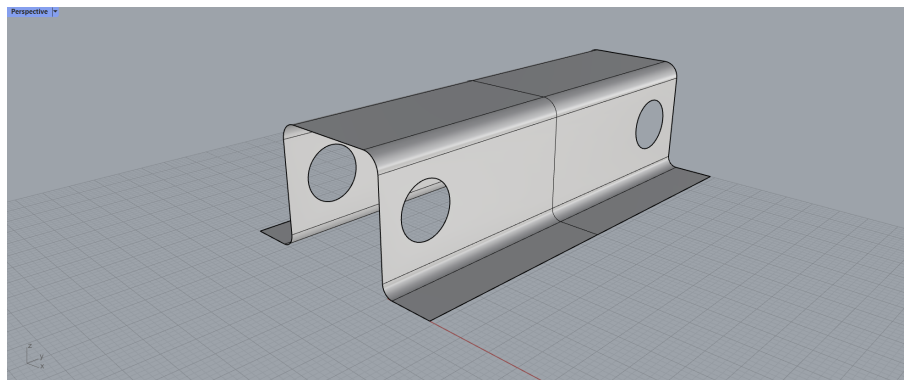


**Figure 6.2:** Surface drawn in Rhinoceros

1. Importing the surface saved in STEP format
2. Meshing the substrate with the automesh function, imposing a maximum element size and a very fine mesh tolerance [Fig:6.3]
3. Remeshing the vertical surfaces of the substrate to have lower computational costs [Fig.6.3]

By doing so the meshed substrate part is shown in Fig.6.3 and is important to underline that two new keywords are created:

1. Part, which defines the part main properties, such as material information, section properties, thermal properties and meshing adaptivity;
2. Element, which group and list together all the elements present in the model, in this particular case under the 'SHELL ELEMENT CARD' that define each shell element by four nodes, instead for example for the adhesive, which is a box solid element, all the element are defined by eight nodes and are listed under 'SOLID ELEMENT CARD'

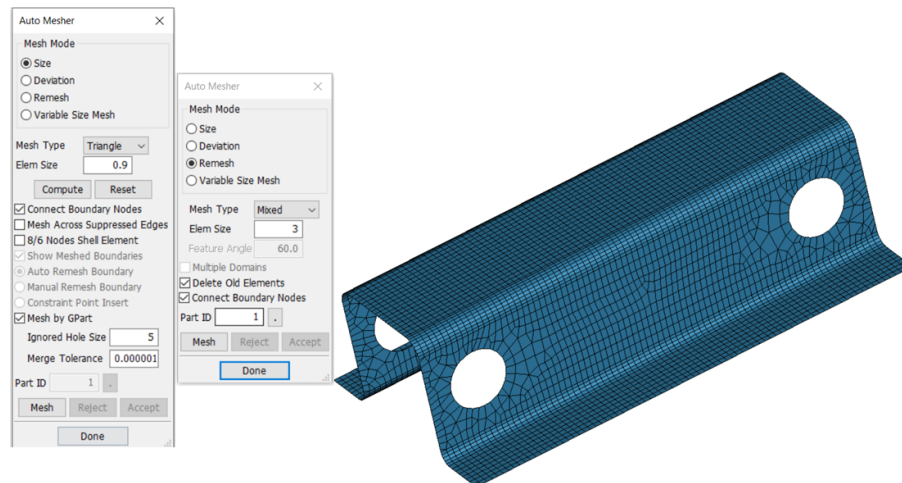


**Figure 6.3:** Automesher function: In the left side there is the implementation of the auto-mesh function and the re-meshing process of the vertical surfaces, while in the right side of the figure there is the meshed substrate

The part must be converted in "PART\_COMPOSITE", this is a very useful keywords when the model must simulate a part made of composite material and in particular by layer of composite material, indeed in this card it is possible to define the number of layer that are present in the part, the material, the orientation of each single layer and also the thickness of it. This procedure must be repeated two time, one for each single substrate. The geometry of the adhesive can be modelled directly inside the Prepost software, because can be easily represented by a box solid. The latter can be created by the function 'Shape Mesher' inside the 'Mesh' panel. This simple function permit to create a box solid by defining the extremes and also the number of element in each direction[Fig.6.4A]. In this particular case the properties of the solid object are described in the following figure [Fig.6.4B]. The geometries are not in contact because, as is possible to see in the next sections, the contact card chosen expect an offset between the contact surfaces, which is the half of the thickness of the substrates.

When the 3 geometries are well defined the model looks like the following [Fig.6.5]:

- The blue part is the fixed substrate
- The red part is the moving substrate
- The green part in the middle which is not really well visible is the adhesive

Is also important to underline that in order to conclude the section related to the geometry it is necessary to define the mathematical element formulation. The

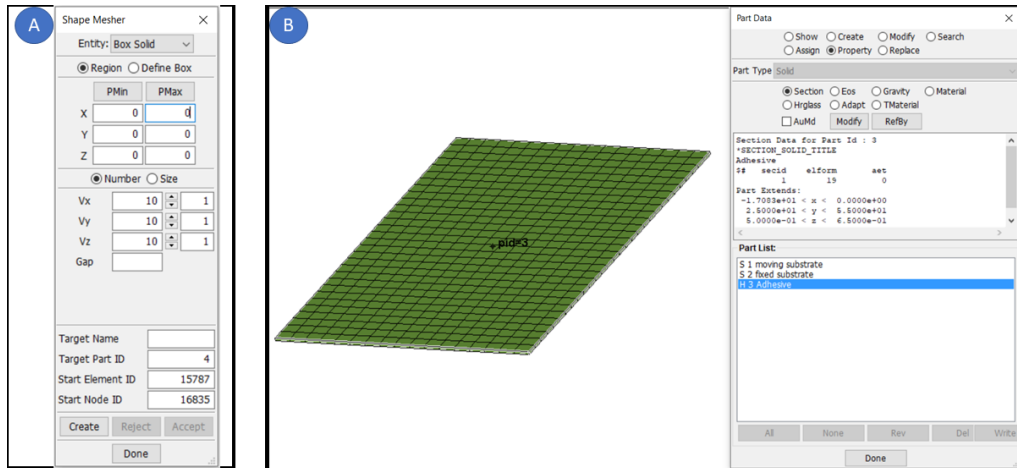


Figure 6.4: Box solid geometric property

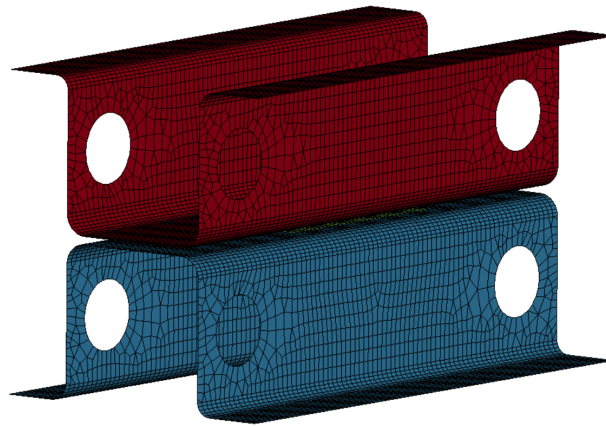


Figure 6.5: Complete geometry model

solid element represent a cohesive element so is obligatory to create a card 'SECTION\_SOLID' where it is possible to choose between two element formulation the number 19 and the number 20, the nineteenth was chosen. For what it concerns the shell element, due to the fact that the 'PART\_COMPOSITE' card was used it is possible to define in that card the element formulation for the shell without creating a new one, in this case the element formulation chosen was the number 16.

### 6.1.2 Material model

The next very important step is to define the material of each part, in this model two material must be defined:

1. Carbon fiber prepreg

## 2. Adhesive material

**Substrates material model**

The substrates are made of prepreg carbon fiber which is possible to model on LS-Prepost using a lot of possible and different material model. In our specific case, the goal of the study was not the simulation of the behaviour of the material itself but the load exchanged between the substrate and the adhesive, which means that the material model to choose doesn't necessary have to simulate the internal behaviour like the delamination. The material model that was used is `MAT_ENHANCED_COMPOSITE_DAMAGE` (MAT\_54-55) [Fig.6.6] which is an improved version of the composite model material type 22. The main parameters

Keyword Input Form

MatDB RefBy Pick Add Accept Delete Default Done 1 Carbon\_fiber

Use \*Parameter  Comment (Subsys: 1 trazione\_comp.k) Setting

\*MAT\_ENHANCED\_COMPOSITE\_DAMAGE\_(TITLE) (054/055) (1)

TITLE  
Carbon\_fiber

1	MID	RO	EA	EB	(EC)	FRBA	(PRCA)	(PRCB)
	1	1.460e-09	5.800e+04	5.800e+04	0.0	0.1200000	0.0	0.0
2	GAB	GBC	GCA	(KF)	AOPT	ZWAY		
	3900.0000	1950.0000	3900.0000	0.0	2.0000000	0.0		
3	XP	YP	ZP	A1	A2	A3	MANGLE	
	0.0	0.0	0.0	0.0	1.0000000	0.0	0.0	
4	V1	V2	V3	D1	D2	D3	DFAILM	DFAILS
	0.0	0.0	0.0	0.0	0.0	0.0	0.0600000	0.0
5	TFAIL	ALPH	SOFT	FBRT	YCFAC	DFAILT	DFAILC	EF5
	1.100e-08	0.0	0.8500000	0.0	2.0000000	0.0072000	-0.0960000	0.0
6	XC	XT	YC	YT	SC	CRIT	BETA	
	453.00000	439.00000	453.00000	439.00000	0.0718000	54.0	0.0	
7	PEL	EPSF	EPSR	TSMD	SOFT2			
	0.0	0.0	0.0	0.0	0.8500000			
8	SLIMT1	SLIMC1	SLIMT2	SLIMC2	SLIMS	NCYRED	SOFTG	
	0.0	0.0	0.0	0.0	0.0	0.0	1.0000000	
9	LCXC	LCXT	LCYC	LCYT	LCSC	DT		
	0	0	0	0	0	0.0		

Total Card: 1 Smallest ID: 1 Largest ID: 1 Total deleted card: 0

**Figure 6.6:** Material model 54-55 used for each the substrates

of the card are: [30]

- RO is the mass density
- EA, EB and EC are the Young's moduli in the longitudinal, transverse and normal direction. The latter is not used
- GAB, GBC and GCA are the shear moduli in the three directions

- AOPT define the material axes option, which for this case has a value of 2, that means globally orthotropic material with the axes define through the vector defined in the parameters A1, A2 and A3
- DFAILM is the maximum strain for the matrix both in tension or in compression, when the strain reaches the DFAILM value the element is completely removed. This parameter is active only if the maximum strain for the fiber tension is bigger than zero (DFAILT>0)
- TFAIL is the time step size criteria for element deletion
- SOFT is the softening reduction factor for the material strength in crashfront element, which means that this factor reduces the strength of the closest element ahead of the crush front.
- YCFAC is the reduction factor for compressive fiber strength after matrix compressive failure
- DFAILC maximum strain for fiber compression, the layer in the element is completely removed after the maximum compressive strain in fiber direction is reached
- XC and XT are the longitudinal compressive and tensile strength
- XC and YT are the transverse compressive and tensile strength
- SC is the shear strength in the ab plane
- SOFT2 is the softening reduction factor for material strength in crashfront elements
- SOFTG is softening reduction factor for transverse shear moduli GBC and GCA in crashfront elements

For what it concerns the criteria that was chosen is the number 54 which exploit the 'Chang matrix failure criterion' instead of 'Tsai-Wu criterion'. Experimentally the substrates did not fail during the tests so is not really relevant the choice of the failure criterion.

### **Adhesive material model**

For what it concerns the LS-Dyna material model to simulate the behaviour of the two adhesives, the MAT\_138 have been chosen. This material also known as

MAT\_COHESIVE\_MIXED\_MODE which follows a bi-linear traction-separation law 6.7. In the card material the following parameters have to be set:

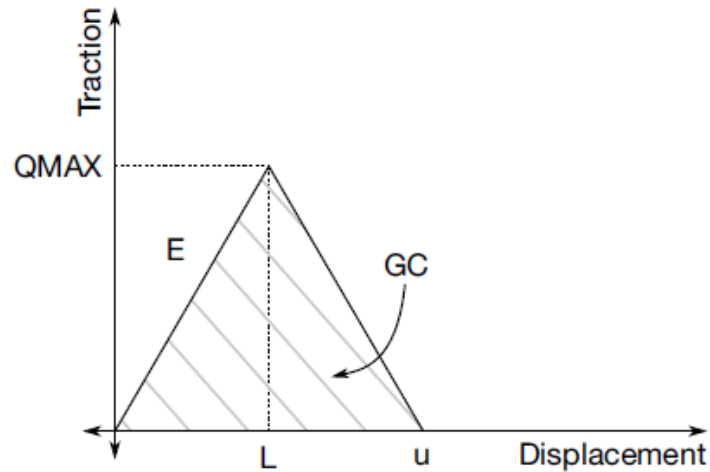


Figure 6.7: Bi-linear traction separation law for MAT\_138

- RO : mass density
- EN, ET: the stiffness in the normal plane and in the transversal one
- GIC, GIIC: The energy release rates for mode I and for mode II
- XMU: exponent of the mixed mode criteria
- T, S: peaks of traction in normal and tangential direction
- UND, UTD: ultimate displacements in the normal and tangential direction

The linearity both in the loading process and in the softening process, provides a simple relation for the two energy release rates:

$$\begin{aligned} GIC &= T \frac{UND}{2} \\ GIIC &= S \frac{UTD}{2} \end{aligned} \quad (6.1)$$

The software checks that the displacements at the peaks (both in normal and tangential directions) are smaller than the two ultimate displacements (UND and UTD) before running [Fig.6.7]. The error checks is done exploiting the formulation de-

scribed in Eq.6.2.[30]

$$\begin{aligned}\frac{u}{L} &= \frac{(2GIC)}{EN\left(\frac{T}{EN}\right)^2} > 1 \\ \frac{u}{L} &= \frac{(2GHC)}{ET\left(\frac{S}{ET}\right)^2} > 1\end{aligned}\quad (6.2)$$

### 6.1.3 Boundary Conditions

One of the most important passages requested during a numerical model creation is the imposition of the boundary conditions. LS-Prepost give to the user a lot of possible boundary conditions in this particular case study two different restriction have to be made:

1. where the specimen is fixed to the fixture it is important to impose the right constraints
2. the moving specimen must be under a prescribed motion equal to the one that the traction machine impose in the reality

#### Boundary SPC set

For what it concerns the first point in the list above, this particular constraints can be set thanks to the keyword 'BOUNDARY\_SPC\_SET'. Inside this particular keyword it is possible to determine which degree of freedom has to be lock or free, but first of all it is necessary to select the nodes that will undergo that constraints. The nodes can be selected by creating a 'NODE\_SET' using the 'CREATE ENTITY' command, by doing so it is easy to select all the possible nodes, in this particular case in the figure [Fig.6.8] the selected nodes are highlighted both in the moving substrate and in the fixed substrate.

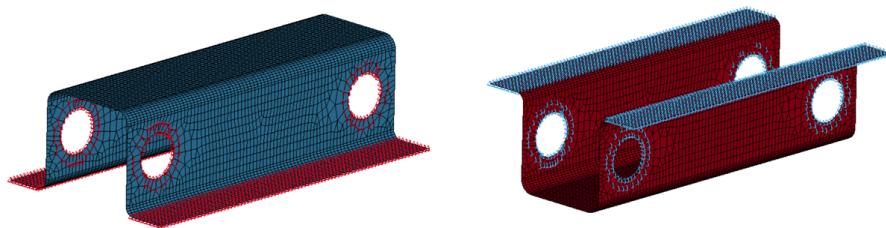


**Figure 6.8:** Set of nodes to be properly constrained

Once the two sets are defined it is possible to create the boundary condition assigning to the sets the correct constraints, in particular in the Fig.6.9 it is possible to see which degree of freedom is locked and which one is not, it is noticeable that only the translation along z of the moving substrate is free (a value of zero means no constraint), instead all the other possible movement are locked.

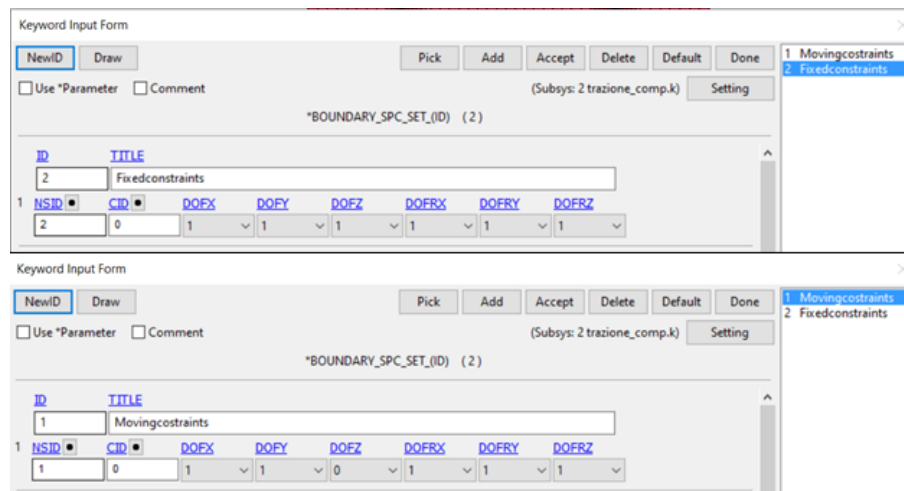


Figure 6.9: BOUNDARY\_SPC constraints cards

## Boundary Prescribed motion set

The second boundary condition that is needed in the model is the one about the traction speed imposed by the traction machine and transmitted to the moving substrate. This kind of constraint can be assigned thanks to the 'BOUNDARY\_PRESCRIBED\_MOTION\_SET' keyword. In the latter, as is noticeable in the Fig.6.10, it is needed to define:

- NSID: the set of nodes to which the condition must be applied
- DOF: the degree of freedom to which the condition must be applied
- VAD: the type of curve is going to be considered (velocity in our case)
- LCID: the curve that describes the motion value (velocity, previously defined) versus time
- SF: Load curve scale factor

In order to load a curve which describes the motion it is necessary to firstly define one and this is possible by creating an additional card 'DEFINE\_CURVE' where is possible to define a curve by its own points Fig.6.11.

ID	TITLE
1	Imposed motion

1	NSID	DOF	VAD	LCID	SF	VID	DEATH	BIRTH
1	1	3	0	1	10.0000000	0	1.000e+28	0.0

2	OFFSET1	OFFSET2	MRB	NODE1	NODE2
0.0	0.0	0	0	0	0

Figure 6.10: Boundary\_Prescribed\_Motion card

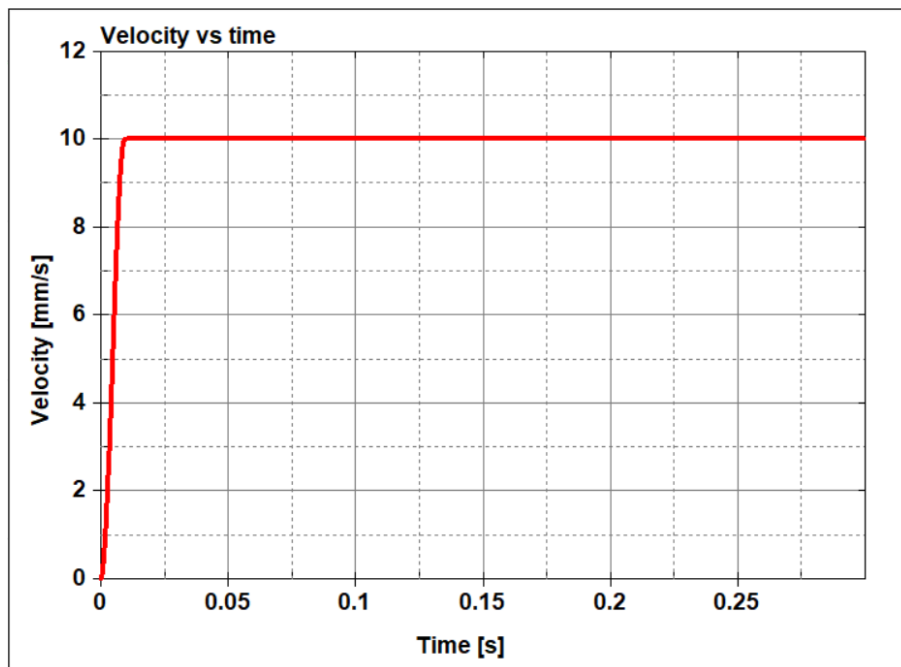


Figure 6.11: Velocity imposed by the traction machine versus time

During the simulation of an arcan test the boundary conditions need to be changed, in fact the value of DOF in the 'Prescribed motion set' card needs to be changed depending on the type of load to apply (shear means y translation instead tensile means z translation), obviously the in the 'Spc constraint' of the moving substrate is necessary to be consistent with what we are changing.

### 6.1.4 Contact

CONTACT\_TIED\_SHELL\_EDGE\_TO\_SURFACE\_CONSTRAINED\_OFFSET is the contact type that was adopted, which ties both translational and rotational degrees of freedom of nodes to a surface (CONTACT\_TIED\_SHELL\_EDGE\_TO\_SURFACE) and preserves the distance between the nodes and the surface (CONSTRAINED\_OFFSET). In general contacts can be implemented with two different algorithms:

1. Penalty based algorithm for which the contact treatment is internally represented by linear springs between the slave nodes and the nearest master segments. The stiffness of these springs determines the force that will be exchanged in the contact;
2. Constraint based algorithm is based on the imposition of constraints directly in the global equations:
  - Transformation of the nodal displacement components of the slave nodes along the contact interface
  - Eliminating the normal degree of freedom of the slaves nodes
  - Interpenetrating nodes are moved back to surface

Using the 'CONSTRAINED\_OFFSET' option a kinematic approach is used, and exchanged moments are computed. The CONSTRAINED option cannot be used with rigid bodies. One important consideration that have to be taken into account is about the distance between the substrates. The thickness of the substrates is defined in the 'PART\_COMPOSITE' card and is equal to the thickness of a single layer multiplied by the number of layers that have been used. The thickness of the shell is extruded from the mid-plane in both directions. The thicknesses of the adhesives are equal to 0.2mm for the epoxy and 1.5mm for the polyurethane, therefore is possible to compute the distance between the substrates considering that the contact surfaces must have a distance equal to half the total substrate's thickness [Tab.6.1] [Fig.6.12].[28][31]

The Value imposed in the contact keyword are shown in the Fig.6.13 and are the following:

- SSID and MSID are the slave and master set ID that are selected to interact during the contact, such as the elements in the two top surfaces of the

Epoxy Adhesive		
N. of layers	Substrate's thickness	Distance of shells
2	1mm	1.2mm
4	2mm	2.2mm
Polyurethane Adhesive		
N. of layers	Substrate's thickness	Distance of shells
2	1mm	2.5mm
4	2mm	3.5mm

**Table 6.1:** Offset distance between shells of different thickness in the epoxy case simulation

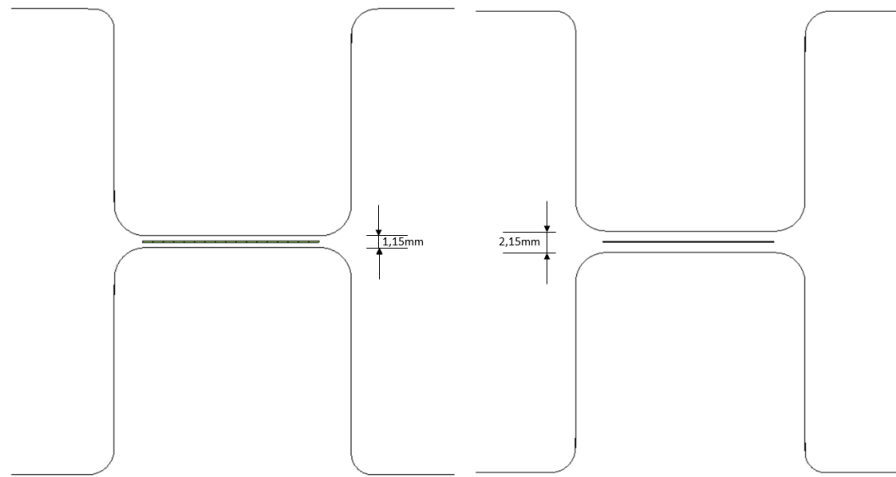


**Figure 6.12:** Offset distance between shells of different thickness in the epoxy case simulation

substrates are the master degrees of freedom, while all the nodes of the part 'Adhesive' are considered as slave elements.

- SSTYP and MSTYP let the user to define the type of slave and master set ID which in particular are SHELL\_ELEMENT\_SET for the master and PART\_SET for the slave
- FS is the static coefficient of friction
- VDC is the viscous damping coefficient in percent of critical
- DT is the death time, which define when the contact surface is deactivated
- SFS, SFM, SFST, SFMT, FSF and VSF are scale factors all set up to the default value of 1.

Keyword Input Form

NewID Draw Pick Add Accept Delete Default Done 1 (1) Contact

Use \*Parameter  Comment (Subsys: 1 trazione\_comp.k) Setting

\*CONTACT\_TIED\_SHELL\_EDGE\_TO\_SURFACE\_CONSTRAINED\_OFFSET\_ID/TITLE/MPP(THERMAL) (1)

1 CID TITLE  
1 Contact

MPP1  MPP2

2 IGNORE BCKET LCBCKT NS2TRK INITITR PARMAX UNUSED CPARM9  
0 200 3 2 1.0005 0

3 UNUSED CHKSEGS FENSE GRPABLE  
0 1.0 0

4 SSID MSID SSTYP MSTYP SBOXID MBOXID SPR MPR  
3 1 3 1 0 0 0 0

5 ES FD DC VC VDC FENCHK BI DT  
1.0000000 0.0 0.0 0.0 20.000000 0 0.0 1.000e+20

6 SFS SFM SSI MST SFST SFMT FSE YSE  
1.0000000 1.0000000 0.0 0.0 1.0000000 1.0000000 1.0000000 1.0000000

Thermal  T\_Friction  A  AB  ABC  ABCD  ABCDE  ABCDEF

Total Card: 1 Smallest ID: 1 Largest ID: 1 Total deleted card: 0

Figure 6.13: Contact keyword

### 6.1.5 Output set up

The last step before running the proper simulation is the definition of the output that have to be computed and shown at the end of the numerical process. The aim is to have a comparison between the real tests and the numerical results, then the following output need to be analyzed :

- Force involved: ASCII file which contains RCFORC SPCFORC SECFORC
- Graphical output: BINARY\_D3PLOT

#### DATABASE\_RCFORC

LS\_Dyna can write a lot of possible output files concerning the contact. The first one used in this project is called DATABASE\_RCFORC, which is an ASCII file containing resultant contact forces both for slave and master side of each contact interface. The time interval between outputs is set to 0,002s.

#### DATABASE\_SPCFORC

With this card is possible to compute the force that are involved in the elements where a constrained boundary condition is imposed. The output file is an ASCII file and as for the previous one the time interval between outputs is set to 0,002s.

### DATABASE\_SECFORC

In order to double check the forces in the contact region, one more ASCII file can be written by using the 'DATABASE\_SECFORC' keyword. The latter needs a plane of reference in order to define the region where the force and moment have to be computed. In the model three different cross section planes are defines, in particular in the mid plane of the adhesive and two in proximity of the contact surfaces in each substrate 6.14.

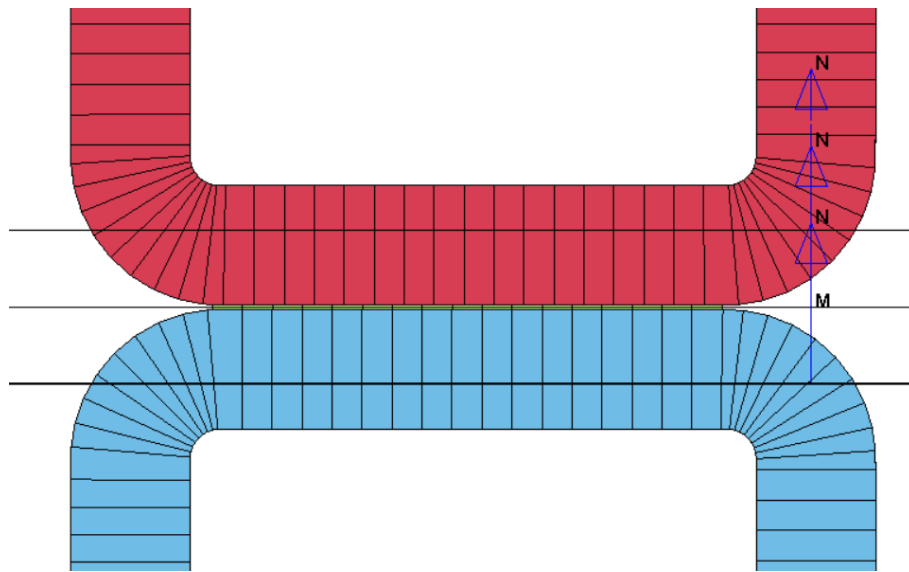


Figure 6.14: Cross sections

### DATABASE\_BINARY\_D3PLOT

This is a graphic output, which prints the model at each stage. The number of stage is defined through the time step size, smaller the step size, bigger will be the number of plot created.

## 6.2 Results

In this final section the numerical results obtained by the software will be showed and compared to the results previously obtained in the experimental tests, described in 4. As a first target only the elastic linear part and the peak load were tried to simulate. The configurations that have been simulated are the following:

- 
- Pure shear loading condition: in fig.6.15a and fig.6.15b is possible to see the comparison between the numerical and experimental curve in the pure shear loading case for both the adhesives and both the thicknesses of the substrates. A good fitting between the numerical curve and the experimental one in both the two cases involving the thicker substrates, instead for what it concerns the thinner substrate, the numerical curve of the epoxy adhesive does not fit well the experimental curve, but the reason is probably that in the experimental tests the substrates have been partially delaminated.
  - Pure tensile loading condition: in fig6.16 the numerical results are compared with the experimental one in the pure tensile loading conditions for both adhesives and thicknesses involved in the analysis. The tests involving the polyurethane have been simulated in a pretty good way in the first elastic part and for what it concerns the peak load, instead an optimization of the softening part, in both cases, was not studied. For what it concerns the epoxy joints, for both of the thicknesses, some problems occurs during the simulations that do not permit a good representation of the real tests. For sure in the future studies a good fitting could be achieved with a more in-depth analysis but unfortunately will not be presented in this thesis work.

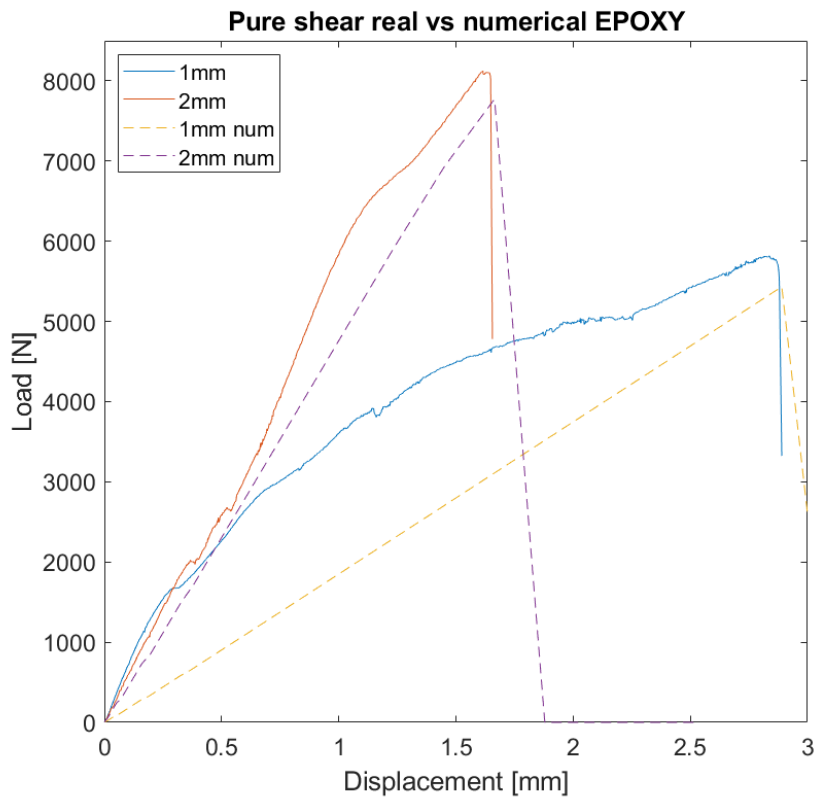
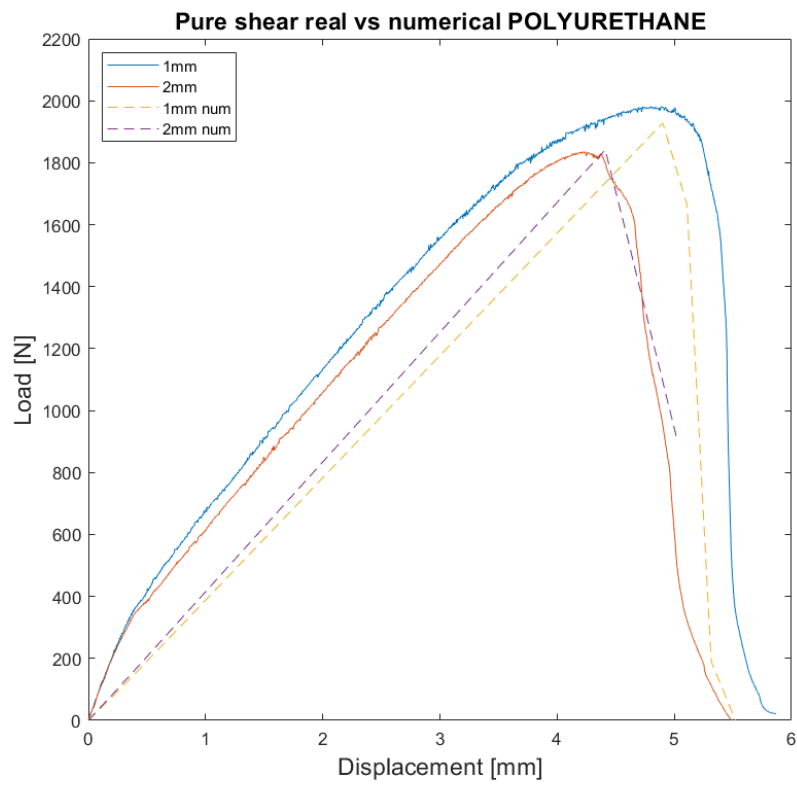
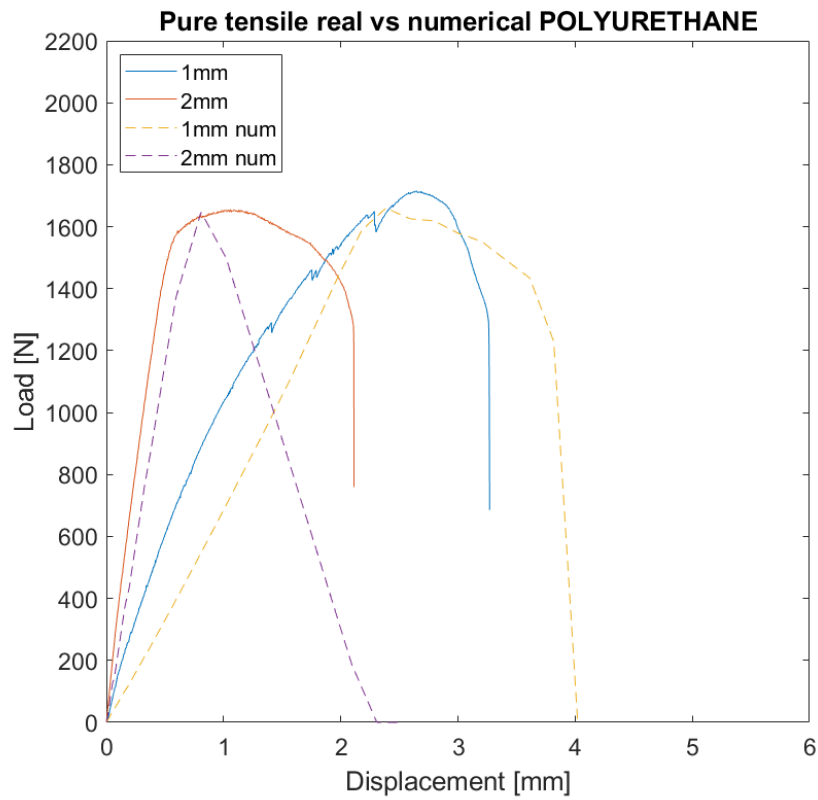
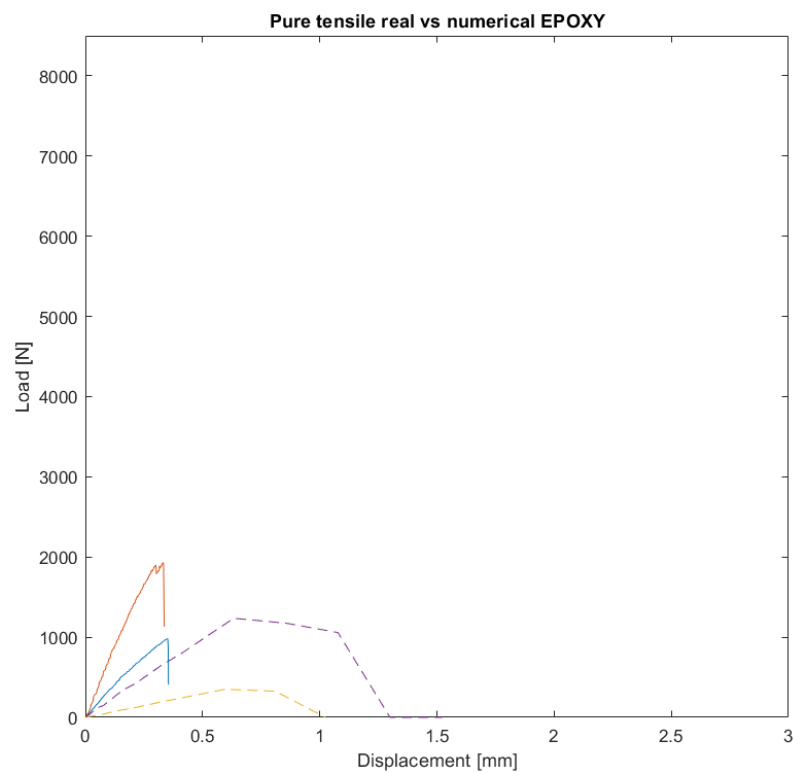


**Figure 6.15:** Comparison between real and numerical curve in the pure shear conditions



(a) POLYURETHANE



(b) EPOXY

**Figure 6.16:** Comparison between real and numerical curve in the pure shear conditions

## 7. Conclusion

This thesis work is based on the characterization of adhesive joints. Two adhesives have been used: structural epoxy adhesive and a more ductile bi-component polyurethane adhesive. The adhesives have been tested by using an Arcan fixture.

In the first part the manufacture of the specimens testable with the Arcan fixture have been studied and designed. After designing it, an aluminum mold was manufactured by folding procedures. The substrates were manufactured by using pre-preg sheets of carbon fiber, that were laid down in the mould, put under vacuum and cured in the oven following a proper curing cycle. After the substrates were cut and drilled, they were glued two by two with the adhesives, using a bonding area of 17 mm by 15 mm, that was delimited by transparent tape..

With the specimens ready, the experimental test have been done by exploiting a traction machine with the arcan fixture mounted on it. The polyurethane adhesive have been tested in 5 different loading conditions, such as pure shear ( $0^\circ$ ), mixed loading conditions ( $30^\circ$ ,  $45^\circ$  and  $60^\circ$ ) and pure tensile ( $90^\circ$ ). For what it concerns the epoxy adhesive just three configurations have been studied, such as pure shear ( $0^\circ$ ), mixed loading condition ( $45^\circ$ ) and pure tensile ( $90^\circ$ ).

The results confirm a correlation between the thickness of the substrate and the adhesive response moreover, the change in the loading conditions did not act equally in the two adhesives, due probably to the their difference in stiffness. For what it concerns the polyurethane adhesive increasing the thickness of the substrate in the adhesive joint, the load displacement curve is steeper, which means an higher stiffness of the joint. The load directions, like the thickness of the substrate, influence the stiffness of the joint, higher the angle of traction, higher the stiffness of the joint. For this particular adhesive, which is very flexible, the load carrying capacity of the adhesive joint is not really influenced by the angle of the load, differently from the stiffness, which increases with the loading angle as shown by the decrease in displacement corresponding to the peak load. The stiffer structural epoxy adhe-

sive showed a huge decay in the loading carrying capacity increasing the angle of application of the load for both the thicknesses of the substrates. The stiffness of the adhesive joint is not following a decreasing or increasing path but is stiffer in the 45° configuration than in the pure load configurations but it was noticed that the peak of the load occurs sooner in the pure tensile configuration and it occurs always later decreasing the loading angle. Finally in the end of the thesis a simulation model is created and the results are presented and compared to the experimental ones. Just the 0° and 90° configurations were simulated and the numerical results obtained were pretty realistic for the polyurethane adhesive joint in both shear and tensile loading conditions. For what it concerns the epoxy adhesive the simulation did not fit very well with the real curves in the pure tensile condition, and due to lack of time no in-depth analysis has been done to fit well real and numerical curves. Instead in the pure shear load configuration, also for the epoxy joint, a good curve fit between the real and numerical case has been obtained.

For the future studies an improved simulation model could be designed in order to obtain numerical results that will be closer to the real experimental curves.

## 8. Bibliography

- [1] Antonio Pizzi and Kashmiri L Mittal. *Handbook of adhesive technology, revised and expanded*. CRC press, 2003.
- [2] Giovanni Belingardi et al. “Thermoplastic adhesive for automotive applications”. In: *Adhesives-Applications and Properties* (2016), pp. 341–359.
- [3] R Ciardiello et al. “Experimental investigation on adhesively bonded U-shaped metallic joints using the Arcan test”. In: *Journal of Advanced Joining Processes* (2020), p. 100010.
- [4] *Alleggerimento dei veicoli elettrici*. URL: <https://www.plastmagazine.it/alleggerimento-dei-veicoli-elettrici/> (visited on ).
- [5] *Born electric*. URL: <https://www.ilpost.it/filippozuliani/2011/09/05/born-electric/> (visited on ).
- [6] Jean-Yves Cognard et al. “Analysis of the nonlinear behavior of adhesives in bonded assemblies—Comparison of TAST and Arcan tests”. In: *International Journal of Adhesion and Adhesives* 28.8 (2008), pp. 393–404.
- [7] Lucas FM Silva, Andreas Öchsner, and Robert D Adams. “Introduction to adhesive bonding technology”. In: *Handbook of adhesion technology*. 2011.
- [8] MD Banea and Lucas FM da Silva. “Adhesively bonded joints in composite materials: an overview”. In: *Proceedings of the Institution of Mechanical Engineers, Part L: Journal of Materials: Design and Applications* 223.1 (2009), pp. 1–18.
- [9] G Belingardi and G Chiandussi. “Stress flow in thin-walled box beams obtained by adhesive bonding joining technology”. In: *International journal of adhesion and adhesives* 24.5 (2004), pp. 423–439.
- [10] Lucas FM Da Silva, Andreas Öchsner, and Robert D Adams. *Handbook of adhesion technology*. Springer Science & Business Media, 2011.
- [11] Dr Kopeliovich. “Dmitri. 2014”. In: *Fundamentals of adhesive bonding* ().

- 
- [12] Józef Kuczmazewski. *Fundamentals of metal-metal adhesive joint design*. Lublin University of Technology, 2006.
- [13] *3M Science Applied to Life*. URL: [https://www.3m.com/3M/en\\_US/bonding-and-assembly-us/resources/science-of-adhesion/common-stress-types-adhesive-joints/](https://www.3m.com/3M/en_US/bonding-and-assembly-us/resources/science-of-adhesion/common-stress-types-adhesive-joints/) (visited on ).
- [14] Josué Quini and Gerson Marinucci. “Polyurethane Structural Adhesives Applied in Automotive Composite Joints”. In: *Materials Research* 15 (June 2012), pp. 434–439. DOI: [10.1590/S1516-14392012005000042](https://doi.org/10.1590/S1516-14392012005000042).
- [15] Shio-Ching Lin and Eli M Pearce. “High-performance thermosets”. In: (2005).
- [16] *Adhesive.org*. URL: <https://www.adhesives.org/adhesives-sealants/science-of-adhesion/design-of-adhesives-bonds/types-of-adhesives> (visited on ).
- [17] *fracturemechanics.org*. URL: <https://www.fracturemechanics.org/modes123.html> (visited on ).
- [18] J.R.J. Wingfield. “Treatment of composite surfaces for adhesive bonding”. In: *International Journal of Adhesion and Adhesives* 13.3 (1993), pp. 151–156. ISSN: 0143-7496. DOI: [https://doi.org/10.1016/0143-7496\(93\)90036-9](https://doi.org/10.1016/0143-7496(93)90036-9). URL: <http://www.sciencedirect.com/science/article/pii/S0143749693900369>.
- [19] Haim Abramovich. *Advanced Aerospace Materials: Aluminum-Based and Composite Structures*. Walter de Gruyter GmbH & Co KG, 2019.
- [20] Bryan Harris et al. “Engineering composite materials”. In: (1999).
- [21] Theodore E Matikas. “Analysis of load transfer behaviour and determination of interfacial shear strength in single-fibre-reinforced titanium alloys”. In: *Advanced Composites Letters* 16.5 (2007), p. 096369350701600504.
- [22] Timotei Centea, Lessa K Grunfelder, and Steven R Nutt. “A review of out-of-autoclave prepregs—Material properties, process phenomena, and manufacturing considerations”. In: *Composites Part A: Applied Science and Manufacturing* 70 (2015), pp. 132–154.
- [23] Seong-Soon Hwang et al. “Cure kinetics and viscosity modeling for the optimization of cure cycles in a vacuum-bag-only prepreg process”. In: *The International Journal of Advanced Manufacturing Technology* 99.9 (2018), pp. 2743–2753.

- 
- [24] *EasyComposite*. URL: <https://www.easycomposites.co.uk/learning/introduction-to-out-of-autoclave-prepreg-carbon-fibre> (visited on ).
- [25] Kenneth H Huebner et al. *The finite element method for engineers*. John Wiley & Sons, 2001.
- [26] Claudio Canuto. *Numerical modelling, Discretization by finite element*. University Lecture DISMA: Dipartimento di scienze matematiche PoliTO. 2019.
- [27] Klaus-Jürgen Bathe. *Finite element procedures*. Klaus-Jurgen Bathe, 2006.
- [28] LS-DYNA Theoretical Manual. “Livermore software technology corporation”. In: *Livermore, CA* 199 (2006).
- [29] Massachusetts Dassault Systemes SolidWorks Corp. Concord. *Understanding Non- linear Analysis*. Klaus-Jurgen Bathe, 2008.
- [30] John O Hallquist. “LS-DYNA® Keyword User’s Manual Volume II Material Models”. In: *Livermore, California, USA* (2013).
- [31] *LS-Dyna Support*. URL: <https://www.dynasupport.com/tutorial/ls-dyna-users-guide/contact-modeling-in-ls-dyna> (visited on ).